CATIONIC POLYMER ENHANCED HYDROLYSIS OF CORNSTARCH FOR THE PRODUCTION OF BIOFUELS

A Dissertation
Presented to
The Academic Faculty

by

Kendra Maxwell

In Partial Fulfillment
of the Requirements for the Degree
Doctor of Philosophy in the
School of Chemical and Biomolecular Engineering

Georgia Institute of Technology
May 2012

CATIONIC POLYMER ENHANCED HYDROLYSIS OF CORNSTARCH FOR THE PRODUCTION OF BIOFUELS

Approved by:

Sujit Banerjee, Advisor
School of Chemical and Biomolecular Engineering
Georgia Institute of Technology

Preet Singh
School of Materials Science and Engineering
Georgia Institute of Technology

Sven Behrens
School of Chemical and Biomolecular Engineering
Georgia Institute of Technology

Lakeshia Taite
School of Chemical and Biomolecular Engineering
Georgia Institute of Technology

Danny Haynes
Eka Chemicals
AkzoNobel

Date Approved: March 19, 2012

ACKNOWLEDGEMENTS

I would like to take this opportunity to thank those who have made this thesis possible. First of all, I would like to thank my advisor Dr. Sujit Banerjee for guiding me through my graduate studies and helping me develop the thinking process necessary for research. I also greatly appreciate all of the helpful comments and guidance given to me from my thesis committee: Sven Behrens, Danny Haynes, Preet Singh, and Lakeshia Taite. I would like to thank the Institute of Paper Science and Technology (IPST) and member companies, Eka Chemicals, and Dupont for their financial support of my graduate studies. Thanks also goes out to my fellow lab mates past and present including John Reye, Sandeep Mora, Jian Lu, Tuan Le, and Swati Rao for their support and advice along the way. In addition, I would like to thank my undergraduate lab mates Alison Krantz, Helina Desta, and Kevin Gray for their experimental contributions, and helping me learn to be a better leader and mentor. To all Georgia Tech and IPST faculty and staff, thank-you for your assistance and making my time at Georgia Tech enjoyable.

I would like to thank my fellow graduate students who experienced this journey with me for their support and the unforgettable memories. I also would like to thank my friends for their patience and never-ending encouragement along the way. Last but not least, I would like to thank my parents for instilling in me the importance of education and perseverance.

TABLE OF CONTENTS

LIST OF TABLES

LIST OF FIGURES

SUMMARY

The mechanism through which a charged polymer cationic polyacrylamide (C-PAM) operates to increase the rate of cornstarch hydrolysis was investigated. The main objective was to determine the major factors that affect the mechanism so that these parameters may be adjusted to achieve optimal hydrolysis rates. A combination of analytical methods including dynamic light scattering, optical imaging, and uv-vis spectroscopy were used to study polymer, starch, and enzyme interactions as a function of process conditions. It was found that C-PAM binds strongly to starch granules, increasing solubilization and decreasing onset gelatinization temperature. Granule swelling was unaffected by C-PAM. Both binding of enzyme to cornstarch, and rate of cornstarch hydrolysis were found to increase in the presence of C-PAM. By analogy to previous work on cationic polymer promoted hydrolysis of cellulose, it was proposed that the polymer reduces the charge on the starch surface through a “charge-patch” mechanism. Because both enzyme and substrate are negatively charged, the positively charged polymer reduces the charge repulsion experienced by the approaching enzyme. This leads to stronger enzyme-substrate binding, and faster hydrolysis. There is a mirror image relationship between viscosity of the medium and hydrolysis rate, which allows optimization of these parameters with enzyme and C-PAM dosage. Overall, the polymer addition reduced enzyme dose by 62% depending on the conditions used, so this method could have significant economic impact on the industrial conversion of starch to ethanol.

CHAPTER 1: INTRODUCTION

A rise in the economic development of the world has led to an increase in demand for oil-based fuel sources, particularly in the transportation sector. As oil is a nonrenewable resource, its supply is rapidly being depleted, causing the market to become increasingly volatile and unpredictable. In addition, the use of these oil-based fuels have largely contributed to environmentally harmful greenhouse gas emissions (Mussatto et al., 2010). As a result, renewable, sustainable, more cost effective alternative fuel sources are being sought to meet increasing energy demands.

Due to the maturity of the technology, biofuels are the most promising transportation fuel alternative in the short term (Nigam & Singh, 2011). They are the favored option in that they are renewable and biodegradable. In addition, biofuels would increase supply security and would reduce green house gas emissions. Biofuels can be produced from forestry, agricultural or municipal waste sources. The most common biofuel currently being produced commercially is ethanol using sugarcane, corn, and cellulosic material as the feedstock (Mussatto, et al., 2010). In the United States corn is the major feedstock material used, reaching a production of 13.5 billion gallons of ethanol in 2010 (RFA, 2011).

Ethanol from corn is mainly produced through either the dry grind or wet milling process. The focus of the dry grind process is to maximize ethanol yield, while the wet milling process produces ethanol in addition to other value added products. The majority of the ethanol in the United States is produced using the dry grind method, as it is the least energy intensive process (Rendleman & Shapouri, 2007). In the dry grind process, corn is ground, and then mixed with water to form a slurry. The slurry is then cooked, and enzymes are added to convert the starch to sugar. Next, yeast is added to ferment the sugars into ethanol. Finally, the mixture is distilled and dehydrated to produce fuel grade ethanol (Bothast & Schlicher, 2005).

Although the dry grind method is an established technology, further increases in process efficiency are needed to ensure long-term economic sustainability. Many approaches have been taken to boost process efficiency including the development of corn hybrids with higher extractable starch (Bothast & Schlicher, 2005; Haefele et al., 2004), enhancement of enzyme stability and performance (Robertson et al., 2006; Sivaramakrishnan et al., 2006), and improvements in process technologies (Montalbo-Lomboy, 2008; Rendleman & Shapouri, 2007). Many of these technologies, though promising, are not yet efficient or cost-effect enough for widespread commercialization.

Cationic polyacrylamide (C-PAM), a flocculating polyelectrolyte has been found to increase the rate of enzymatic hydrolysis of multiple biomass feedstock

including cellulosic fibers, starch, and sludge (Reye et al., 2009). Increasing the rate of starch hydrolysis would allow for a higher yield of product, and lower energy and input supply costs. The purpose of this study was to investigate the mechanism through which C-PAM increases the starch hydrolysis rate, and to specifically answer the following questions:

1. How does C-PAM interact with starch in solution, and how strongly does this interaction affect starch gelatinization?
2. How does C-PAM interact with enzyme in solution and how strongly does this interaction affect enzyme binding, activity, and stability?
3. How does C-PAM affect starch hydrolysis and what are the optimum conditions for C-PAM enhanced hydrolysis of starch?

To this end, the specific objectives of this thesis were to:

- Characterize interactions of C-PAM with cornstarch and determine the effect of C-PAM on gelatinization and hydrolysis of cornstarch
- Characterize interactions of C-PAM with starch hydrolyzing enzymes and determine the effect of C-PAM on enzyme binding and activity
- Propose a mechanism to account for both C-PAM-starch-enzyme interactions and the increase in hydrolysis rate in the presence of C-PAM

Fundamental studies of polymer-substrate and polymer-enzyme interactions relevant to starch hydrolysis are presented. The results of this study will provide insight into the mechanism of a novel method to increase the rate of starch to

glucose conversion. In addition, the findings of this study could be useful for similar polymer-enhanced hydrolysis systems that have been shown to operate through similar means with other biomass sources and polymers.

The remaining chapters are organized as follows: chapter 2 reviews relevant literature on biomass, flocculation, and enzymatic hydrolysis of biomass. Chapter 3 provides the experimental techniques and procedures used to complete this research. Chapter 4 reports results and discussion of starch-polyelectrolyte, enzyme-polyelectrolyte, and enzymatic hydrolysis studies, respectively. The thesis concludes with Chapter 5, which provides overall conclusions and suggestions for future work.

CHAPTER 2: LITERATURE REVIEW

2.1. Starch

Starch is a major energy storage component in cereal grains such as corn, wheat, sorghum, rice, tubers (potato), and roots (tapioca and sweet potato). In corn, starch makes up approximately 71% of the corn kernel (Van Beynum & Roels, 1985).

2.1.1. Starch composition

Starch is a glucose polymer with the general formula $(C_6H_{10}O_5)_n$. It is a mixture of two glucose polymers: the linear polymer amylose, and the branched polymer amylopectin. Amylose is a linear polymer of repeating glucose units linked at the α-1-4 glycosidic bond, containing up to 6000 glucose units depending on the origin of the starch (Figure 1). Amylose chains may contain trace amounts of branching. In cornstarch, amylose makes up approximately 28 %(w/w) of the starch, with an average degree of polymerization (DP) of 800 (Van Beynum & Roels, 1985). Amylopectin molecules contain branched glucose chains connected at the α-1-6 linkages in addition to α-1-4 linked glucose chains, as seen in Figure 2. Amylopectin typically contains about 2,000,000 glucose units, making it one of the largest naturally occurring biopolymers.

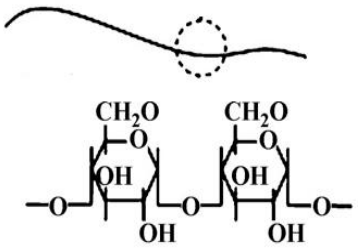

Figure 1: Chemical structure of amylose

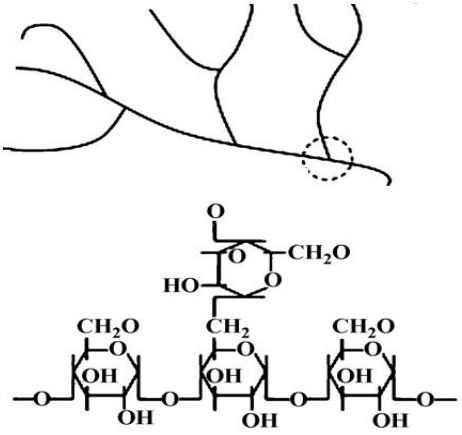

Figure 2: Chemical structure of amylopectin

2.1.2. Starch granule structure

Starch granules have complex structures made up of several amylose and amylopectin starch molecules. Starch molecules have an abundance of hydroxyl groups, which are attracted to each other, forming hydrogen bonds between adjacent amylose and amylopectin molecules (Robertson, et al., 2006). These hydrogen-bonding forces pull the polymer chains together into crystalline bundles to form starch granules as illustrated by the “hairy billiard ball” model Figure 3. The crystalline bundles are interspersed between less ordered amorphous

regions of the granule, and are responsible for holding the starch granule together. Due to the size of amylopectin, it is a major component of the crystalline regions. About 25-50% of the total volume of a typical starch granule is crystalline.

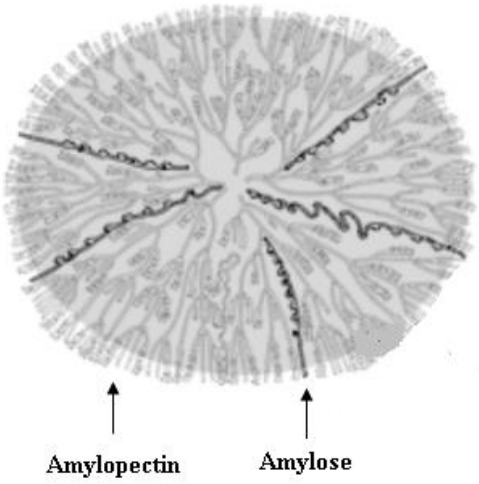

Figure 3: Model of starch granule structure

2.1.3. Starch swelling and gelatinization

Starch granules are partially insoluble in water. They must typically undergo a multi-stage process called gelatinization in order to solubilize the particles. A schematic of the process is shown below in Figure 4. At low temperatures, starch is insoluble because of hydrogen bonding forces between starch molecules. Though the hydrogen bonding forces are weak, the large numbers of bonds involved keep the granules from dissolving in cold water. When starch granules in water are heated from 20-60 ^{o}C, they absorb water that disrupt the weak hydrogen bonds, and allow them to swell (Xie et al., 2006). At this phase

the process is reversible. With further heating, the granules begin to rupture and collapse, releasing starch chains into solution, leaving a viscous dispersion of swollen granule fragments and dissolved starch molecules. The point at which the process becomes irreversible is called the initial or onset gelatinization temperature. For cornstarch granules, this generally occurs between 65-80 ^{o}C (Van Beynum & Roels, 1985). Further heating above the gelatinization temperature causes further hydrogen bonding disruption, swelling, and crystalline structure melting.

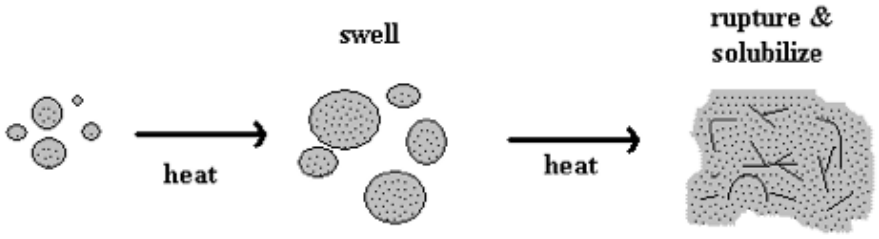

Figure 4: Gelatinization of starch granules

Starch gelatinization has been widely studied, and factors that affect gelatinization include water availability, agitation, salt concentration, and addition of other hydrocollolloids (Xie, et al., 2006). Reducing the availability of water reduces the amount of water that is able to absorb and swell the starch granules, hindering the gelatinization of starch. As a result, higher temperatures are needed to begin the gelatinization process for low water containing systems as is generally the case for commercial starch processing systems. Shear stress or agitation can be applied to enhance the disruption of starch granules and

subsequent gelatinization. Electrostatic interactions induced by salt concentration can have significant effects on gelatinization. Jane (Jane, 1993) found that negatively charged ions repel the –OH groups on starch and stabilize the starch. As a result higher onset gelatinization temperatures are required. The degree of repulsion was found to be proportional to the charge density of the ion. Alternately, positive cations were attracted to the starch molecules, which caused starch destabilization and lowered onset gelatinization temperatures.

The interaction of starch with other hydrocolloids has been of great interest in recent years as many hydrocolloids have been shown to affect starch gelatinization with potential implications for the food industry. A wide range of starch-hydrocolloids systems with various preparation methods and analysis tools have been used (BeMiller, 2011). As a consequence, many different and sometimes conflicting results and mechanisms have been proposed. From these studies it can be concluded that due to the complexity of the starch-hydrocolloid system, several mechanism are likely to be operating depending on system parameters such has colloid type, starch composition, and concentration.

2.2. Enzymatic Hydrolysis of Starch

2.2.1. Enzymatic hydrolysis of starch

Starch can be converted to simpler sugars by acid or enzymatic hydrolysis, but commercially, most hydrolysis today has been replaced by enzymatic hydrolysis, as enzymatic hydrolysis has many advantages over acid hydrolysis. Enzymes have higher specificity, so products can be developed with more control.

Secondly, enzymatic hydrolysis is performed under milder conditions, which results in fewer side reactions and lower operating costs (Nigam & Singh, 2011) .

Starch must first be hydrolyzed to single glucose units before being fermented into ethanol. In the United States, starch extracted from corn (corn milling) is the major feedstock for ethanol production. There are two types of industrial corn milling processes (Figure 5): wet milling and dry milling. In the dry grind process, the purpose is to maximize ethanol yield (Kwiatkowski et al., 2006). In the wet milling process, other high value products are produced in addition to ethanol (Bothast & Schlicher, 2005; Taylor et al., 2001). The majority of the ethanol in the United States is produced using the dry grind method, however the hydrolysis steps are essentially the same for both processes (Sanchez & Cardona, 2008).

Cooking, liquefaction, and saccharification are the three main stages in industrial starch hydrolysis. The starch solution is brought to high temperatures (90-110 ^{o}C) in a jet cooker to gelatinize the starch molecules. Without gelatinization, starch granules are less soluble and will not hydrolyze as efficiently as gelatinized starch. Alpha-amylase is added at this phase to aid in solubilization. In the liquefaction step, additional alpha-amylase enzyme is added after reducing the temperature to between 70-90 ^{o}C, the optimal temperature for most alpha-amylase enzymes. The alpha-amylase breaks the starch molecules into a mixture of shorter length starch pieces called dextrin. In the final hydrolysis step called saccharification, the temperature of the starch slurry is lowered to between

50-70 ^{o}C, and a second enzyme, glucoamylase, is added which converts the dextrin to glucose. (Sanchez & Cardona, 2008).

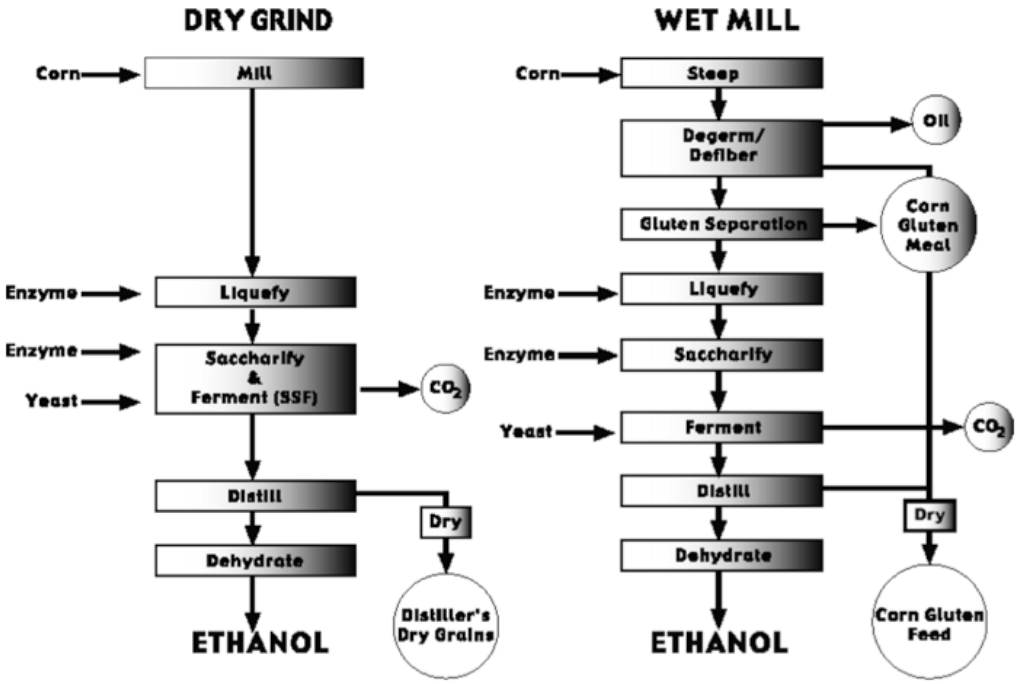

Figure 5: Ethanol production from corn (Bothast & Schlicher, 2005)

2.2.2. Starch hydrolyzing enzymes

Amylases are enzymes that hydrolyze starch. They are present in all organisms, play an important role in carbohydrate breakdown, and vary in activity from species to species. Hence, amylases from a particular source are chosen industrially based on the specific application that the amylase will be used for (Sivaramakrishnan, et al., 2006). Most amylases used for hydrolysis come from fungus and bacteria because of cost effectiveness and relative ease of production from these sources.

Alpha-amylase enzyme cleaves inner α-1-4 glycosidic bonds of the starch molecule, breaking it into smaller starch fragments called dextrin. The major end products of alpha-amylase are glucose, maltose, maltotriose, maltotetraose, maltopentaose, and maltohexaose (Nigam & Singh, 2011). Alpha-amylase produced from bacterial sources including *B. subtilis*, *B. licheniformis,* and *B. amyloliquefaciens* are commonly used in industry because of their thermostability (Sivaramakrishnan, et al., 2006) . Optimum alpha-amylase activity occurs at temperatures between 70-90 ^{o}C, and pH of 6-7.

The second major enzyme used industrially is glucoamylase enzyme, which attacks external α,1-4 and α,1-6 linked glucose units of amylose and amylopectin, respectively, producing single glucose units. Glucoamylases used commercially are generally extracted from fungal strains *Aspergillus niger* or *Rhizopus sp*. (James & Lee, 1997). The molecular mass of fungal glucoamylases ranges between 27-112 kDa. For most glucoamylases, the optimum range of pH is 4.5-5.5, while the optimum temperature is between 40-60 ^{o}C.

2.2.3. Technologies to improve starch hydrolysis efficiency

Efforts to improve the efficiency of the starch conversion generally fall into three categories:

- Input improvements: corn hybrids for higher ethanol yield
- Process or equipment improvements

- Technologies to improve enzyme performance

Input improvements

Seed companies are working to develop corn hybrids that yield higher levels of ethanol. Hybrids can be separated into two different types: those developed with higher extractable starch and those with higher fermentable constituents called high total fermentables (HTF) corn. The Pioneer seed company reported increases in ethanol of up to 4% with their HTF corn brand (Bothast & Schlicher, 2005). Several challenges exist for widespread commercialization of corn hybrid technology. Corn hybrids with higher starch or fermentable content would mean lower yields of other potentially valuable side products. The cost of corn hybrids must be comparable to that of regular corn (Rendleman & Shapouri, 2007).

Process and equipment Improvements

There are several ongoing areas of experimental research to improve process efficiency, a few of which are highlighted below. One potential technology being explored is the replacement of the traditional batch reactor used in starch saccharification by the continuous membrane reactor (Sarbatly & England, 2004). In this reactor, glucose is produced and extracted continuously. Hindrances to the commercialization of this technology include accumulation of high molecular mass oligosaccharides, and inactivation of enzymes.

Montalbo-Lomboy investigated the feasibility of replacing the jet cooking step with ultrasonification for solubilization of the granules (Montalbo-Lomboy, 2008).

Comparing jet cooking to ultrasonification pretreatment, they found only minor differences in ethanol conversion, yet energy needs for ultrasonification were lower than that for jet cooking. In order for ultrasonification to be economically feasible, savings from reduced energy costs would have to outweigh the higher capital cost of the ultrasonification installation. Other techniques are focused on improving separation technologies for better product recovery (Taylor, et al., 2001).

Enzyme improvements

Of the various areas being investigated, improvements in enzyme have great promise in the short term. Improving the performance of hydrolyzing enzymes is of interest, as the enzymes would provide immediate economic benefits without large adjustments to the process. One way to achieve this is to screen for enzymes with inherently higher activity and stability. Other methods include adding stabilizing agents, chemical modifications, enzyme immobilization, and protein engineering (Sivaramakrishnan, et al., 2006).

Most commercial enzymes used today are not capable of hydrolyzing raw ungelatinized starch granules. However raw starch hydrolysis would eliminate viscosity issues, and reduce energy costs associated with high temperature processing. As a result, amylases that can digest raw starch have been investigated. Iefuji et al compared the raw starch digesting ability of a thermostable alpha-amylase from the yeast *Cryptococcus sp. S-2 and* Taka amylase (Iefuji et al., 1996). Alpha-Amylase from *Cryptococcus sp. S-2* exhibited

a strong activity towards raw potato starch but weaker activity for wheat, corn, rice and sweet potato starches. Low temperature processing would mean that both liquefaction and saccharification could be combined, and simultaneous use of alpha-amylase and glucoamylase would be possible. More than 80 naturally occurring raw starch digesting enzymes have been reported (Robertson, et al., 2006). Raw starch hydrolyzing enzymes present many challenges, including the requirement of limited substrate processing capability, higher enzyme loading requirements, and slower rates of conversion. Raw starch digesting enzymes would reduce energy costs, but would reduce process efficiency as compared to traditional methods.

Enzyme engineering and immobilization

One way to improve enzyme performance is to engineer enzymes with the desired properties. In recent years, many enzymes have been developed that are more thermostable (Declerck et al., 2003) and active at wider ranges of pH values (Shaw et al., 1999). Another method to improve the activity of the amylases has been to immobilize the enzymes during processing. The catalytic activity of enzymes is dependent on the structure and conformation of the enzyme. Changes to the conformation caused by physical or chemical damages can lower the activity and performance of the enzymes. Thus, protection of the enzyme can result in higher overall stability and activity. Many different materials and techniques have been used to immobilize alpha-amylase (Gangadhara et al., 2009; Lim et al., 2003), but most agents are polymer based. Retained activity of as much as 90% activity for up to 20 hydrolysis cycles have been reported using

calcium-alginate gel capsules as the immobilizing agent (Sivaramakrishnan, et al., 2006). Though immobilization increases the life of the enzyme, the overall enzyme activity often suffers (Khalil et al., 2001).

Activating and stabilizing additives

It has been documented that cations Ca^{2+}, Na+, K+, NH4+ and bovine serum albumin have thermostabilizing effects on alpha-amylase (Sivaramakrishnan, et al., 2006). Polyols (ethylene glycol, propenediols and glycerol), dimethylformamide and dimethyl sulfoxide increased the half-life of *B. stearothermophilus* alpha-amylase twofold. These compounds stabilized the enzyme against thermal denaturation through ionic interactions (Brumm & Teague, 1989).

Recently several investigators have reported on the enzyme stabilizing effect of cationic polyelectrolytes on lactate dehydrogenase, alcohol dehydrogenase, and glucose dehydrogenase (Hatti-Kaul & Andersson, 1999; Khalil, et al., 2001; Nishibue et al., 1996). In these studies, electrostatic interactions played a prominent role in the stabilization of the enzyme.

Little work has been done on polymer-starch hydrolyzing enzyme systems. In a study by Yoon et al, ten non-ionic polymer additives including seven polyethylene glycols (PEGS) of varying molecular weight, two polyvinyl alcohols (PVA) of varying molecular weight, and a polyethylene containing material Triton X-100 were tested for their ability to activate and stabilize alpha amylase from *B. amyloliquefaciens* and *B. lichenformis* (Yoon & Robyt, 2005). The effect of

additive concentration, order of addition and reaction time were studied at 25 ^{o}C. Each additive was found to stabilize and increase the activity of the amylase. They postulated that the additives bind to the proteins to create a single tertiary structure resulting in maximum enzyme activity. The experiments were carried out at room temperature in dilute concentrations, conditions not used in industrial starch liquefaction and saccharification. The ability of these polymers to enhance activity under typical starch converting conditions was not studied.

As mentioned in the previous studies, polymers (Yoon 2005) and electrolyte cations such as Ca^{2+} (Sivaramakrishnan, et al., 2006), have both been shown to enhance the performance of alpha-amylase. It follows that polyelectrolytes should yield positive effects on the performance of alpha-amylase, yet little work has been done on polyelectrolyte enhanced starch hydrolysis systems. Preliminary results show an increased rate of conversion in the presence of the polyelectrolyte, cationic polyacrylamide (C-PAM) for both cellulase and alpha-amylase (Reye, et al., 2009). Further understanding of the polyelectrolyte behavior is crucial to understanding polyelectrolyte enhanced hydrolysis of starch.

2.3. Polyelectrolytes

Polyelectrolytes are water-soluble polymers that carry a charge along the polymer backbone. They are used in a wide range of industries including the water treatment, oil recovery, mineral processing and paper industries (Bratby, 1980). Their main use is to promote flocculation of colloidal suspensions for the

purpose of solid-liquid phase separation. Polyelectrolyte flocculants can be anionic, or cationic. Common flocculants include:

- Anionic: hydrolyzed polyacrylamide; polyacrylic acid (PAA); polyvinyl sulfate;
- Cationic: poly(dimethylammonium chloride), (PDADMAC); cationic polyacrylamide (C-PAM); polyethylene imine (PEI)

Polyacrylamide-based polyelectrolytes are commonly used in industry as they are easily synthesized (Figure 6). Propylene is first converted to acrylonitrile, which is then converted to acrylamide. The acrylamide monomers can then be polymerized into polyacrylamide.

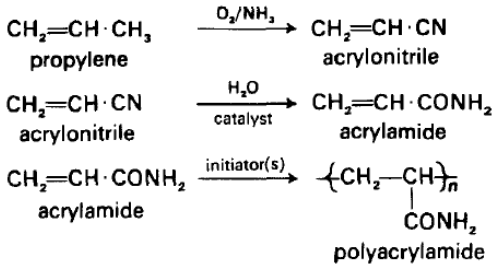

Figure 6: Polyacrylamide synthesis from propylene

Polyacrylamide alone is not a polyelectrolyte because it bears no charge and must be further chemically altered to create the charged polymer. Anionic polyacrylamides can be hydrolyzed in the presence of NaOH to produce a co-polymer of acrylamide and acrylate (Figure 7), or co-polymerized with an anionic monomer such as sodium acrylate, as shown in Figure 8 (Bratby, 1980).

In a similar manner, cationic polyacrylamides are prepared by co-polymerization of acrylamide with a various cationic monomers. Typical co-monomers are shown in Figure 9 (Mortimer, 1991).

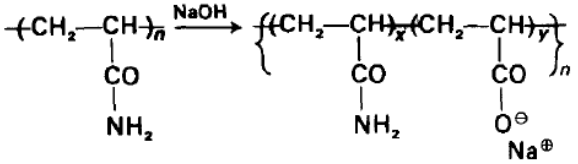

Figure 7: Synthesis of an anionic polyacrylamide via hydrolysis

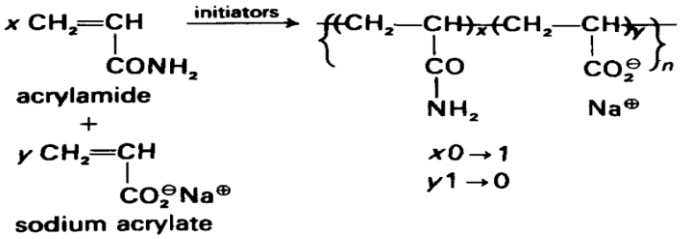

Figure 8: Synthesis of an anionic polyacrylamide via co-polymerization

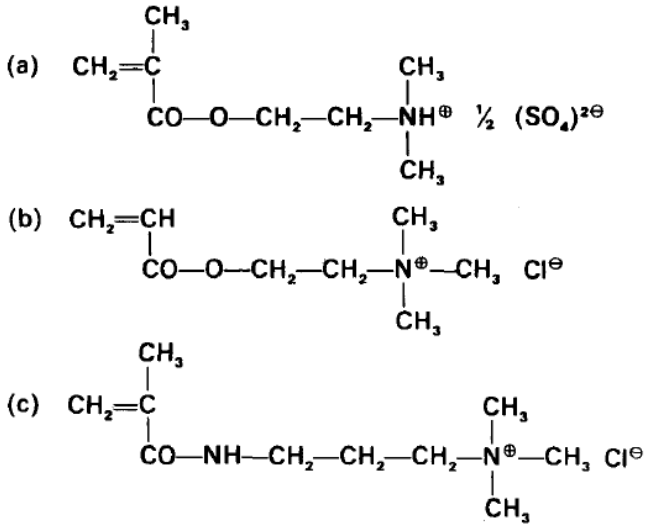

Figure 9: Typical cationic co-monomers for acrylamide.
(a) Dimethyl amino ethyl methacrylate, sulphate salt (DMAEMA sulphate);
(b) acryloyloxethyl-trimethyl ammonium chloride (AETAC);
(c) methacrylamido proyl trimethyl ammonium chloride (MAPTAC)

The most important properties of polyelectrolytes are their molecular weight and charge density. Typical molecular weights of C-PAM are on the order of 4-6 million g/mol (Hubbe et al., 2009). Polymers adopt a random coil configuration in solution, although because of intra-molecular repulsion, polyelectrolytes typically have a larger effective size than their nonionic polymer counterparts. Polyelectrolyte size is largely dependent on ionic strength. At high ionic strength, the charge on the polyelectrolyte is screened, thereby lowering repulsion. As a result, the polymer will adopt a more coiled configuration.

Charge density, the measure of ionization per polymer chain, is also an important factor in the effectiveness of a polyelectrolyte. For those polymers created by hydrolysis, the higher the degree of hydrolysis, the higher the charge density. Charge density can be expressed as mole % ionization or meq/g.

2.3.1. Polyelectrolyte destabilization

Polyelectrolytes are primarily used for solid-liquid phase separation. Most particles suspended in an aqueous solution have a net negative charge due to ionization of groups on the particle surface. The “like” negative charge causes particles in solution to repel each other, thereby causing the particles to stabilize and remain suspended in solution (Mortimer, 1991). Polyelectrolytes are used to destabilize the colloidal particles by overcoming the repulsive forces between suspended particles. When they are added to an aqueous solution, several processes are initiated. The key steps in polyelectrolyte destabilization are outlined in Figure 10 and include the following:

(i) mixing of suspension for even dispersal of polymer among the particles

(ii) adsorption of polymer chains onto particles

(iii) compression and relaxation of polymers on particle surfaces

(iv) flocculation of polymer adsorbed particles via bridging or charge patching

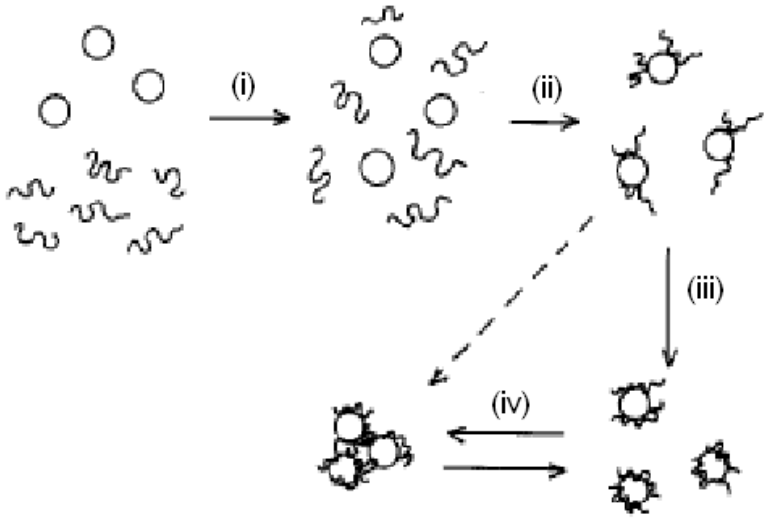

Figure 10: Key steps in polymer induced particle destabilization: (i) Mixing (ii) Polymer Adsorption (iii) Polymer relaxation (iv) Flocculation (John, 1988)

(i) Mixing

Because of the high molecular weight of polyelectrolytes, their diffusion is slow. For that reason, adequate mixing is needed to evenly disperse polyelectrolyte throughout the suspension. Generally, increasing the intensity of mixing increases the efficiency of the destabilization process (John, 1988).

(ii) Polymer Adsorption

The effectiveness of a polyelectrolyte in destabilizing a colloidal suspension is largely dependent on the ability of the polymer to adsorb onto the surface of a suspended particle. A widely accepted model of polymer adsorption is depicted in Figure 11 (Napper, 1983). Polymers can adsorb to several different surfaces at one time, or adsorb to a single particle surface at several segments on the polymer. Attachments on the particle surface are called trains. Once attached, the polymers extend into the solution via polymer tails and loops.

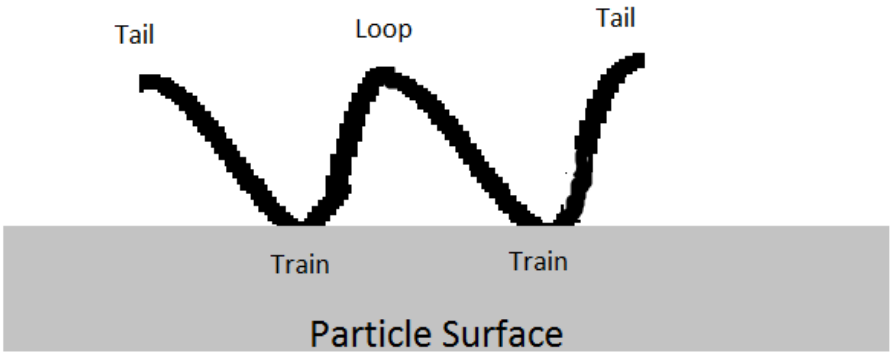

Figure 11: Adsorbed polymer chain

Polymer adsorption is a generally irreversible process due to the high affinity of polymers for substrate surfaces (Smith-Palmer & Pelton, 2002). Once attached, the chances of all attached segments of an adsorbed polymer detaching at once are low. The extent of polymer adsorption and polymer conformation is largely driven by electrostatic and ionic interactions as detailed below.

Absorption Affinity

The affinity of a polyelectrolyte towards a surface will be high when the charge of the surface and polyelectrolyte are the opposite of each other due to electrostatic interactions. The higher the polyelectrolyte charge, the greater the polymer-surface attraction, which results in a significantly flatter polymer configuration on the particle surface, as illustrated in Figure 12. Decreasing the charge density of a polyelectrolyte reduces the intra-molecular repulsion felt by the polymer, and higher amounts of polymer are able to adsorb on the surface in thicker adsorbed layers (Claesson et al., 2005).

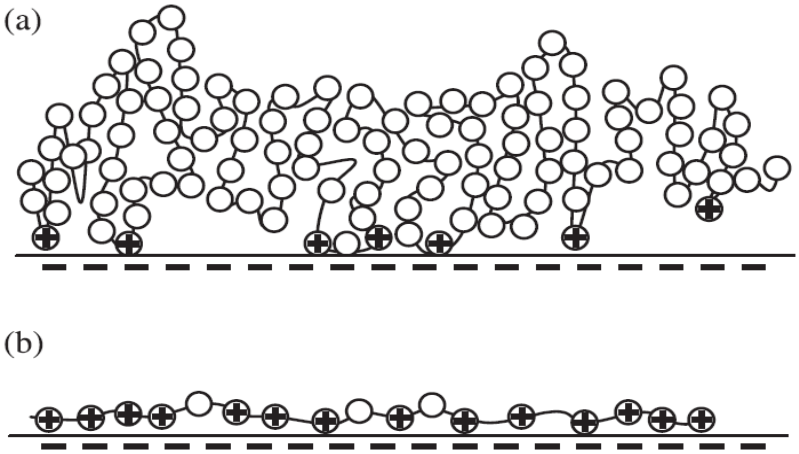

Figure 12: Effect of charge density on oppositely charged surfaces. (a) low charge density (b) high charge density (Claesson, et al., 2005)

Salt concentration also significantly affects electrostatic polymer-particle interactions. Polyelectrolytes have an extended confirmation in low salt concentrations due to intra-molecular repulsions of “like” charged constituents on the polymer. When a salt such as NaCl is added to a solution, the oppositely

charged electrolytes begin to neutralize or screen the charge on the polyelectrolyte, reducing their intra-molecular repulsion. As a result, the polymers assume increasingly coiled confirmations at high salt concentration. These salt induced conformational changes lead to lower directly bound polymer segments and thicker layers of adsorbed polymer. The adsorbed amount of polymer may increase or decrease with higher salt concentration depending on the non-electrostatic polymer to surface affinity (Claesson, et al., 2005). In some cases, the amount of polymer adsorbed first increases, then decreases with increasing salt concentration (Solberg & Wagberg, 2003; Sukhishvili & Granick, 1998). The initial increase is due to reduced intra-molecular repulsion which allows more polymers to adsorb to the surface. Adsorption weakens at higher salt concentration due to competition with smaller ions for surface sites, lowering polymer-surface affinity.

Polyelectrolytes only adsorb to surfaces of the same charge if the non-electrostatic affinity is high enough to overcome repulsion. In these cases a certain salt concentration is usually needed to promote polymer adsorption. Salts with divalent cations have been found to be quite effective in facilitating polyelectrolyte adsorption (Berg et al., 1993; Claesson, et al., 2005)

Adsorption Kinetics

Since it is reasonable to assume that every collision will lead to attachment of one or more polymer segments to a particle in the initial stages of adsorption,

estimates of the adsorption rate can be made in terms of the collision rate (John, 1988):

$$-\frac{dn_2}{dt} = k_{ads} n_1 n_2 \quad (1)$$

Where $-\frac{dn_2}{dt}$ is the rate of disappearance of polymer in solution due to adsorption, k_{ads} is the adsorption rate coefficient, and n_1 and n_2 are the number concentrations of the particle and polymer, respectively. Initial rates of adsorption will be high, followed by a much slower rate due to fewer sites being available for adsorption.

The adsorption rate coefficient depends on a number of factors including the size of polymer and particle, and degree of agitation (Hogg, 1999). In unstirred solutions, the rate of collision frequency will be governed by "Brownian" motion, the random movement of particles due to thermal energy. Assuming particles behave as spherical molecules, the adsorption rate coefficient for Brownian diffusion can be estimated by the Smoluchowski expression:

$$k_{ads} = \frac{2kT}{3\eta}\frac{(R_1+R_2)^2}{R_1 R_2} \quad (2)$$

When particle collision is induced by agitation, the Smoluchowski equation is:

$$k_{ads} = \frac{4}{3} G(R_1 + R_2)^3 \quad (3)$$

Where k is the Boltzmann constant, T the absolute temperature, the viscosity, G shear rate, and R_1 and R_2 the effective radii of the particle and polymer (John, 1988). For most practical applications, polymer is added under shear conditions and the latter equation is more suitable. For these cases, the rate of collision is expected to increase strongly with increasing size of the suspended molecules and increasing rates of hydrodynamic shear.

(iii) Adsorbed Polymer Compression

Once a polymer adsorbs onto the surface of a particle, it will undergo a change in conformation in which the polymer chain will begin to relax and lie flat onto the surface. Consequently, the final adsorbed layer will be much thinner than the initial polymer. Enarsson and Wagberg (Enarsson & Wagberg, 2008) found that the adsorption of C-PAM molecules in solution with a hydrodynamic diameter of 100 nm formed layers of thickness of only about 10 nm. The rate of relaxation was too fast to measure, but was estimated to be on the order of seconds.

The relaxation rate greatly depends on the rate of adsorption and total amount of polymer adsorbed. When the amount of polymer adsorbed is high, there is limited opportunity for the polymer to relax. It follows that at high rate of adsorption brought about by high polymer concentration or agitation, polymer relaxation will be hindered (De Witt & Van de Ven, 1992; Van De Ven, 1994). At low rates of adsorption, polymers will have more time to achieve a flatter confirmation, resulting in less adsorption of polymer.

2.3.2. Polyelectrolyte flocculation

Adsorbed polymer will cause the particles to destabilize and form aggregates (flocs) via flocculation. There are two main mechanisms through which flocculation occur:

a) Polymer Bridging

b) Patched Charge adsorption

Polymer Bridging

When adsorbed polymer chains contain loops and trains that extend out into solution, those segments will entangle with other particles, forming a “bridge” between adjoining particles (Figure 13). The basic principles of the bridging mechanism are well established (Bratby, 1980; John, 1988). In order for bridging to occur, there must be a balance between the amount of adsorbed polymer and the number of unoccupied surface sites available for polymer attachment. Thus there is an optimum dosage of polymer that will give maximum flocculation. At surface coverage above this level flocculation will be hindered, as there will not be enough surface sites available for polymers to attach and form bridges. In addition if too high a level of polymer is adsorbed, particles will begin to undergo a charge reversal, causing the particles to re-stabilize back into solution. La Mer postulated that optimum flocculation occurs when the fraction of surface covered by polyelectrolyte is 0.5 (La Mer, 1966). However, surface coverage is greatly dependent on other factors such as the conformation of adsorbed polymer and the rate of adsorption. For this reason, many studies have observed optimum flocculation at surface coverage of much less (John, 1973).

Bridging flocculation is often possible in systems where polyelectrolyte and particles bear the same charge. In such cases, adsorption and subsequent flocculation is induced by ionic salts in solution (O'Gorman & Kitchener, 1974).

Effective bridging occurs when polymer loops and trains extend out enough into solution to overcome intra-molecular repulsion. The more a polymer train or loop extends into solution, the more effective the bridging capability. Polymer extension is largely a function of charge density, ionic strength, and molecular weight, as these factors influence polymer conformation in solution. High charge density polymers repel from surfaces of the same charge, but exhibit strong intra-molecular repulsion resulting in extended confirmations ideal for bridging. Thus, an optimum charge density would be the balance of these competing effects. Michaels found an optimum degree of hydrolysis (charge density) for polyacrylamides to be about 30% (Michaels, 1954). Ionic strength indirectly affects bridging by influencing charge density effects. A great deal of experimental work has shown that better flocculation occurs with linear polymers of higher molecular weight (Shatat et al., 2008) because of the ability of these chains to form bridging loops that extend further out into solution.

Charge Patch

In the charge patch mechanism (Figure 13)**,** polyelectrolytes destabilize particles by adsorbing onto the surface of oppositely charged particles, thus reducing the net surface charge of the particles. In the charge patch mechanism,

polyelectrolytes are almost completely adsorbed onto the surface in a flat conformation due to strong electrostatic attraction (Claesson, et al., 2005). Polyelectrolytes adsorb in highly charged “patches” of opposite charge on the surface, and flocculation is initiated due to decreased particle repulsion. Because electrostatic attractions drive this mechanism, charge density has been found to be more of an important factor than molecular weight. Polyelectrolyte surface patching has been observed by atomic force microscopy (Pfau et al., 1999).

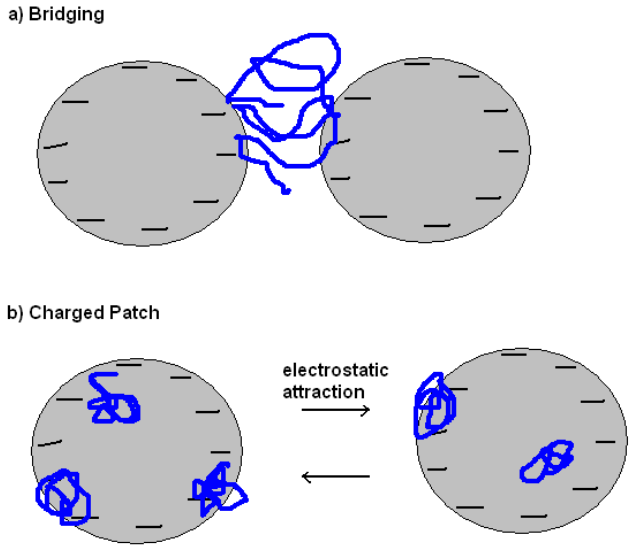

Figure 13: Schematic of flocculation via (a) bridging and (b) charge patching.

In some cases, the bridging and charge patch mechanisms operate in conjunction with each other, while in other cases one mechanism will dominate the other. Adsorbed polymer conformation also plays a role in determining which mechanism is dominant. If adsorbed polymers are allowed enough time to relax on the particle surface, electrostatic patch effects will dominate. If not enough

time is given, or if polymer adsorption is too high to allow for equilibrium to be reached, bridging will be the dominant mechanism (Gregory & Barany, 2011).

2.4. ***Polyelectrolyte Enhanced Hydrolysis***

As mentioned above, polyelectrolytes have been shown to enhance the rate of hydrolysis of both fiber and cornstarch. Though little work has been done on polyelectrolyte enhanced hydrolysis of cornstarch, considerable work has been done to investigate the polyelectrolyte-enhanced fiber hydrolysis mechanism (Mora et al., 2011; Reye, Lu, et al., 2011; Reye, Maxwell, et al., 2011; Reye, et al., 2009). Commercial cationic polyacrylamides (C-PAM) were first screened for their effect on the performance of amylase on corn starch and cellulose on fiber (Reye, et al., 2009). C-PAMs varying in charge, molecular weight, and the degree of branching were used. The intent of the screening was to identify polymer properties that most significantly affected hydrolysis. Several members of the C-PAM family were effective in enhancing the hydrolysis of both the cornstarch and fiber to varying degrees. As a result, it was concluded that the effect of C-PAM is non-specific because it boosted the performance of two different systems.

A typical effect of C-PAM on the alpha-amylase-induced hydrolysis of cornstarch at 50 ^{o}C is shown in Figure 14. The rate of glucose generation increased with increasing C-PAM concentration up to 100 mg/l, but a higher polymer dose of 1,000 mg/l inhibited the rate. Analogously, bleached hardwood fiber was hydrolyzed by 1 g cellulase (Optimase CX 40L)/l with and without C-PAM. The

enzyme formulation contained three components: endoglucanase, which cuts the fiber into smaller strands, exoglucanase, which hydrolyzes the strands to cellobiose, and β-glucosidase, which converts the cellobiose to glucose. The C-PAM was added at a concentration of 1000 mg/l (38% active ingredient). Here, dissolved Total Organic Carbon (TOC) generated from the breakdown of fiber was measured. The rise in TOC was much more pronounced in the presence of C-PAM. The C-PAM also accelerated the rate of fiber length reduction. Though the effect was small, it demonstrated that the C-PAM affects more than one enzyme present in the cellulase preparation. C-PAM did not break down the fiber in the absence of the enzyme.

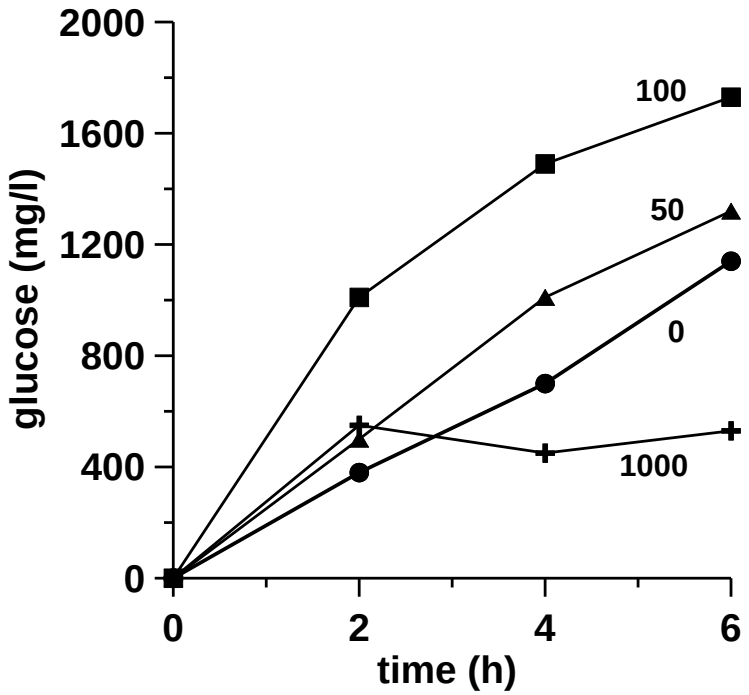

Figure 14: Effect of a C-PAM on hydrolysis. The values in the plot represent C-PAM concentration in mg/l

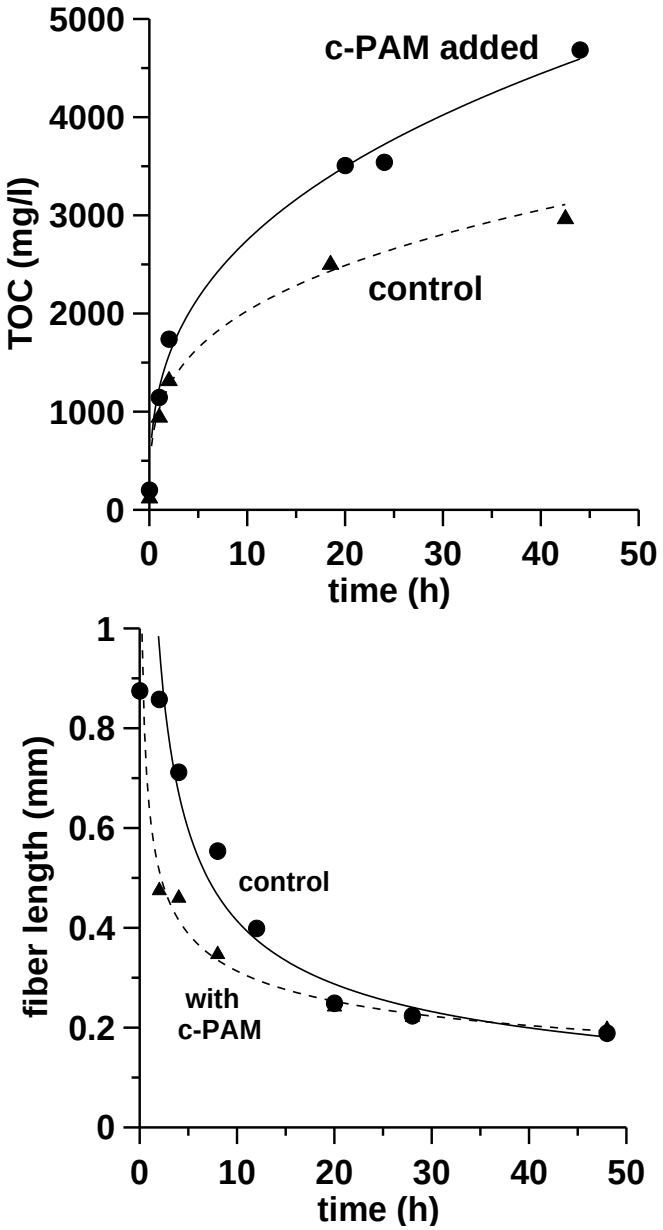

Figure 15: Effect of C-PAM on hydrolysis of 1g/l cellulase on bleached hardwood fiber (top) and effect of C-PAM on the change in fiber length during hydrolysis (bottom)

2.4.1. Polyelectrolyte effect on enzyme-fiber binding

The binding of cellulase to fiber was also measured with and without C-PAM. The fiber was formed into handsheets, one set of which was treated with 200 mg/l C-PAM solution for 30 minutes. A second set was exposed to the same volume of water for the same period. The handsheets were dried at room

temperature and soaked in 1-5 g/l cellulase at 4 ^{o}C for 20 minutes. The protein content of the enzyme remaining in the supernatant was determined and the amount of enzyme bound to the sheet determined by the difference. As shown in Figure 16, the polymer increased the binding of enzyme to fiber. Therefore it was concluded that enhancement of fiber hydrolysis is due to the increased binding of the enzyme induced by the C-PAM.

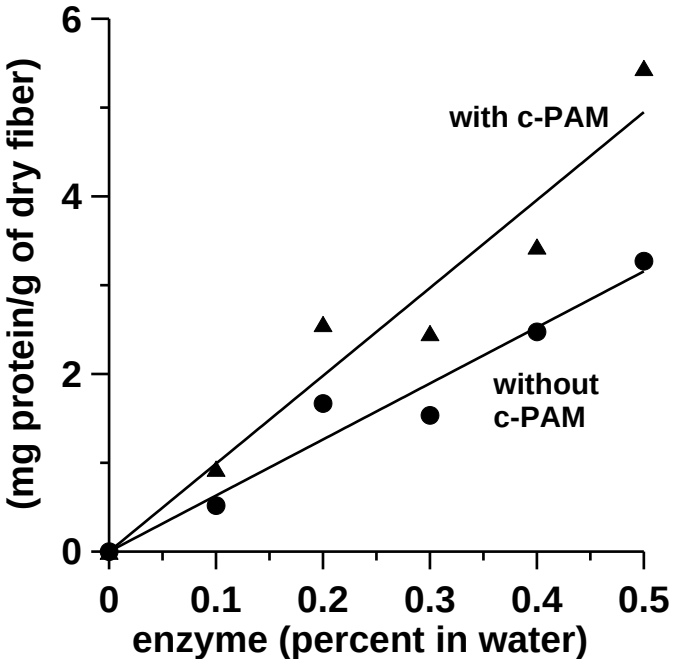

Figure 16: Effect of 1000 mg/l C-PAM on the binding of cellulase (volume of stock enzyme solution to volume of water) to bleached softwood kraft fiber

To further understand the role of binding in the C-PAM enhanced fiber hydrolysis, the effect of C-PAM on cellulase enzyme activity was studied (Reye, Maxwell, et al., 2011). The association of cellulase enzyme with polymer was determined first, followed by association of polymer to fiber. Equilibrium constants for the sorption of cellulase on C-PAM-treated fiber dispersed in water were then calculated. The C-PAM almost completely attached to the fiber under the

conditions used (Reye 2010) indicating that the enzyme binds similarly to either free or bound C-PAM, i.e. the fiber does not interfere with the association of C-PAM and enzyme. The C-PAM increases binding by 50-100%, which is also the amount by which the rate of hydrolysis is increased by the C-PAM. A comparison of changes in binding to that of the rate of glucose generation was only qualitative because different conditions (temperature, enzyme loading) were used for binding and hydrolysis. Reye et al (Reye, Maxwell, et al., 2011) postulated that the increased enzyme binding induced by the C-PAM can account for the hydrolysis rate increase observed. C-PAMs are known to agglomerate solids through a patching mechanism (charge neutralization). It was proposed that when C-PAM is added, it neutralizes a section of the fiber surface. Because the enzyme and fiber are both negatively charged, neutralization of the fiber charge by the C-PAM would remove the repulsive charge barrier between enzyme and fiber that would otherwise exist and a faster rate would result.

The relative affinity of enzyme for fiber in the absence and presence of C-PAM was expressed as dimensionless partition coefficients ($K_{f/w}$), which is the ratio of enzyme associated with the fiber to that present in an equal weight of solution (Mora, et al., 2011). Results are illustrated in Figure 17. Without polymer, $K_{f/w}$ remained constant as a function of enzyme concentration, i.e. a Langmuir isotherm is followed. In the presence of C-PAM, a Freundlich isotherm (n = 1.7, r^2 = 0.992) was obtained. As discussed previously, C-PAM primarily promotes attack on the amorphous region. Consequently, the shift in adsorption was

attributed to binding of C-PAM to the amorphous regions of the fiber.

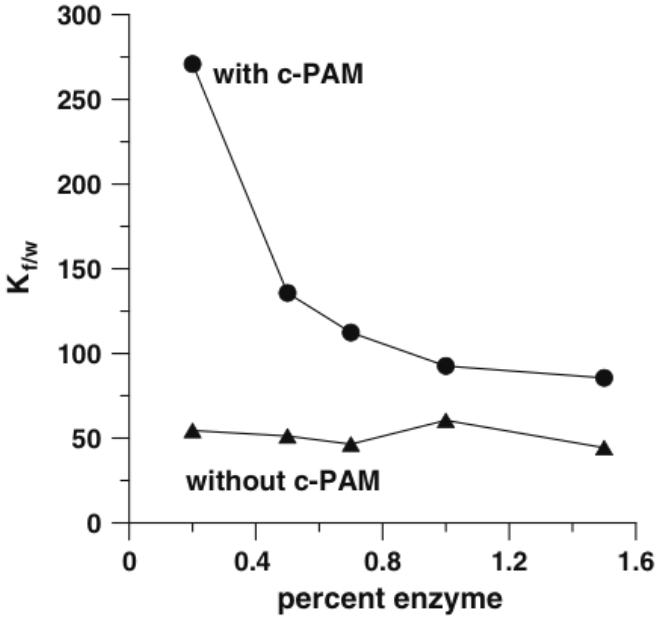

Figure 17: Fiber:water partition coefficient of cellulase on 2% softwood fiber in water at 4 ^{o}C. Circles represent measurements where 1 g of fiber was treated with 0.1 g C-PAM in 100 mL. of water (Mora, et al., 2011)

2.4.2. Polyelectrolyte property and process condition effects

The mechanism was further explored by studying enzyme attack, effect of agitation, C-PAM addition, and C-PAM charge (Reye, Lu, et al., 2011). The commercial cellulase used in the initial experiments contained three groups of enzymes. The endoglucanases attack and fragment the fiber. Exoglucanases then work on the fiber and fiber fragments, releasing cellobiose units, which are then rapidly converted to glucose by cellobiase. The kinked (amorphous) regions of the fiber are especially vulnerable to attack by endoglucanase. Therefore to understand the effect of C-PAM on the action of endoglucanase, changes in kink angle and fiber length were studied. The addition of C-PAM led to a faster drop

in kink angle, indicating that the C-PAM increased the rate of endoglucanase enzyme. The effect on C-PAM on exogluconases was not explored in the study.

The effect of agitation was then explored. Shaking was ineffective as an agitation method as the level of agitation was not high enough to stop floc formation. Floc formation reduces the surface area accessible to the enzyme and would therefore offset the rate enhancing effect of C-PAM. Agitation by stirring proved most effective. Enhancement of C-PAM mediated fiber hydrolysis was shown to exhibit an optimum level of agitation. The initial increase in rate can be attributed to inhibition of floc formation by increased agitation. At levels beyond the peak rate, shear forces damage the enzyme, decreasing the rate of hydrolysis.

The effect of the point of C-PAM addition was examined by adding C-PAM at different periods during fiber hydrolysis, ranging from the start of hydrolysis (time 0), through after 6 hours of hydrolysis. It was found that the best results are obtained when C-PAM was added after four hours. Any further delay decreased the benefit because hydrolysis had substantially advanced and floc formation was no longer a significant factor. As short fibers do not floc easily, delaying the addition of C-PAM takes advantage of its rate enhancing ability without the inhibition by flocculation.

Three polymers of varying mol% cationicity were added during fiber hydrolysis to study the effect of C-PAM charge. There was no significant difference in the rate of hydrolysis as a function of the three polymers used, indicating that the rate of fiber hydrolysis is generally independent of the C-PAM charge.

For fiber hydrolysis, some overall conclusions were reached: C-PAM primarily enhanced the performance of the endogluconase enzyme by associating the enzyme to the amorphous region of the fiber. Enzyme binding to fiber alone followed a Langmuir isotherm. On the other hand, in the presence of C-PAM, binding of the enzyme followed a Freundlich isotherm and increased the amount of binding (Mora, et al., 2011; Reye, Maxwell, et al., 2011). It was proposed that the polymer mainly operated via a “patching” flocculation mechanism which reduced fiber-enzyme repulsion, thereby promoting enzyme binding and hydrolysis (Reye, Lu, et al., 2011).

CHAPTER 3: Materials and Methods

3.1. Introduction

Chapter 3 describes experimental techniques and procedures used throughout the thesis work. This includes explanations of methods for characterization of enzymes, polyelectrolytes, and substrate, and the study of how these constituents interact with each other. Experiments are divided into three groups: starch-C-PAM interaction experiments, enzyme-CPAM interaction experiments, and C-PAM-added starch hydrolysis experiments.

3.2. Materials

3.2.1. Starch

Unmodified regular cornstarch (73% amylopectin and 27% amylose) obtained from Sigma-Aldrich (S4126), St. Louis, Mo was used in all experiments unless otherwise specified. The moisture content of the starch at room temperature was $10 \pm 1\%$ (db, 120 ^{o}C, 24h, 3 replications). High amylose cornstarch (70% amylose) and unmodified waxy cornstarch (<1% amylose) purchased from Sigma-Aldrich (S4180 and S9679, respectively) were also used in experiments to determine the effect of amylopectin/amylose ratio on C-PAM aided processing.

Starch samples came in a dry white powder form. Basic size characterization of cornstarch granules was conducted using light scattering as measured by a Malvern Droplet Particle Size Analyzer Series 2600 based on the principles of laser light diffraction. The setup contains a particle suspension unit, which

provides a uniform liquid suspension and pumps the solution across the path of the detector. At room temperature aqueous solutions of the 0.1 w/v% starch were prepared with distilled water. The suspension unit was run to maintain a homogenous solution, which prevented the starch from settling. Starch solutions were pumped through the flow cell. Particle size distributions were immediately generated. The flow cell and suspension unit were flushed and cleaned out between each starch sampling. The average particle diameter was 15.8±0.4 μm from 5 replications. The average particle size distribution is shown below in Figure 18.

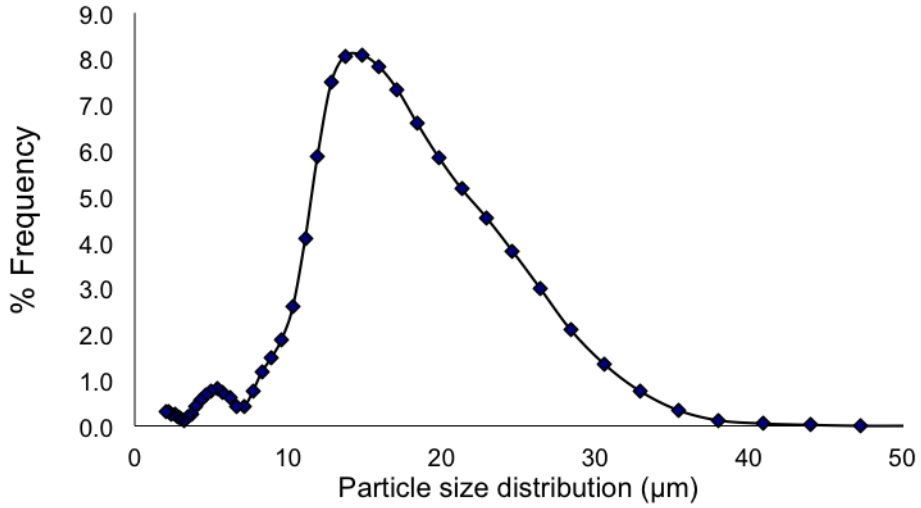

Figure 18: Particle size distribution of regular cornstarch

3.2.2. Enzymes: alpha-amylase and glucoamylase

B. amyloliquefaciens alpha-amylase (BAN 480L) and glucoamylase (NS 22032) obtained from Novozymes (Franklinton, NC) were used in all experiments unless otherwise noted. Protein concentrations of the alpha-amylase and glucoamylase

determined by the BCA protein assay (Thermo Scientific) were 38.0±0.2 mg/ml and 254±1 mg/ml (3 replications), respectively.

3.2.3. C-PAM

The C-PAM used most extensively was XP10025, a 40% cationicity polymer from Eka Chemicals, Marietta, GA. XP10023 (10% cationicity) and XP10033 (80% cationicity) polymers were also used. This series of C-PAM is based on co-polymers of acrylamide and [2-(acryloyloxy)ethyl] trimethylammonium chloride as shown in Figure 19.

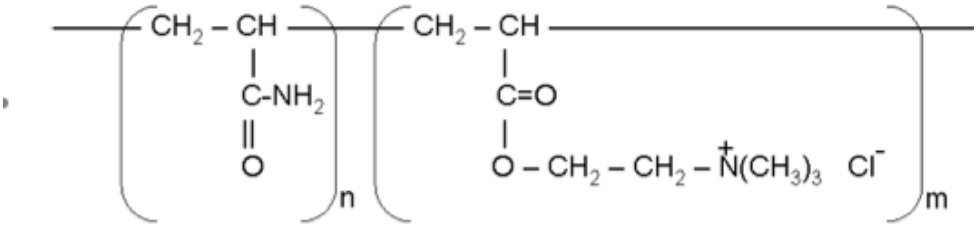

Figure 19: XP series copolymer composition, acrylamide (left) and [2-(acryloyloxy)ethyl] trimethylammonium chloride (right)

A summary of number average molecular weight ranges of these polymers is shown in Figure 20. Raw C-PAM samples came in the form of a dry white granule. For experimentation, C-PAM granules were dissolved in deionized water and agitated by a stirrer for one hour prior to use in any experiment.

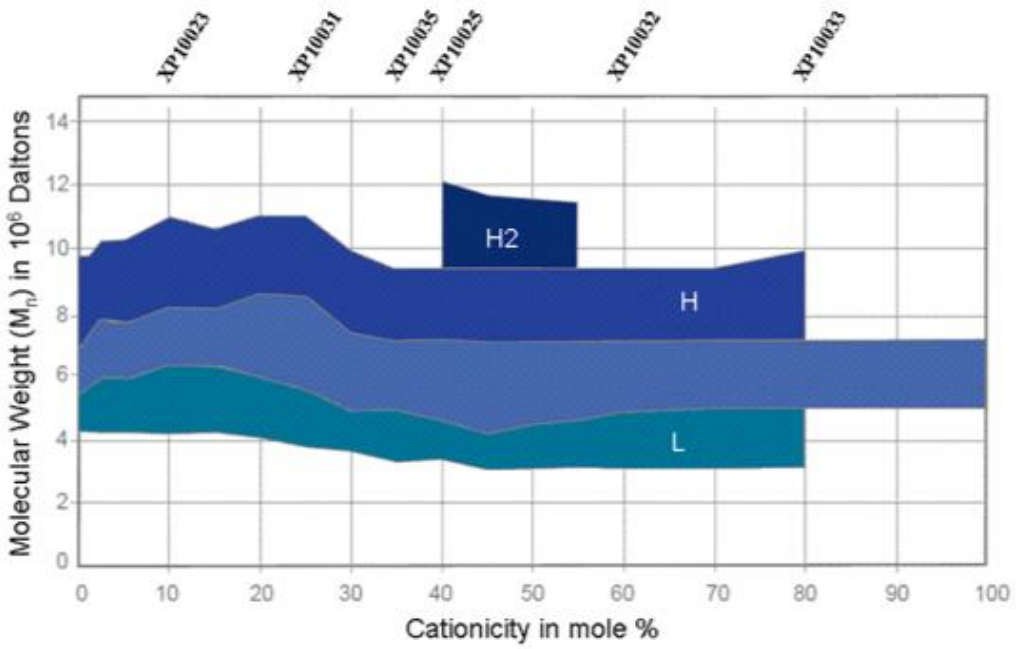

Figure 20: Molecular weight ranges for C-PAM XP series (modified diagram from http://www.snfinc.com/)

Because C-PAM gradually loses charge through hydrolysis (Aksberg & Wagberg, 1989), zeta potential measurements were taken of C-PAM over 24 hours to determine the stability of C-PAM at hydrolysis conditions. C-PAM (100 ppm) in a 0.2 M phosphate buffer solution of pH 6 was heated to 50 ^{o}C. Zeta potential measurements of the samples were taken using a Malvern Zetasizer 3000 instrument. The experiment was repeated at a temperature of 70 ^{o}C. Each experiment was repeated in triplicate. The results, shown in Figure 21, indicate that the polymer is slightly more stable at the lower temperature. While there is some charge loss, the polymer retains most of its charge under typical cornstarch hydrolysis conditions of 1 hour duration at both 50 ^{o}C and 70 ^{o}C.

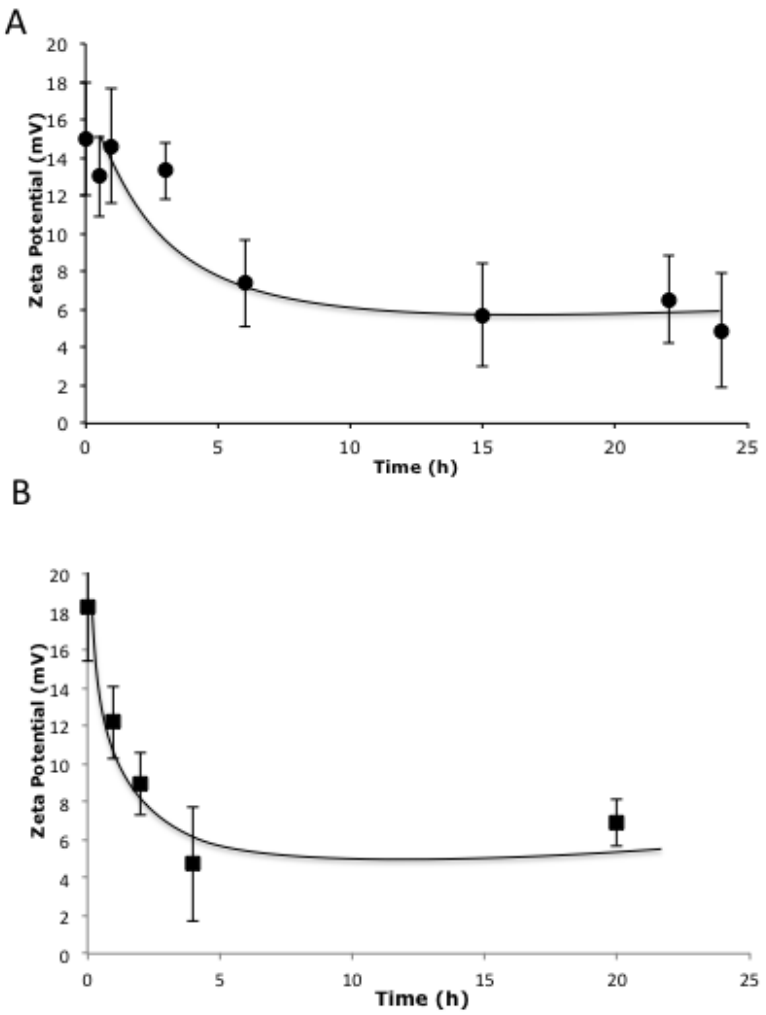

Figure 21: Zeta potential (stability) of 100 ppm C-PAM (40 mol%) at (A) 50 ^{o}C and (B) 70 ^{o}C in a pH 6 phosphate buffer. Each point is an average of eight measurements.

3.3. Starch-C-PAM Interactions

3.3.1. C-PAM adsorption to starch using charge titration

Charge titration is used to evaluate polyelectrolyte adsorption and complexation. The particle charge detector consists of a cylindrical test cell with a fitted displacement piston as shown in Figure 22.

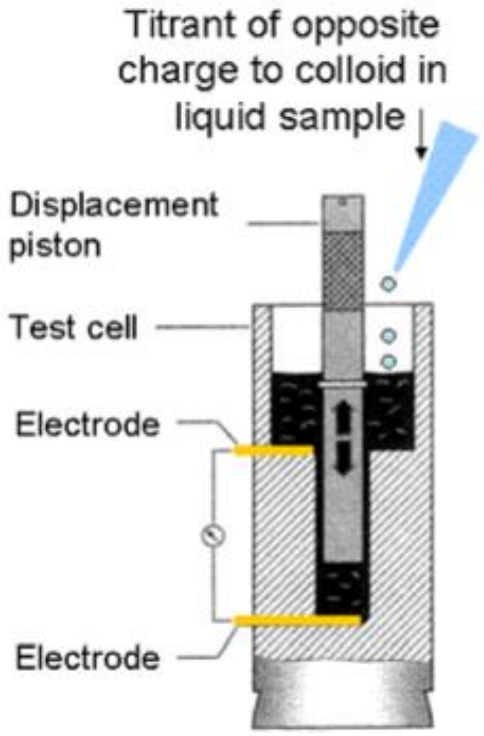

Figure 22: Schematic of charge particle detector

The charge of ions in solution can be measured by streaming current in mV. A streaming current of 0 mV denotes zero charge and neutralization of the sample. To quantitatively measure charge, an oppositely charged polyelectrolyte titrant of known charge density is added to the sample. The titrant is added until the charge of the sample is neutralized and the charge of the sample can be calculated from the amount of titrant needed to neutralize the sample according to the following equation:

$$Q = \frac{V \cdot c}{m} \cdot F \qquad (4)$$

where Q is the total charge amount (C/g; 96.5C/g = 1 meq/g), V the volume of

titrant consumed (L), c the titrant concentration (mole/L, 0.001N), m the amount of active substance in the sample (grams), and F is Faraday's constant (96,485 C/mole). The detection limit of the charge detector is approximately 1 ppm depending on sample specifications.

The adsorption of C-PAM to starch was measured by the solution depletion method (Guillen et al., 2007; Leloup et al., 1991; Noh & Vogler, 2006) by adding starch at various concentrations to 20 ppm of a c-PAM (40% cationicity). The samples were shaken at 25^{o}C for 30 minutes and centrifuged at 3,000 RCF for 15 min. The supernatant was charge-titrated against PVSK (potassium polyvinyl sulfate) using a MÜTEK PCD-03 particle charge detector from BTG Americas. The amount of C-PAM adsorbed to the starch was determined from the difference in charge between C-PAM alone and that of the starch/c-PAM samples. The dimensionless partition coefficient of the C-PAM, K, was calculated as the ratio of the amount of C-PAM adsorbed to starch to the amount of C-PAM still in the water solution (of equal weight). The analytical uncertainty due to duplicate measurement was 6%.

3.3.2. Effect of C-PAM on starch swelling and solubility

Starch swelling and solubility are critical factors associated with starch gelatinization. Therefore, the effect of C-PAM on swelling and solubility was studied in detail. Swelling measurements were made with 2% starch suspensions containing varying amounts of C-PAM. The samples were heated at different temperatures for 30 minutes and immediately centrifuged for 15 minutes

at 3,000 RCF. The resulting pellet was weighed, dried at 105 °C for 24 hours and reweighed. The swelling power was calculated as the ratio of the mass of the hydrated substrate to that of the dry pellet. The total amount of soluble starch in solution as a function of C-PAM concentration and temperature was determined by measuring the total dissolved organic carbon concentration (DOC) in solution by a Shimadzu TOC-V_{CSH} instrument. The measurement uncertainty was 11%. The swelling of cornstarch particles was also studied using light microscopy to monitor changes in granule particle size as swelling occurred. C-PAM (100 ppm) in a pH 6 phosphate buffer was placed in a bath at 50 or 70 ^{o}C for 30 minutes. After cooling to room temperature, the samples were examined with an Olympus BH-2 microscope at 100x magnification. Photos were taken using a Pixera digital microscope camera. Assuming cornstarch particles granules to be circular in shape, image analysis software (ImageJ) was used to calculate the average diameter and the particle size distribution of the images after converting pixels to μm with reference images of known length. Images of samples with more than 300 granules were used. The results were averaged from three images.

3.3.3. Effect of C-PAM on starch viscosity and gelatinization

To determine the effect of C-PAM on starch during gelatinization, viscosity measurements were taken. A C-PAM solution was prepared at room temperature by dissolving 0.1 g dry wt. in deionized water using a mechanical stirrer. The C-PAM solution was mixed with starch (32 g, dry wt.) so that the final starch concentration was 8 w/v%. Each sample had a total of 400 mL. The mixture was then heated in a Grace Instruments M3500 viscometer from 20 ^{o}C to

90 ^{o}C (2.5 ^{o}C/min) at a shear rate of 400 s^{-1}, and held at those conditions for forty minutes. Viscosity as a function of time and temperature was measured for each starch-C-PAM system. The onset temperature of gelatinization was taken as the temperature at which the change in viscosity over the change in temperature began to significantly increase.

3.4. Enzyme-C-PAM Interactions

3.4.1. Enzyme-C-PAM complex studies using dynamic light scattering and UV-vis spectroscopy

Dynamic light scattering

Dynamic light scattering (DLS), also known as photon correlation spectroscopy (PCS) or quasi-elastic light scattering (QELS), is a technique that can be used to determine the size distribution of particles in solution. DLS is commonly used to study polymer-protein interactions in solution.

In this technique, light is emitted through a solution of particles and can be monitored by a light detector in the instrument. Before reaching the detector, the light is scattered by the particles in solution undergoing diffusive Brownian motion. The distance that the scattered waves travel to the detector varies as a function of time and these fluctuations in time can be correlated to the translational diffusion coefficient of the particles in solution. Using the Stokes-Einstein equation, the diameter for a spherical particle moving through a liquid with a low Reynolds‘s number can be calculated from the translational diffusion

coefficient as shown in equation 5, where k_B is Boltzmann's constant, T is the temperature of the medium in K, η is the viscosity of the liquid medium (in centipoise), and d is the particle diameter.

$$D = \frac{k_B T}{3\pi\eta d}, \left[cm^2 / \sec\right] \tag{5}$$

DLS was also used to study the stability of enzyme and polymer molecules. The mechanism of destabilization is a two-stage process as depicted in Figure 23 (Iyer & Ananthanarayan, 2008). The enzyme molecule in its native active state N, exists in equilibrium with its partially destabilized state U. With further denaturing, the protein reaches a point of irreversible destabilization U, where the enzyme becomes inactive. Protein destabilization occurs by an unfolding of the enzyme structure. DLS can be used to monitor the change in protein size as the protein structure unfolds and destabilizes. Proteins can be denatured by chemical, physical, or thermal means. In this study, DLS was used to characterize the stability of the enzyme as well as C-PAM as a function of parameters such as ionic strength, pH, and temperature.

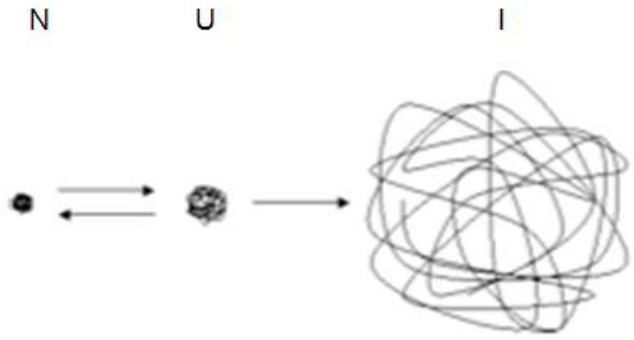

Figure 23: Schematic of enzyme unfolding as a function of deactivation

DLS was also used to study enzyme-C-PAM interactions in solution and determine the extent to which C-PAM complexes to enzyme. Measurements were made with a 90 Plus Analyzer from Brookhaven Instruments. C-PAM and alpha-amylase solutions were made in a 0.2 M pH 6 phosphate buffer. Measurements were made with 1% v/v alpha-amylase (0.6 mg/mL final concentration) with polymer concentrations ranging from 0-1000 mg/L in a pH 6 phosphate buffer at room temperature. The size of the enzyme-polymer complex was measured as a function of C-PAM concentration and charge. Using these measurements, dissociation constants for the C-PAM-enzyme complex were determined. The purpose was to gain insight into the C-PAM properties that influence the interaction between the C-PAM and enzyme.

UV-vis spectroscopy

Ultraviolet-visible spectrophotometry (UV-vis) is another method that can be used to monitor the change in protein concentration. UV-vis spectroscopy measures the absorption of compounds in the visible and near ultraviolet wavelength regions between 200-800 nm. The concentration of an absorbing molecule such as a protein can be determined using the Beer-Lambert law (Equation 6),

$$A=\varepsilon l C \tag{6}$$

where ε is the molar absorption coefficient ($M^{-1}cm^{-1}$), l the light path length, and C the protein concentration (M).

Samples for this study were prepared as were the DLS samples. Spectrophotometric measurements were carried out using a Shimadzu UV-Visible spectrophotometer with a path length of 1 cm. Solutions of alpha-amylase, C-PAM, and alpha-amylase-C-PAM mixtures were prepared at various concentrations. A spectrum of each sample was then recorded over 200-350 nm. While alpha-amylase has a peak at a wavelength of 280 nm, C-PAM does not. Therefore, the difference in alpha-amylase absorbance of each sample was used to determine the concentration of protein associated to C-PAM. Dissociation constants for each C-PAM to enzyme system were then determined using a modification to the method of Elodi (Elodi et al., 1972).

3.4.2. Effect of C-PAM on enzyme to starch binding

For the bimolecular binding of alpha-amylase enzyme [E] to starch [S] at equilibrium,

$$[S] + [E] \leftrightarrow [ES] \tag{7}$$

the dissociation constant K_d can be expressed as

$$K_d = \frac{[E][S]}{[ES]} \tag{8}$$

Dissociation constants of alpha-amylase with and without C-PAM were obtained by a modification of the Warren method (Warren et al., 2011). The binding of enzyme to C-PAM treated starch was measured by adding C-PAM to a suspension of cornstarch in water at 4 ^{o}C. The low temperature was used to minimize hydrolysis. Enzyme was added at a final concentration of 0.6% and the suspension shaken cold for 30 minutes. It was then centrifuged at 13,400 RCF

for 10 minutes and the enzyme in the supernatant determined by protein analysis with a Pierce BCA protein assay kit. The amount of enzyme in the supernatant was taken as the amount of free, unbound enzyme, $[E]_{free}$. The amount of enzyme bound to cornstarch, $[E]_{bound}$, was then determined by subtracting $[E]_{free}$ from initial enzyme amount $[E]_o$.

Dissociation constants were determined using a one site-binding model

$$[E]_{bound} = \frac{B_{\max}[S]}{K_d + [S]} \tag{9}$$

where B_{max} is the maximum enzyme binding, and [S] the starch concentration. A linear plot of this model according to the Scatchard equation

$$\frac{[E]_{bound}}{[S]} = \frac{B_{\max}}{K_d} - \frac{[E]_{bound}}{K_d} \tag{10}$$

was then constructed to determine B_{max} and K_d of alpha-amylase on starch in the presence of C-PAM. The enzyme absorbed was calculated as:

$$\%EnzymeBound = \frac{[E]_{bound}}{[E]_0}\%100 \tag{11}$$

Measurement uncertainty from duplicate measurement was 1%.

3.4.3. Effect of C-PAM on enzyme activity and stability

Alpha-amylase activity was determined by a modification of the Street-Close method (Street & Close, 1956; Yoo et al., 1987). Raw cornstarch (5 mL of a 1% w/v suspension in pH 6 phosphate buffer was incubated in a water bath at 37 ^{o}C. The reaction was started by adding 1 mL of enzyme to the cornstarch suspension. After 10 minutes the reaction was stopped by adding 5 mL of 0.1 M

HCl and placing the vessel in an ice bath. Samples were analyzed for glucose using the Megazyme glucose oxidase/peroxidase (GOPOD) assay kit. One alpha-amylase activity unit (U) is the amount of enzyme that releases 1 μmol of glucose/min at pH 6 and 37 ^{o}C using D-glucose as a standard.

The activity of glucoamylase was determined using the same method but in a pH 4 buffer solution. One glucoamylase activity unit is the amount of enzyme required to produce 1 μmol of glucose/min at pH 4 and 37 ^{o}C, using D-glucose as a standard. The activity of alpha-amylase was 3.5 ± 0.6 μmol/min/mL of glucose from starch at pH 6 and 37^{o}C. The activity of glucoamylase was 116.5 ± 1.7 μmol/min/mL. Each activity measurement is an average of experiments conducted in triplicate.

The effect of C-PAM preparation method on alpha-amylase activity was studied by adding C-PAM (XP10025) to samples in three different ways. For the control experiment with no C-PAM, cornstarch and alpha-amylase solutions were prepared separately. The two solutions were then mixed to start the reaction. In the second sample, C-PAM was added to only the cornstarch solution so that when mixed with the alpha-amylase solution, the final concentration of C-PAM would be 167 ppm. In the third, C-PAM was added to only the enzyme solution so that when mixed with the cornstarch solution, the final concentration of C-PAM would be 167 ppm. For the last sample, half of the C-PAM was added to the

cornstarch solution and the other half added to enzyme solution so that when mixed the final CPAM concentration would be 167 ppm.

To study the effect of C-PAM concentration on enzyme activity, C-PAM was added at 0-1500 ppm to alpha-amylase, and 0-167 ppm to glucoamylase. The effect of ionic strength was also explored by determining the activity of alpha-amylase in the presence of C-PAM with varying ionic strength. Alpha-amylase was added to solutions of C-PAM ranging from 0-167 ppm, and $CaCl_2$ ranging in concentration from 0.1-9.0 mM concentration.

To study the effect of pH on enzyme activity, buffer solutions with pH between 3-8 were used in solutions with and without C-PAM. The effect of C-PAM on alpha-amylase activity at different temperatures was explored by measuring enzyme activity at temperatures ranging from 30 to 90 ^{o}C. The stability of the alpha-amylase enzyme in the presence of C-PAM was determined by measuring activity periodically for 8 hours.

To study the effect of amylose/amylopectin ratio on activity in the presence of C-PAM, the activity of alpha-amylase on 1% solutions of high amylose cornstarch (70% amylose) and unmodified waxy cornstarch (<1% amylose) were determined in the presences of 208 ppm of C-PAM and compared to the activity of regular cornstarch in the presence of C-PAM using the procedure described above.

3.5. Hydrolysis of Cornstarch

3.5.1. Alpha-amylase experimental procedure

Hydrolysis experiments were conducted based on typical industrial conditions (Bothast & Schlicher, 2005). C-PAM-starch suspensions were prepared by adding solutions of C-PAM to 30, 8, or 1 w/w% dry basis starch suspensions. Control samples contained no C-PAM. To start the reactions, alpha-amylase (0.2% cornstarch dry basis unless otherwise indicated) was added to the suspensions, and the suspensions were placed in a water bath at 70 ^{o}C with agitation at 250 RPM unless otherwise noted. Samples of the reaction were taken periodically throughout the course of the reaction, filtered using a 0.2 μm GHP syringe, then analyzed for glucose, DOC, and Brix.

3.5.2. Glucoamylase experimental procedure

An experiment to determine the effect of C-PAM on the rate of glucoamylase hydrolysis was conducted using the following procedure: an 8 w/v% solution of cornstarch was prepared. Alpha-amylase at 0.2 w/v% (dry cornstarch basis weight) was added to the sample, and the sample was placed in a water bath at 70 ^{o}C to start the reaction. After hydrolysis for sixty min, a sample was taken from the solution and analyzed for Brix and glucose. The hydrolyzed cornstarch solution was then separated into two equal volumes. C-PAM (100 ppm, 40 mol% cationicity) was then added to one of the solutions and both samples were then placed in a water bath at 50 ^{o}C. Glucoamylase (0.02 v/v%) was added to both starch solutions to start the glucoamylase hydrolysis reaction. Samples of the

reaction were then taken periodically throughout the course of the reaction, filtered using a 0.2 μm GHP syringe, and analyzed for glucose.

3.5.3. Hydrolysis experiments

Several hydrolysis experiments were conducted with varying parameters to determine their effect on sugar yield, and are listed in Table 1. To study the effect of C-PAM concentration on hydrolysis, three concentration of C-PAM (30, 100, and 300 ppm) were used to hydrolyze starch at 30 w/v% and 8 w/v%. For the study of cationicity, a 10, 40, and 80 mol% cationicity C-PAM at 100 ppm was used in the hydrolysis of 30 and 8 w/v% starch concentrations. C-PAM polymers of molecular weight 5, 9, and 11 million Daltons were used in the hydrolysis of 8 w/v% starch in order to study the effect of C-PAM molecular weight on sugar yield.

The next experiment was conducted to determine if the order in which the C-PAM was added had any effect on the yield of glucose. This experiment would give important clues towards the mechanism of C-PAM aided hydrolysis. For the first sample in this experiment, the C-PAM (100 ppm) was mixed with the starch prior to the addition of alpha-amylase. For the second sample, the C-PAM was added 5 minutes after the addition of the enzyme. Both samples were hydrolyzed along with a control sample, which contained no C-PAM.

The effect of the enzyme loading in the presence of C-PAM was investigated by adding progressively lower levels of enzyme to 30 w/v% starch suspension with 100 ppm C-PAM.

The next set of experiments was centered on investigating the effect of process conditions on the yield of starch hydrolysis in the presence of C-PAM. To study the effect of temperature, hydrolysis of starch (1 w/v%) was conducted at both 50 ^{o}C and 70 ^{o}C and compared. The purpose of this study was to determine if C-PAM inhibited or enhanced the rate as a function of temperature.

To study the effects of agitation, hydrolysis with agitation speeds of 180, 250, and 500 RPM were used. The Reynolds number, Re, was calculated for each agitation speed. In a cylindrical vessel stirred by a central rotating paddle, turbine or propeller, the characteristic dimension is the diameter of the agitator D. The velocity of the system is ND where N is the rotational speed (revolutions per second). The Reynolds number is then:

$$\mathrm{Re} = \frac{\rho N D^2}{\mu} \qquad (12)$$

where ρ is fluid density in kg/m^3 , and μ is viscosity in kg/m·s. The flow is laminar in the tank for Re<10, turbulent for Re>10^4, and for a range between 10 and 10^4, the flow is transitional, being turbulent at the impeller and laminar in remote parts of the vessel. In our system, D is 5.2 cm, and ρ is fluid density of approximately 1000 kg/m^3. Therefore agitation speeds of 180, 250, 500 RPM in our system correspond to Reynolds numbers of 149, 207 and 413 respectively.

Table 1: Summary of hydrolysis experiments and variables studied

	Variable tested:	Variable values used in experiment*	Starch Concentration (w/v%)	C-PAM concentration (ppm)
1	C-PAM concentration (ppm)	30,100, 300	30, 8	30,100, 300
2	C-PAM cationicity (mol %)	10, 40, 80	30, 8	100
3	C-PAM Molecular Weight-M_n (x10^6 Daltons)	5, 9, 11	8	30
4	C-PAM addition point	C-PAM added before/after enzyme	8	100
5	enzyme loading (v/w% of cornstarch db)	0.2, 0.15, 0.1, 0.05	30	100
6	Temperature (^{o}C)	40, 70	1	30,100, 300
7	agitation (Reynold's number)	149, 207, 413	30	100

*40% cationicity C-PAM (XP10025) was used with an enzyme loading of 0.2 (v/w% enzyme loading) at 70 ^{o}C unless otherwise noted.

3.5.4. Analysis of hydrolyzed products

Glucose analysis

The glucose oxidase/peroxidase (GOPOD) assay kit supplied by Megazyme International Ireland Ltd. was the main method used to analyze samples for glucose concentration. In this assay, glucose oxidase (GO) enzyme oxidizes D-glucose in the presence of oxygen and water to produce D-gluconate and hydrogen peroxide according to the reaction illustrated in Figure 24. The amount of quinoneimine dye produced in the reaction is proportional to the amount of D-glucose reacted. The quinoneimine dye concentration can be measured by the absorbance of the solution at 510 nm.

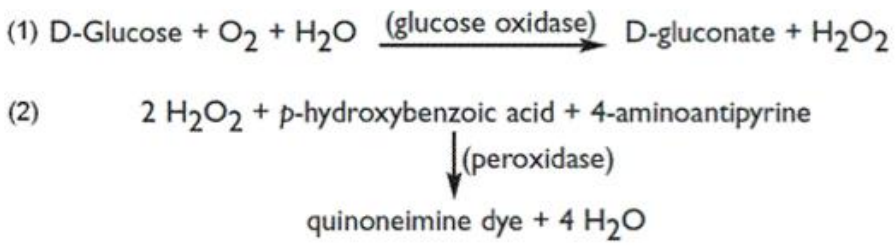

Figure 24: GOPOD glucose analysis reaction

Automation of the glucose analysis procedure was done using a DA3500 Discrete Analyzer from OI Corporation, College Station, TX with an average error from duplicate measurement of 4.5%.

Brix analysis

Brix analysis was the method used in this study to measure total sugar concentration of hydrolysis experiments. Brix is a measurement of the concentration of dissolved solids in a solution commonly used in the starch and sugar industries. Brix can be determined using a digital refractometer which measures the change in refractive index of a solution proportional to dissolved sugar concentration. One degree Brix equals 1 gram of sucrose per 100 mL of liquid at a given temperature, and can also be expressed as mass percentage w/w% solids content. A Sper Scientific 300034 Digital refractometer was used for all experiments. The uncertainty was 0.2 degrees. Brix measurements were expressed as degree Brix. As a control, Brix level of C-PAM and alpha-amylase alone was measured at various concentrations. Both C-PAM and alpha-amylase measurements were below significant detection of the refractometer.

Dissolved organic carbon analysis

Dissolved organic carbon (DOC) analysis was another method used to determine dissolved sugar. DOC measurements were conducted using a Shimadzu TOC-V_{CSH} instrument. Measurement of DOC in this instrument is done via high temperature combustion, in which inorganic carbon in the injected sample is

converted to CO_2 and purged from the system. The remaining (organic) carbon is then combusted in an oxygen rich environment into carbon dioxide (CO_2) and measured by a non-dispersive infrared detector. The resultant CO_2 concentration can then be used to determine the total dissolved organic carbon content (DOC).

3.6. Statistical analysis

Single factor analysis of variance (ANOVA) was conducted using Microsoft Excel and Graphpad InStat 3 statistical software. P-values from control and non-control samples for each experiment were determined and statistical significant correlations were accepted at p-values <0.05.

CHAPTER 4: Results and Discussion

4.1. Introduction

As stated in chapter 1, the purpose of this study was to examine hydrolysis in the presence of C-PAM in order to gain insight into the mechanism. To this end, the chapter is organized in terms of the specific questions introduced in chapter 1: It first reports finding from C-PAM-starch interactions studies, followed by C-PAM-enzyme interactions studies, and finally findings from the C-PAM added hydrolysis studies.

4.2. Starch-C-PAM Interactions

4.2.1. Starch-C-PAM adsorption

Charges of starch, enzymes and select C-PAM samples measured by charge titration are listed below in Table 2. C-PAM, starch and alpha-amylase samples were measured in 0.2 M pH 6 phosphate buffer solution, while glucoamylase was measured in pH 4 0.2 M ph 4 buffer solution. All polyacrylamide samples bore positive charge, and were titrated against a 0.001 N solution of anionic PVSK polyelectrolyte. Starch, fiber, and enzymes had negative charge, and were titrated against 0.001 N solution of cationic PDADMAC polyelectrolyte.

The adsorption isotherm of 20 ppm C-PAM (40 mol% cationicity) on starch (Figure 25), exhibits a Langmuir-shaped curve. The starch reaches saturation at 0.004 mg C-PAM/mg of starch. The partition coefficient (ratio of C-PAM adsorbed to starch to that dissolved in an equal weight of water), shown in Figure

26, was very high at low starch concentrations. As starch concentration increased, the partition coefficient decreased until reaching a minimum limit value of 107±9.

Table 2: Measured charges (C/g) of experimental materials

Sample	Charge (C/g)
XP10023 (10 mol% cationicity)	123 ± 19
XP10025 (40 mol% cationicity)	268 ± 17
XP10033 (80 mol% cationicity)	283 ± 18
Alpha-amylase	-1.1 ± 0.1
Glucoamylase	-14.7 ± 1.2
Cornstarch	-0.823 ± 0.06
Softwood bleached Kraft fiber*	-0.13 ± 0.05

*Measurement taken from Reye (Reye, et al., 2009).

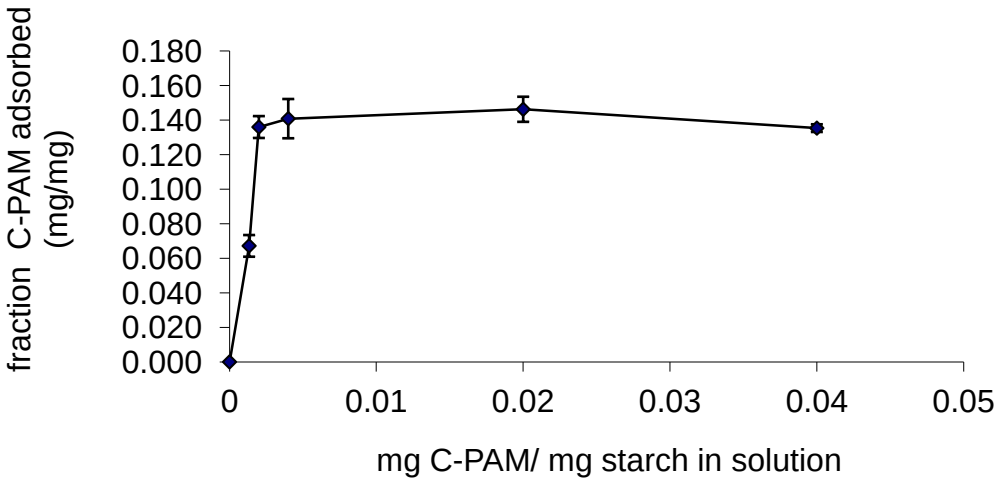

Figure 25: Adsorption isotherm of 40% cationicity C-PAM (20 ppm) to starch.

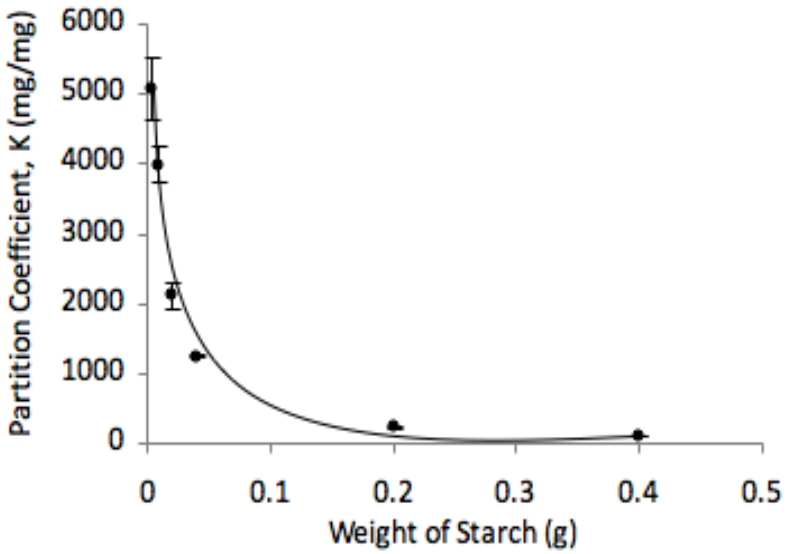

Figure 26: Partition coefficient of 20 ppm C-PAM (40% cationicity) between starch and water in solution.

4.2.2. Swelling and solubility

As shown in Figure 27, the extent of swelling for the cornstarch was low below gelatinization temperatures (< 65 ^{o}C). Above 65 ^{o}C, the swelling power (SP) increased significantly. There was no statistical difference between the SP of cornstarch and that of cornstarch in the presence of 100 ppm and 1000 ppm C-PAM at a given temperature. The SP data were consistent with particle size analysis data collected from microscopic imaging of the cornstarch granules (Figure 28). C-PAM had no significant effect on starch granule size distributions (Figure 29) at both pre (50 ^{o}C) and post (70 ^{o}C) gelatinization temperatures. At 50 ^{o}C, the mean particle size for starch granules with and without C-PAM was 17.1±9 μm, and 16.6±9 μm, respectively. Mean particle sizes for starch at 70 ^{o}C with and without C-PAM were 23.4±10 μm and 23.6±11 μm, respectively.

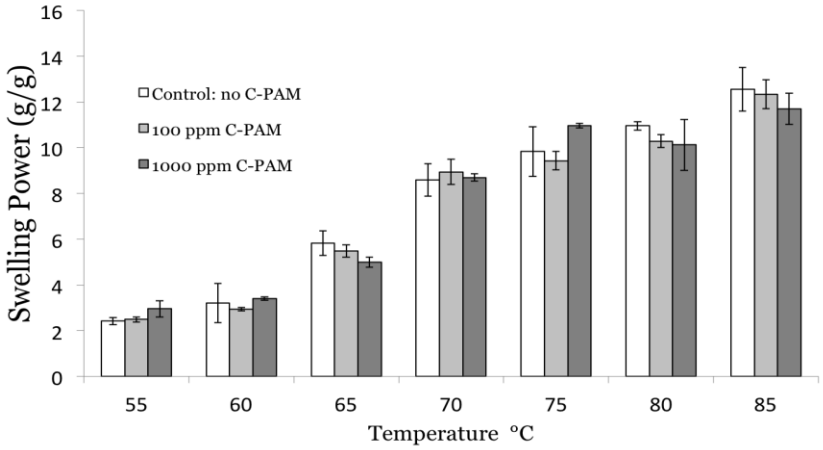

Figure 27: Swelling power (g/g) of cornstarch at different temperatures with C-PAM at concentrations of 100 ppm and 1000 ppm, and without C-PAM (control). Each data point is the mean value of 4 measurements

Temperature (^{o}C)	Cornstarch	Cornstarch with C-PAM
50	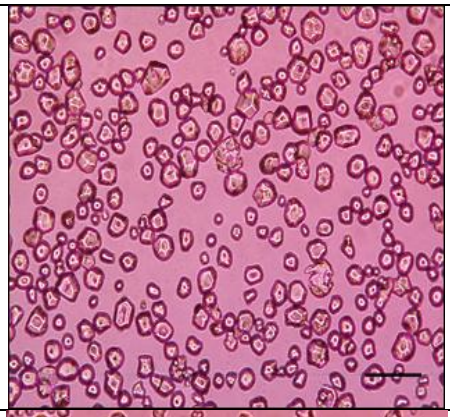	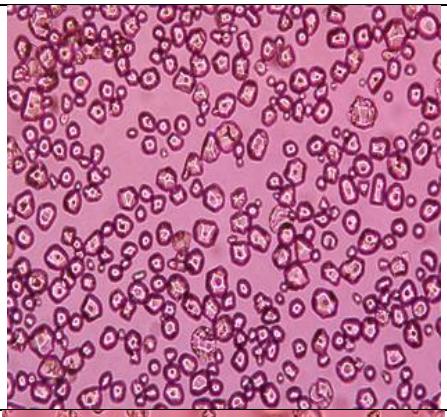
70	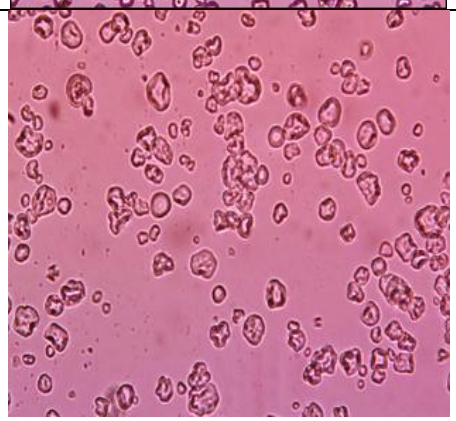	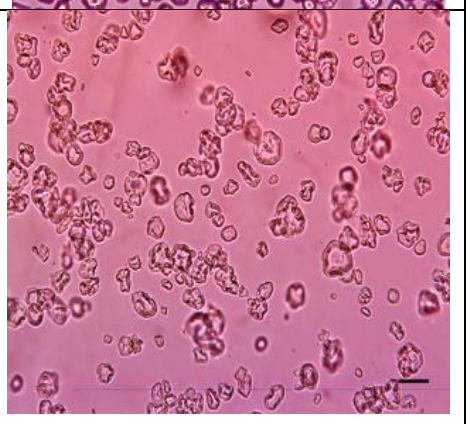

Figure 28: Microscopic images of cornstarch at 50 ^{o}C and 70 ^{o}C with and without 100 ppm C-PAM.

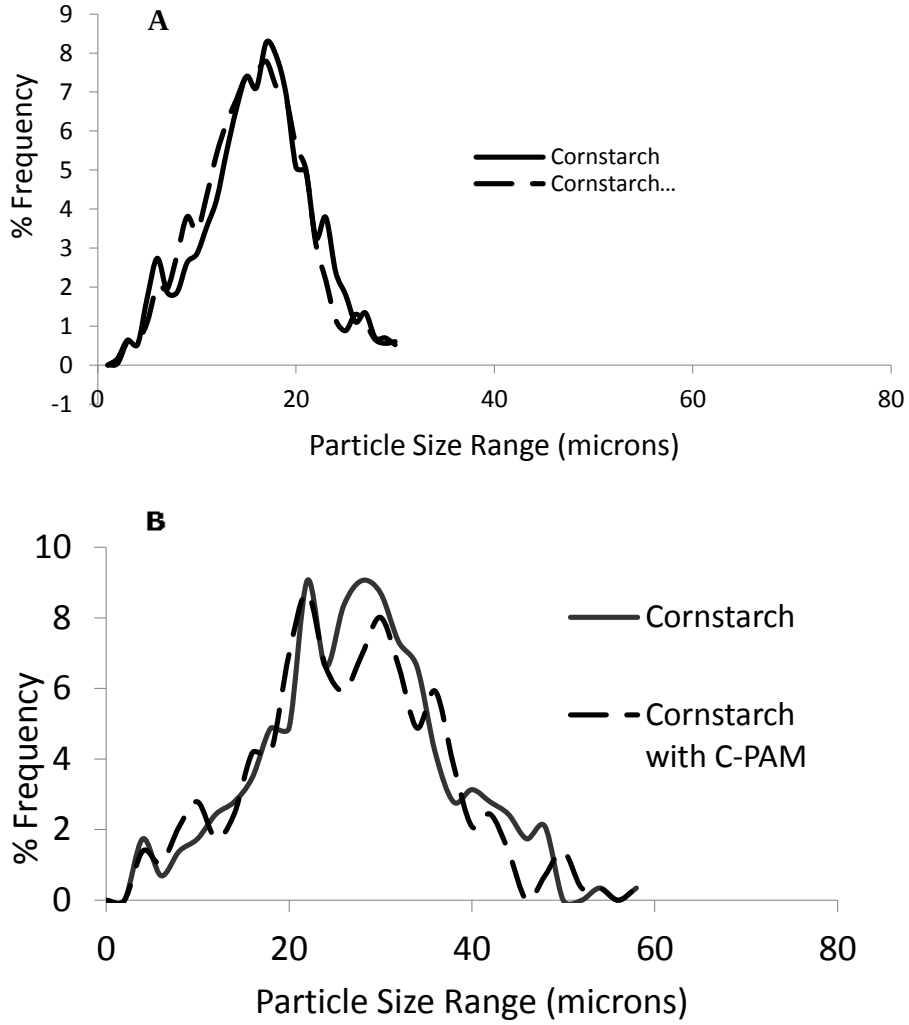

Figure 29: Particle size distribution of cornstarch as collected from image analysis with (dotted line) and without (solid line) 100 mg/l C-PAM at (A) 50 ^{o}C, and (B) 70 ^{o}C.

C-PAM addition had a more pronounced effect on the amount of soluble starch leakage from granules as DOC results show in Figure 30 below. As with SP, the amount of soluble leakage as characterized by DOC, was initially low at pre-

gelatinization temperatures, but increased greatly once samples were heated above typical gelatinization temperatures. Heating the granules in the presence of C-PAM did have an effect on the amount of soluble starch content, but was dependent on the concentration of C-PAM as well as the heating temperature. Heating starch in the presence of 100 ppm starch made no difference to the amount of soluble starch. With 1000 ppm C-PAM, the amount of soluble starch increased considerably even at pre-gelatinization temperatures. At 85 ^{o}C, the addition of C-PAM greatly inhibited the release of soluble starch fragments.

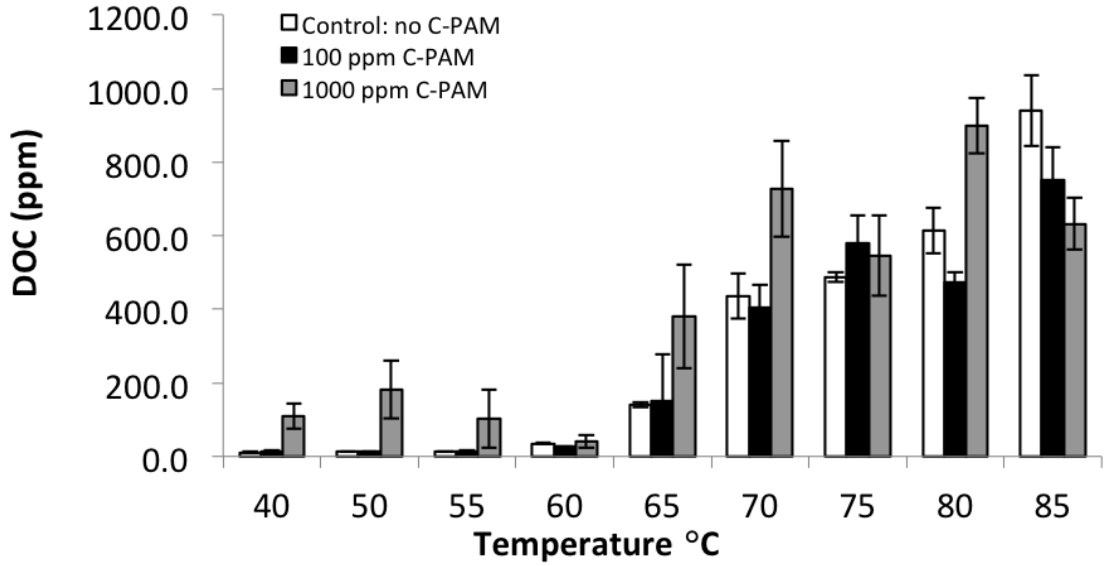

Figure 30: Total soluble solids (DOC) at different temperatures with addition of C-PAM at concentrations of 100 ppm and 1000 ppm, and without C-PAM (control). Each data point is the mean value of 4 measurements.

Table 3: Total soluble solids (DOC) at different temperatures with addition of C-PAM at concentrations of 100 ppm and 1000 ppm, and without C-PAM (control). Each data point is the mean value of 4 measurements.

	DOC (ppm)		
Temperature	Control (No C-PAM)	with 100 ppm C-PAM*	with 1000 ppm C-PAM*
40	12	14	110*
50	13	13	183*
55	13	15	102*
60	36	26*	42
65	141	149	380*
70	437	404	727*
75	488	580	546
80	614	472*	899*
85	940	752*	632*

* data differs significantly from control sample at constant temperature ($p<0.05$)

4.2.3. Effect of C-PAM on starch gelatinization

The onset pasting temperatures and peak viscosities of various starch-C-PAM systems are listed in Table 4 below. The presence of C-PAM significantly reduced the onset temperature (as signaled by a sharp rise in viscosity), as seen in the viscosity-temperature plot of Figure 31. The degree of temperature shift was significantly affected by C-PAM concentration. While all C-PAM polymers (with varying cationicities) reduced the onset gelatinization temperature to some degree, there was no significant difference between C-PAMs with varying cationicity at the same concentration. The onset temperature appeared to exhibit an inversely proportional relationship to peak viscosity; the lowest onset gelatinization temperature was caused by a 300 ppm concentration of 40% cationicity C-PAM, which had the greatest viscosity. Analogously, a 30 ppm concentration of 40% cationicity C-PAM had the lowest peak viscosity, and caused the smallest shift in onset gelatinization temperature.

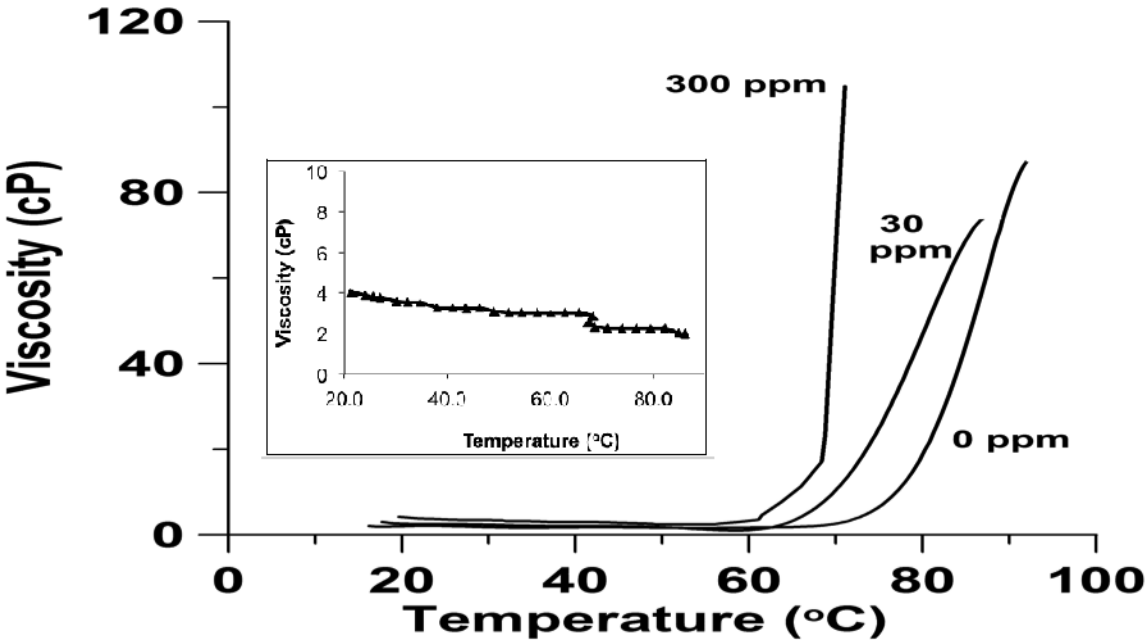

Figure 31: Effect of C-PAM (40% cationicity) on gelatinization temperature as characterized by viscosity (cP). Starch was present at 8 w/v% with 0, 30, and 300 ppm C-PAM. Inset: Viscosity Profile of 100 ppm C-PAM only.

Table 4: Onset gelatinization temperature and peak viscosities of cornstarch in the presence of C-PAM

Sample description	Onset gelatinization temperature (^{o}C)*	Peak viscosity (cP)
Cornstarch	69.6±3	104± 4
Cornstarch + 10% cationicity C-PAM (30 ppm)	61.7±1	148± 3
Cornstarch + 40% cationicity C-PAM (30 ppm)	63.0±3	85± 7
Cornstarch + 40% cationicity C-PAM (300 ppm)	58.0±2	196± 15
Cornstarch + 80% cationicity C-PAM (30 ppm)	64.7±1	76± 5

4.2.4. Discussion of starch-C-PAM interactions results

Adsorption of C-PAM on starch quickly reached maximum saturation, indicating very low levels of C-PAM are required for full starch surface coverage (Figure 25). This type of behavior indicates a relatively high affinity of C-PAM for starch. If the Langmuir model behavior is followed, the partition coefficients remain constant. They decrease with increasing solute:solids ratio if the Freundlich model behavior is obeyed (Kinniburgh, 1986) . In this case, the opposite situation was observed, where partitioning increased with high solute:solids ratios (Figure 26). The anomaly likely arises from the known ability of C-PAM to aggregate small particles in water (Wong et al., 2006). At high relative C-PAM dose (low starch levels) the C-PAM agglomerates starch-derived colloids and starch particles, which are subsequently pelletized during centrifugation; a high partition coefficient results because solids are largely removed from water. At low dosage, the C-PAM is unable to agglomerate all the solids and some of the smaller particles remain in water. The C-PAM associated with these particles appears in the aqueous phase and gives rise to a lower partition coefficient. However, both C-PAM-starch isotherm and partition coefficient results indicated a strong affinity of C-PAM for starch.

When C-PAM is added to a suspension of starch, the strong attraction for and adsorption of C-PAM to starch, causes the insoluble starch particles to stabilize and remain suspended or entrapped within the C-PAM-starch “network”. The network allows for an increased starch surface area that is subjected to forces

within the suspension, thus facilitating increased starch solubilization, even at pre-gelatinization temperatures. Upon further heating, the combination of gelatinized granules, leaked soluble starch, and C-PAM in solution began to pack so tightly around the starch granules (as indicated by high viscosities) that further polymer leakage and swelling become inhibited, accounting for the inhibition of starch solubility observed with C-PAM at 85 ^{o}C.

Changes in solubility, swelling, and onset temperature of gelatinization induced by additives have been observed by many others (Kaur et al., 2008; Mandala & Bayas, 2004; Tester & Sommerville, 2003), though individual results seem to depend largely on specific starch type -additive system combinations. For example, Mandala and Bayas found increased swelling of wheat starch granules in the presence of xanthan, in addition to increased soluble solids at pre-gelatinization temperatures from approximately 2 to 3%. Onset gelatinization temperature can also be raised or lowered by the addition of salts, dependent on nature and concentration of the salt (Jane, 1993; Zhu et al., 2009).

4.3. Enzyme-C-PAM Interactions

4.3.1. Dynamic light scattering (DLS) characterization of Enzyme and C-PAM

Dynamic light scattering (DLS) was used to study the association of C-PAM to enzyme. First, solutions of C-PAM or enzyme were analyzed under various conditions in order to study the effect of these conditions on the polymer and enzyme stability. Then samples containing both C-PAM and enzyme varying by

C-PAM properties and solution conditions were analyzed using DLS to determine the factors which most affected C-PAM-enzyme interactions. Effective diameters represent an average size of the particles in the sample, and are an output of the DLS system.

DLS characterization of alpha-amylase enzyme

Alpha-amylase solutions were prepared in 0.1 M pH 6 phosphate buffer. The particle size distribution of 10 v/v% alpha-amylase, averaged over three measurements, is shown in Figure 32. The enzyme had a bimodal distribution with a major portion in the size range from 4-6 nm corresponding to actual enzyme distribution, and a minor peak at 22-32 nm, which corresponded to clusters of the alpha-amylase. The average effective diameter, an average size of all particles in solution, was 9.1 ± 0.3 nm. Both experimental size distribution and effective diameter were consistent with literature values (Fitter, 2005). The effective diameter of alpha-amylase at varying dilutions is shown in Figure 33. It remained consistent in the range of concentration from 5-25 v/v% with an average size of 11.2 ± 2 nm. At a dilution of 3.75 v/v%, the alpha-amylase began to lose stability, increasing in size to 24.1 ± 0.4 nm. To keep the enzyme in the stable size range, all remaining DLS experiments contained alpha-amylase at 10 v/v%.

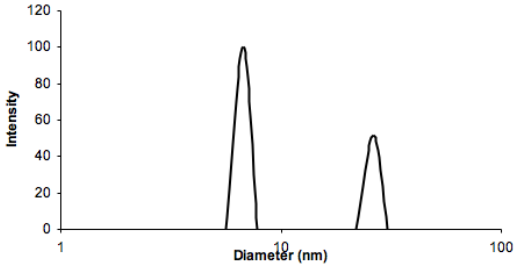

Figure 32: Particle size distribution of 10 v/v% alpha-amylase in pH 6 phosphate buffer. The x-axis is the hydrodynamic diameter (nm), while the y-axis is particle size % frequency.

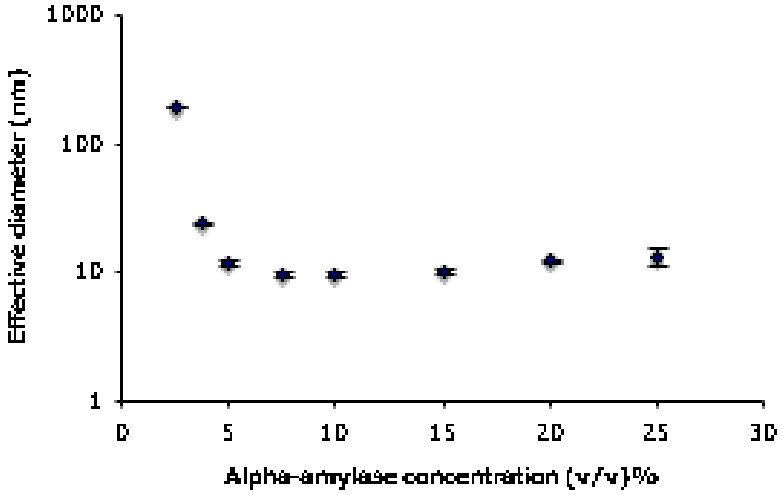

Figure 33: Effect of dilution on the alpha-amylase effective diameter in pH 6 phosphate buffer.

DLS characterization of C-PAM

DLS analysis was conducted for a series of C-PAM samples. A series of varying cationicity (10% - 80%) C-PAM polymers were prepared at 100, 500, and 1000 ppm in pH 6 buffer solution to determine their effect on the particle size distribution. Particle size distributions and corresponding effective diameters are summarized in Figure 34 and Table 5, respectively. Each value is an average of three measurements.

Each distribution exhibited bimodal distributions. Ozeroglu et al. observed a bimodal size distribution for polyacrylamide and offered an explanation for the observed results based on HPLC (Ozeroglu et al., 1996). The smaller distribution centered around 100 nm is attributed to single polymer chains and the larger distribution to that of multi-chain polymer clusters in solution. For a given C-PAM, the effective diameter was highest at the lowest concentration, then reached a minimum at 500 ppm, before increasing in size again at 1000 ppm. These results are consistent with known polyelectrolyte behavior (Dobrynin & Rubinstein, 2005). Polyelectrolytes at low concentration have an extended conformation in solution. As polymer concentration increases, the number of counterions that are able to adsorb on the chains increase, and shrink the size of the chains. At higher polymer concentration the chains begin to entangle, increasing the overall effective size of the polymer. The effective size of the polymer decreased with decreasing cationicity due to a reduction in intra-molecular charge repulsion.

Cationicity (mol %)	100 ppm	500 ppm	1000 ppm
80	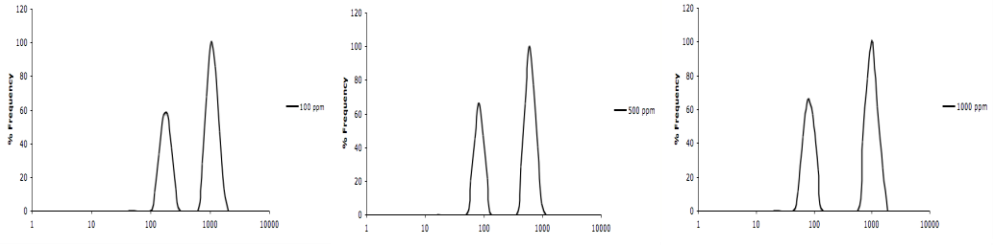		
40	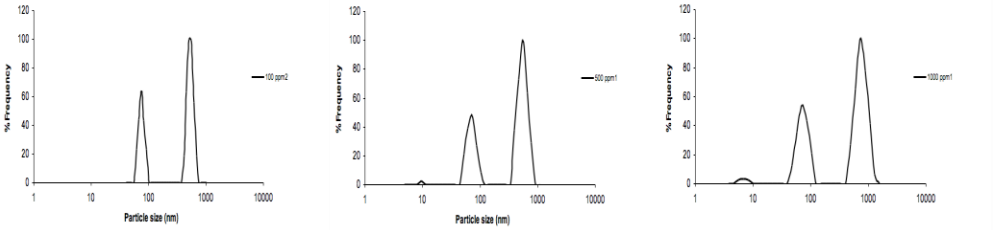		
10	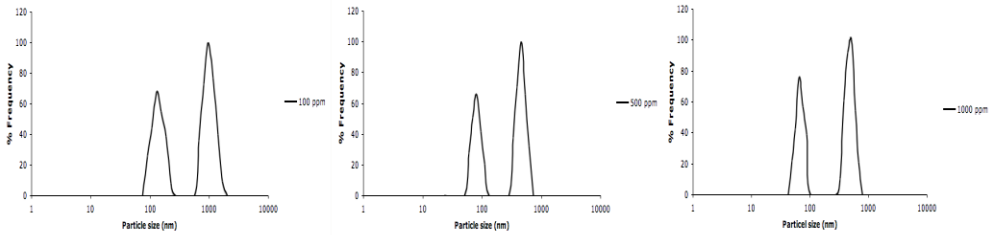		

Figure 34: Particle size distribution of C-PAM as a function of mol% cationicity 80, 40, 10 (top to bottom), and concentrations 100, 500, and 1000 ppm (left to right).

Table 5: Effective diameter of a series of C-PAM polymers as a function of mol% cationicity and concentration.

C-PAM cationicity (% mol)	100 mg/l C-PAM	500 mg/l C-PAM	1000 mg/l C-PAM
80	348±20	212±10	257±26
40	215±16	210±12	245±13
10	302±15	163±5	164±4

DLS: Effect of ionic strength

To assess the effect of ionic strength on enzyme and C-PAM stability, solutions of enzyme or C-PAM were prepared as above but with the addition of 0-2 M sodium chloride. Particle size distributions of alpha-amylase as a function of NaCl concentration are shown in Figure 35. The enzyme exhibited a bimodal

distribution corresponding to the distribution of individual enzyme molecules in solution, and that of the entangled aggregate enzyme molecules. When no salt was present, the effective diameter was 113±41 nm, due to the large concentration of aggregates in solution. The effective diameter of the amylase at 0.02 M NaCl decreased to 17.2±1.1 nm. As salt concentration increased, aggregation decreased until a single alpha-amylase size distribution was exhibited at 1 M NaCl with an effective diameter of 9.7±1.5 nm. Though there was some aggregation at 0.2 M NaCl, the effective size of 9.5 ± 0.5 nm was not significantly different than that of the size at 1 M NaCl. Aggregation decreased with increasing salt concentration because the attraction of the individual enzyme molecules in the aggregated complex was greater for the counter ions in solution than for the weakly complexed aggregate resulting in eventual dissolution of the aggregate particles as ionic strength increased.

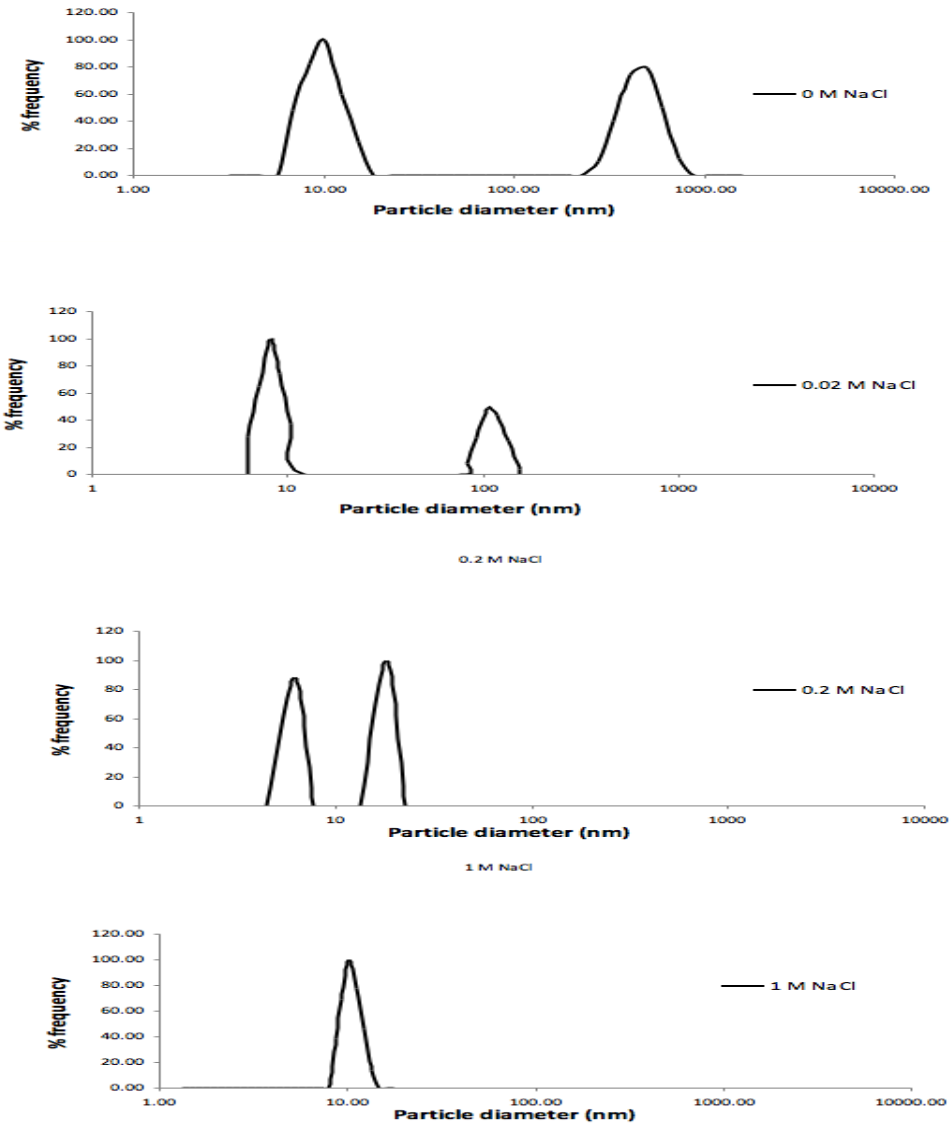

Figure 35: Alpha-amylase (10 v/v%) concentration with the addition of various concentrations of NaCl including (A) no NaCl (B) 0.02 M NaCl, (C) 0.2 M NaCl, and (D) 2 M NaCl

The effect of ionic strength on C-PAM particle size distribution and effective particle size is shown in Figure 36 and Table 6, respectively. At a given concentration, the effective diameter decreased as ionic strength increased from 0.02 M to 0.2 M. Increased ion concentration reduced the intra-molecular

repulsion, resulting in reduced size. There was no significant difference in effective diameter as salt concentration increased from 0.2 M to 1 M, most likely because the polymers had already reached the charge neutralization point.

NaCl concentration (M)	C-PAM concentration (I) 100 ppm	(II) 1000 ppm
(A) 0.02	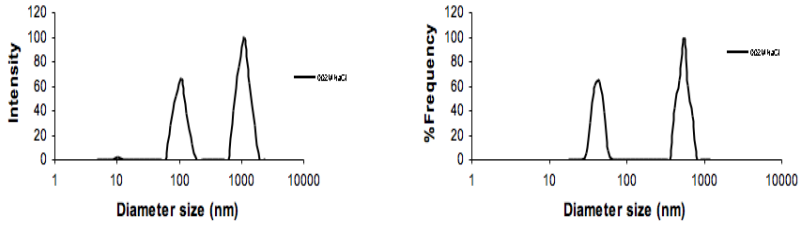	
(B) 0.2	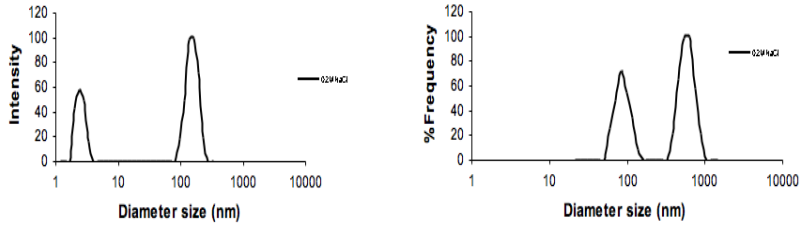	
(C) 1	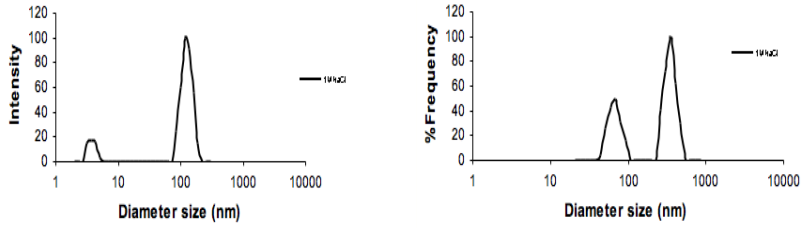	

Figure 36: Effect of ionic strength on 60 mol% C-PAM polymer at (I) column-100 ppm and (II) column -1000 ppm. NaCl was added to a final concentration of (A) 0.02 M, (B) 0.2 M, and (C) 1 M concentration

Table 6: Effect of addition of an ionic salt on effective diameter (nm) of 60 mol% cationicity

NaCl concentration (M)	C-PAM concentration 100 mg/L	C-PAM concentration 1000 mg/L
0.02	285±34	194±3
0.2	155±35	139±26
1	143±9	156±26

DLS: Effect of pH

The effect of pH on the effective diameter of 40 mol% cationicity C-PAM is shown in Table 7. At pH 2, the C-PAM was larger in size than at the other pH levels, most likely as a result of the high number of positive cations present in solution at such low pH, causing the polymer chains to expand due to the increased repulsion.

Table 7: Effect of pH on C-PAM particle size at two different mol% cationicities

	40 mol% cationicity C-PAM	
pH	Effective diameter (nm)	standard deviation
2	334	52
4	287	21
5	249	20
6	260	4
7	236	11
8	257	21
10	231	31

The effect of pH on enzyme particle stability was also studied using DLS. As shown in Figure 37, the effective diameter of 10 v/v% alpha-amylase is greatly dependent on pH. At low (2) and high (8, 10) pH values, the enzyme loses stability and unfolds to sizes of greater than 1000 nm. Results of the experiment repeated for 5 v/v% glucoamylase are shown in Figure 38. Glucoamylase was relatively stable across the complete range of pH values tested with an optimum stability at a pH of 4.

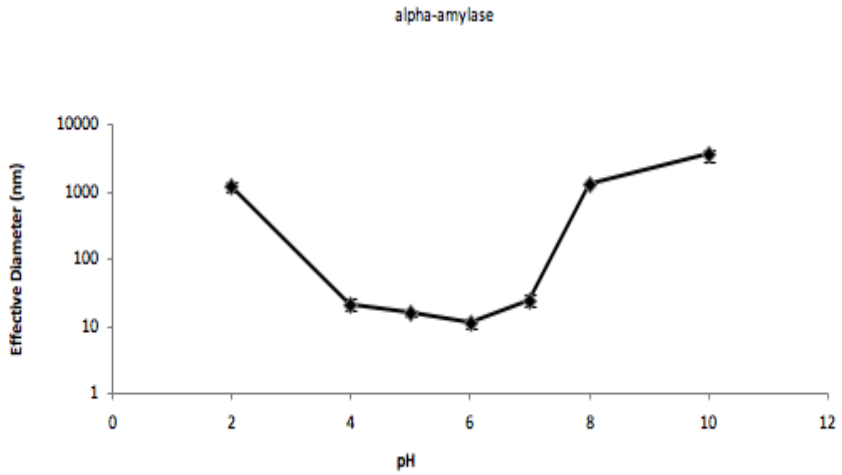

Figure 37: Effective diameter of 10 v/v% alpha-amylase as a function of pH.

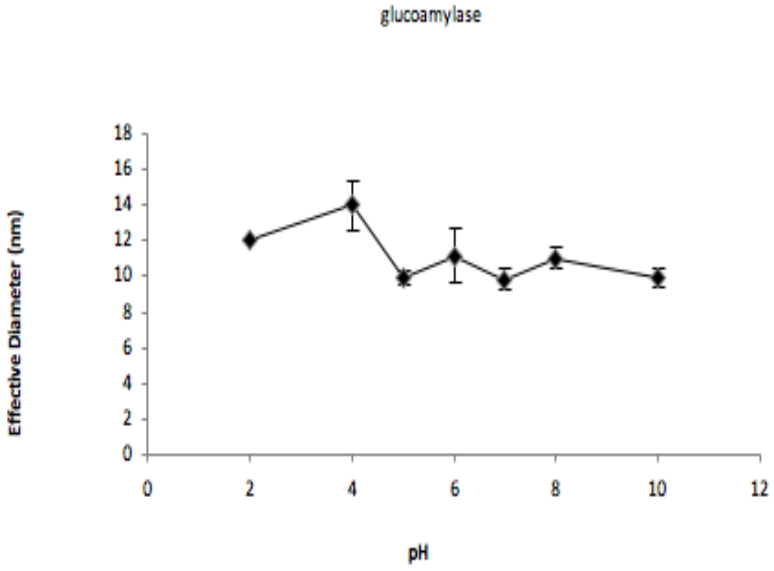

Figure 38: Effective diameter size of 5 v/v% glucoamylase as a function of pH.

DLS: Effect of Temperature

To determine the stability of the C-PAM as function of temperature, samples containing 500 ppm of C-PAM in a pH 6 buffer were heated in the particle size

analyzer at 1°C/minute from 25 °C to 70 °C as effective diameter was recorded. The effective diameter of 10 mol% and 40 mol% cationicity C-PAMs as a function of temperature is shown in Figure 39. Both C-PAMs remained stable from 26-70 °C. The average diameter of the 10 mol% and 40 mol% C-PAM was 171±22 nm and 225±7 nm, respectively.

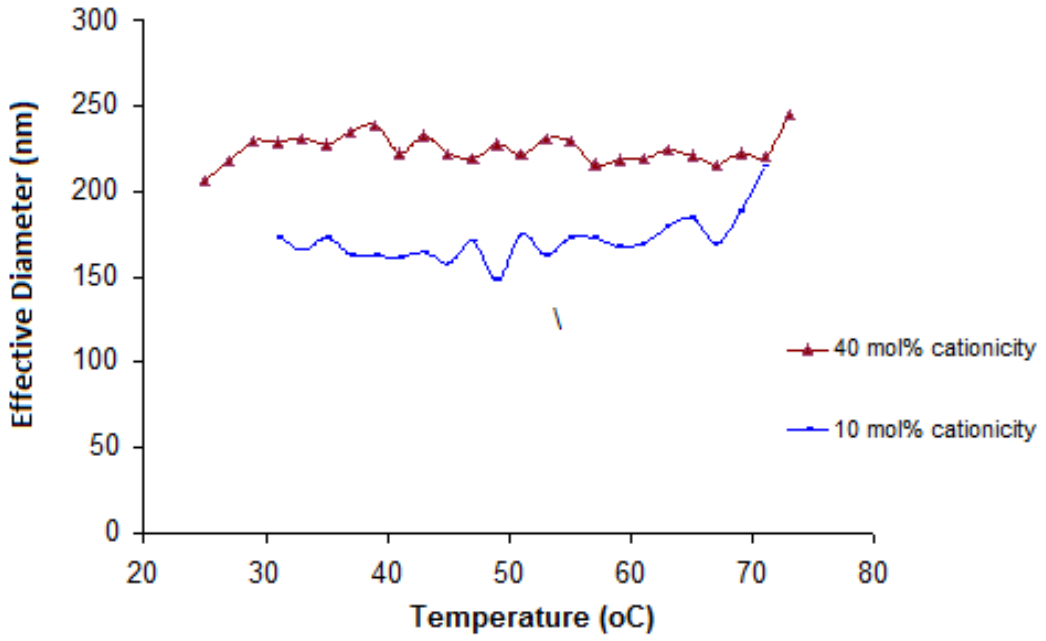

Figure 39: Polymer size of C-PAM as a function of temperature (°C) of 10 mol% cationicity and 40 mol% caationicity C-PAM. C-PAM was present at 500 ppm.

Similar studies were conducted for both alpha-amylase (10 v/v%) and glucoamylase (5 v/v%) enzyme. The gradual destabilization of alpha-amylase can be seen as a function of particle size distribution in Figure 40. The effective diameter of alpha-amylase in a pH 6 buffer as a function of temperature is listed in Table 8. At 24 °C the enzyme is stable with an effective diameter of 10 nm. At

44 ^{o}C, the distribution becomes wider as the enzyme destabilizes and unfolds, and a second distribution can be seen at approximately 100 nm. These effects are more pronounced at 74 ^{o}C. Despite the destabilization there is still a substantial amount of active enzyme at 74^{o}C.

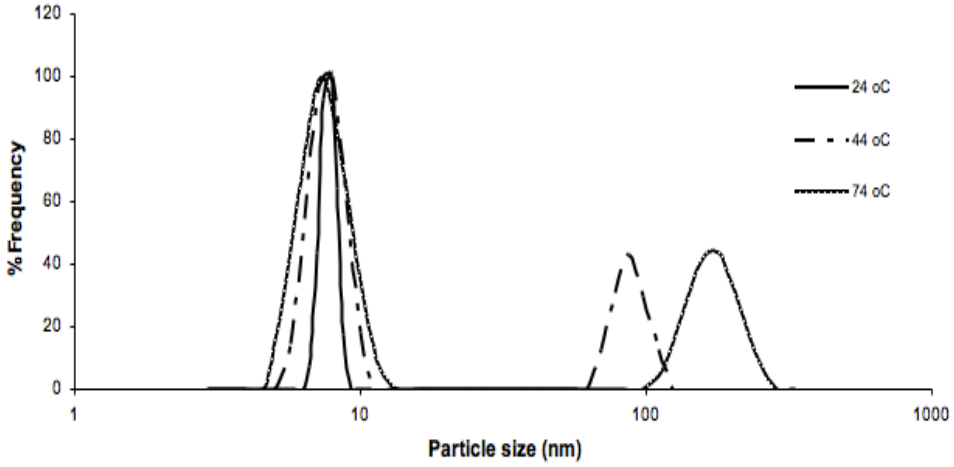

Figure 40: Particle size distribution of 10 v/v% alpha-amylase at 24 ^{o}C, 44 ^{o}C, and 74 ^{o}C.

Table 8: Effective diameter of alpha-amylase (10 v/v%) as a function of temperature.

Temperature (^{o}C)	Effective diameter (nm)
24	10±0.6
34	10.5±0.3
44	29.6± 2
54	41.6± 4
64	49.4± 2
74	60.2± 5

Glucoamylase (5 v/v%) at pH 4 was used for the thermostability study. As can be seen in Figure 41, the glucoamylase remained stable between 25-57 ^{o}C with an effective diameter of 7.8±0.1 nm. At 59±2 ^{o}C, the enzyme denatured rapidly and unfolded to an effective particle size of approximately 1582 nm.

Polymers have commonly been found to stabilize enzymes in solution (Hatti-Kaul & Andersson, 1999; Khalil, et al., 2001; Nishibue, et al., 1996). A study was conducted to determine if C-PAM had any stabilizing effects on glucoamylase. For this study 500 ppm of 10 mol% and 40 mol% C-PAM was added to solutions with the same parameters as the previous glucoamylase temperature study. Both C-PAM samples delayed the temperature at which the effective diameter of the glucoamylase began to increase (Figure 42). With10 mol% C-PAM, the average effective diameter of the solution was 230±20 nm prior to destabilization. In this solution, the size increase began at 61±3 ^{o}C. With 40 mol% cationicity, the effective particle size was 158±10 nm prior to destabilization, and the increase in size occurred at 59±3 ^{o}C, though the difference in effective diameter increase were not significant enough to conclude any stabilization effects as a result of the C-PAM.

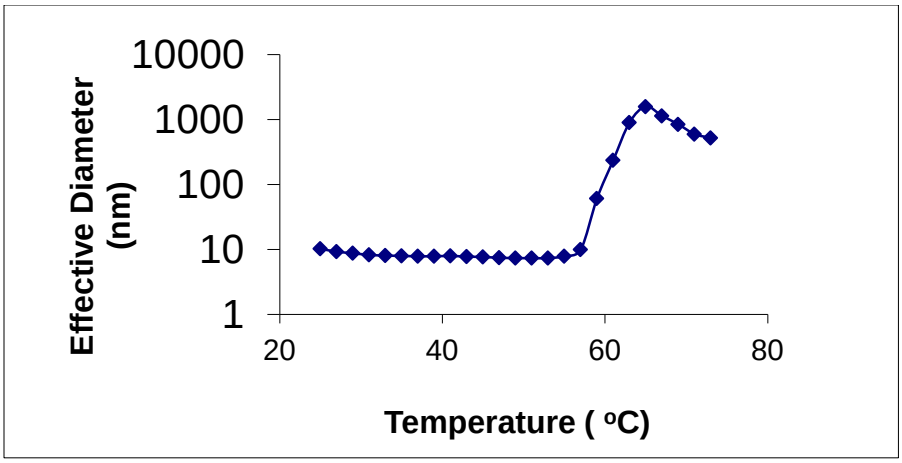

Figure 41: Effective diameter of glucoamylase (5 v/v%) as a function of temperature.

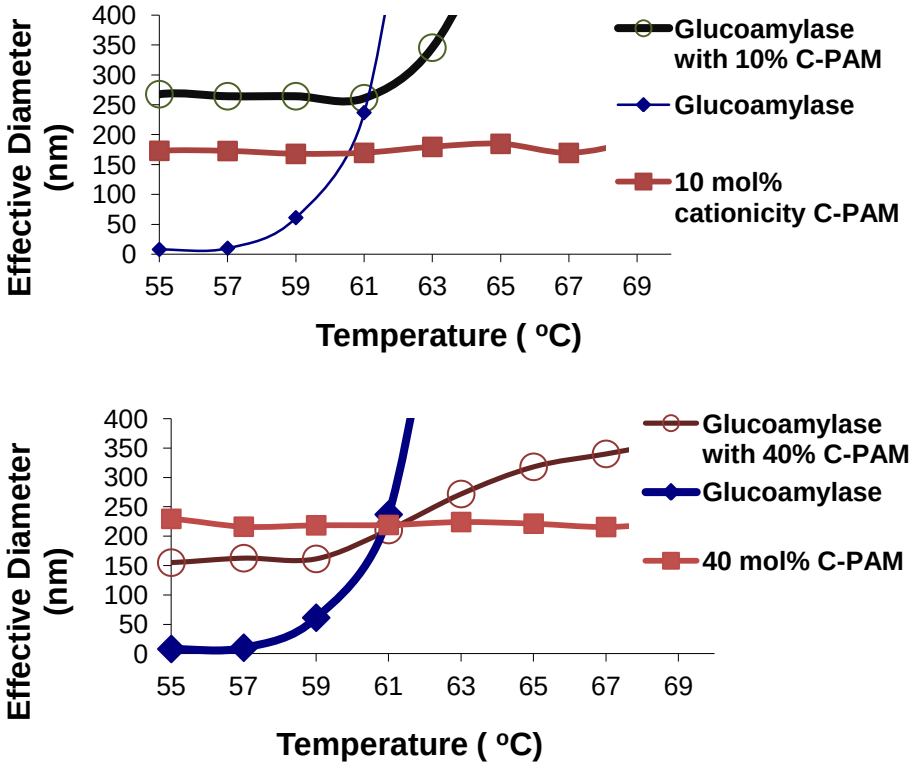

Figure 42: Particle effective diameter (nm) as function of heating of glucoamylase and glucoamylase-C-PAM solutions.

4.3.2. Determination of enzyme to C-PAM dissociation constants

The equilibrium between free enzyme [E] and C-PAM [P], and the enzyme-C-

PAM complex [PE] in solution can be written as

$$[P] + [E] \leftrightarrow [PE] \quad (13)$$

where the dissociation constant K_d is

$$K_d = \frac{[E][P]}{[EP]} \quad (14)$$

Assuming single site coverage, the fractional enzyme saturation on polymer, θ is:

$$\theta = \frac{[EP]}{[E_0]} = \frac{[P]}{[P] + K_d} \quad (15)$$

where $[E_o]$ is the total amount of enzyme in solution. These data can be transformed into a linear plot using the Scatchard equation:

$$\frac{\theta}{[P]} = \frac{1}{K_d} - \frac{\theta}{K_d} \quad (16)$$

If this equation is obeyed then K_d can be obtained by plotting θ/[P] vs. θ, which will yield a slope that is equal to the inverse of K_d.

The size distribution profile for 1000 mg/l of C-PAM in 0.2 M pH 6 phosphate buffer is shown in Figure 43. C-PAM exhibited a bimodal distribution with peaks in the range from 47-103 nm and 490-1068 nm which gave an effective diameter of 245±10 nm. When a10% v/v solution of alpha-amylase (3.8 mg/mL) was added to the same concentration of C-PAM and constant ionic strength, the C-PAM shifted the peaks to a range of 33-70 nm and 217-551 nm, decreasing the effective diameter to 165±2 nm.

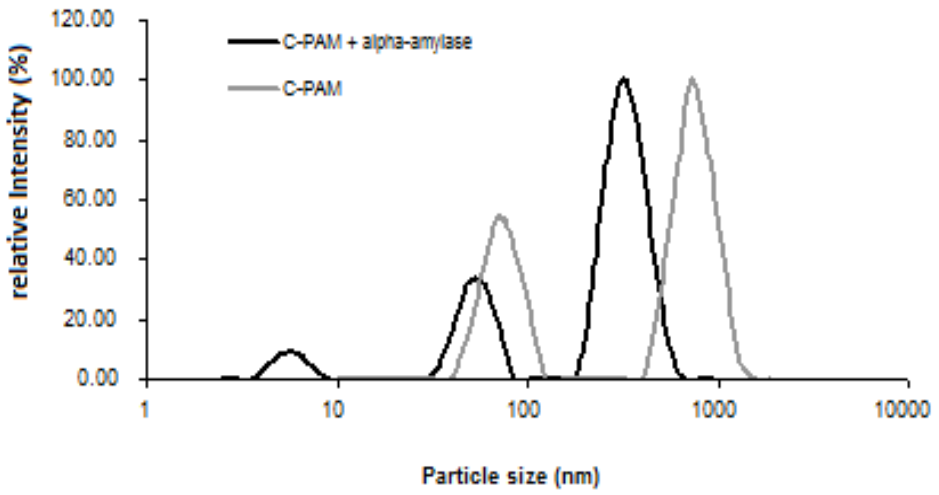

Figure 43: Particle size distribution of 1000 mg/l C-PAM XP10025 (gray) in 0.2 M pH phosphate buffer (pH 6), and the same concentration of C-PAM with the addition of 3.8 mg/l (10 v/v%) alpha-amylase (black).

The difference between the effective diameter of C-PAM (40 mol% cationicity), and the effective diameter of C-PAM in the presence of alpha-amylase, Δd, is plotted as a function of C-PAM concentration in Figure 44. At high C-PAM concentration the effect of the enzyme on polymer size is negligible and Δd approaches zero; at low polymer concentrations, intra-molecular charge repulsion is reduced due to the enzyme-C-PAM association, and the polymer contracts in size. The degree of polymer contraction was found to depend upon the amount of enzyme in solution so that a binding constant could be estimated from Δd. With the assumption that Δd varies linearly with the fraction of bound enzyme, θ,

$$\theta = 1 - \frac{\Delta d}{\Delta d_o} \tag{17}$$

where Δd_o is the change in polymer size in solution in the presence of excess enzyme. Adsorption isotherms for C-PAM to alpha-amylase association were constructed (Figure 45). Values of Δd used to determine adsorption isotherms are shown in Table 9. Dissociation constants were obtained from the Scatchard equation (Figure 46), and are shown in Table 10 as a function of C-PAM cationicity. The lowest cationicity C-PAM had the weakest affinity towards the enzyme with a dissociation constant of 24 $\pm$ 2 nM, while higher cationicity polymers (40% and 80%) exhibited stronger attraction to the enzyme.

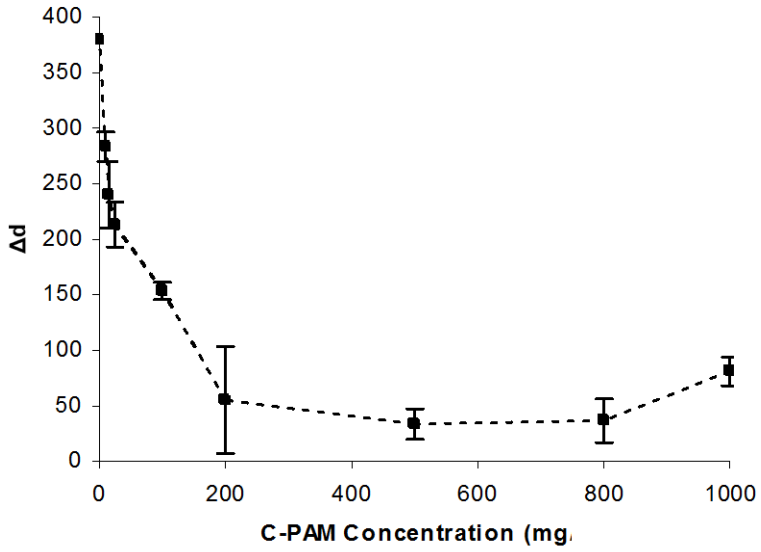

Figure 44: The change in effective diameter, Δd of 40% cationicity C-PAM with the addition of alpha-amylase as function of C-PAM concentration used to calculate alpha-amylase to C-PAM dissociation constants.

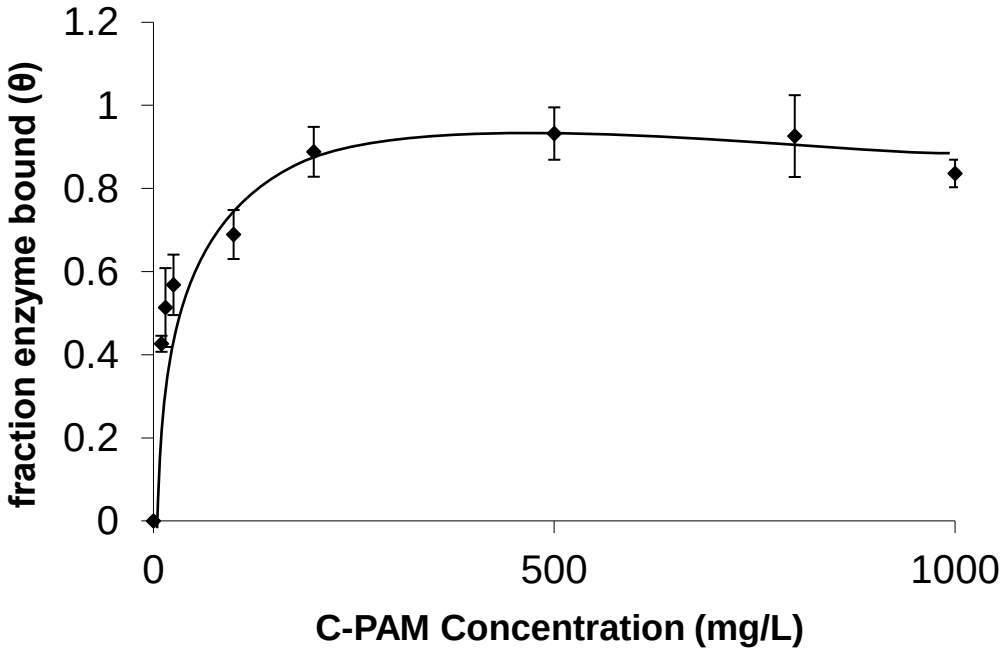

Figure 45: Adsorption isotherm for alpha-amylase to 40% cationicity C-PAM using dynamic light scattering.

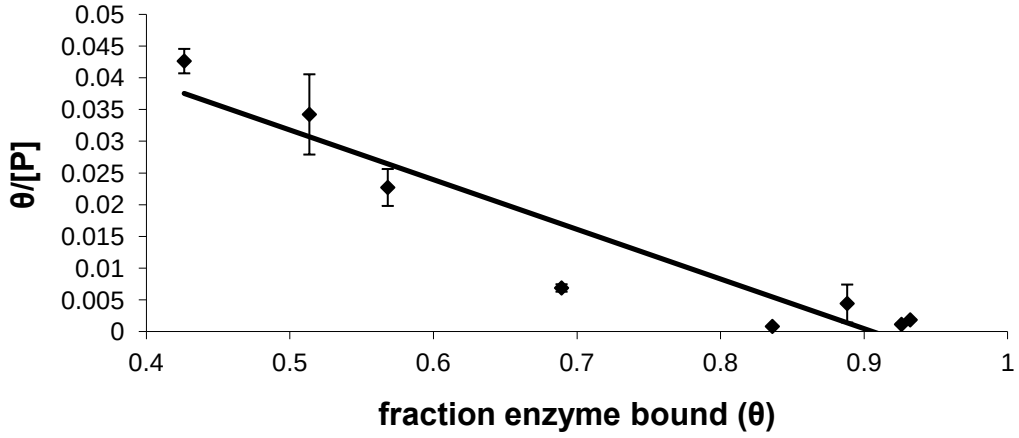

Figure 46: Plot of C-PAM to amylase isotherm data fitted to the Scatchard equation to determine K_d using dynamic light scattering (r^2=0.89).

Table 9: Dynamic light scattering data (effective diameter, nm) for C-PAM and C-PAM-alpha-amylase complex solutions. Corresponding differences in effective diameter (Δd), and calculated bound enzyme fractions are also listed. Values are averages of measurements done in triplicate.

C-PAM cationicity (%mol)	C-PAM concentration (mg/l) [P]	C-PAM effective diameter (nm) Without enzyme	C-PAM effective diameter (nm) With enzyme	Δd	θ
10	1000	164 ± 8	109 ± 3	54	0.89
	800	155 ± 1	100 ± 3	55	0.89
	500	163 ± 4	95 ± 31	68	0.86
	200	231 ± 13	91 ± 6	139	0.72
	100	302 ± 31	65 ± 10	237	0.52
	25	460 ± 39	41 ± 38	419	0.15
	15	453 ± 73	13 ± 1	440	0.11
	0			**494**	0.00
25	1000	218 ± 3	151 ± 7	67	0.82
	800	273 ± 31	163 ± 41	110	0.71
	500	256 ± 16	165 ± 22	92	0.76
	200	221 ± 10	174 ± 15	47	0.88
	100	326 ± 12	167 ± 19	159	0.58
	25	278 ± 80	39 ± 17	239	0.37
	15	292 ± 48	22 ± 8	270	0.29
	10	321 ± 81	13 ± 0	308	0.19
	0			**379**	0.00
40	1000	245 ± 19	165 ± 7	81	0.84
	800	221 ± 20	184 ± 20	37	0.93
	500	186 ± 17	152 ± 10	34	0.93
	200	186 ± 9	130 ± 88	55	0.89
	100	195 ± 12	41 ± 4	153	0.69
	25	242 ± 37	29 ± 4	213	0.57
	15	260 ± 56	20 ± 4	240	0.51
	10	300 ± 26	17 ± 1	283	0.43
	0			**380**	0.00
60	1000	193 ± 3	183 ± 10	11	0.98
	800	227 ± 15	193 ± 14	34	0.93
	500	186 ± 21	161 ± 13	25	0.95
	200	213 ± 14	174 ± 28	39	0.92
	100	322 ± 34	108 ± 6	213	0.57
	25	285 ± 14	15 ± 2	270	0.45
	10	420 ± 106	14 ± 0	405	0.18
	0			375	0.00
80	1000	257 ± 23	123 ± 3	134	0.73
	800	213 ± 8	138 ± 5	75	0.85
	500	212 ± 4	140 ± 2	72	0.85
	200	232 ± 7	149 ± 8	83	0.83
	25	250 ± 44	23 ± 3	226	0.54
	15	287 ± 39	19 ± 2	269	0.46
	10	307 ± 103	14 ± 1	293	0.41
	0				

Table 10: Dissociation constants K_d for alpha-amylase to C-PAM association using dynamic light scattering.

C-PAM (Cationicity)	K_d (nM)
XP10023 (10%)	24.0 ± 1.8
XP10031 (25%)	7.9 ± 0.8
XP10025 (40%)	3.4 ± 0.2
XP10032 (60%)	11.9 ± 0.3
XP10033 (80%)	3.4 ± 0.4

UV-vis spectrophotometry association studies

Dissociation constants were also obtained via UV-vis spectroscopy. Alpha-amylase absorbs light at 280 nm while C-PAM does not absorb in this region. When C-PAM was added to alpha-amylase, the absorbance of alpha-amylase increased slightly (Figure 47).

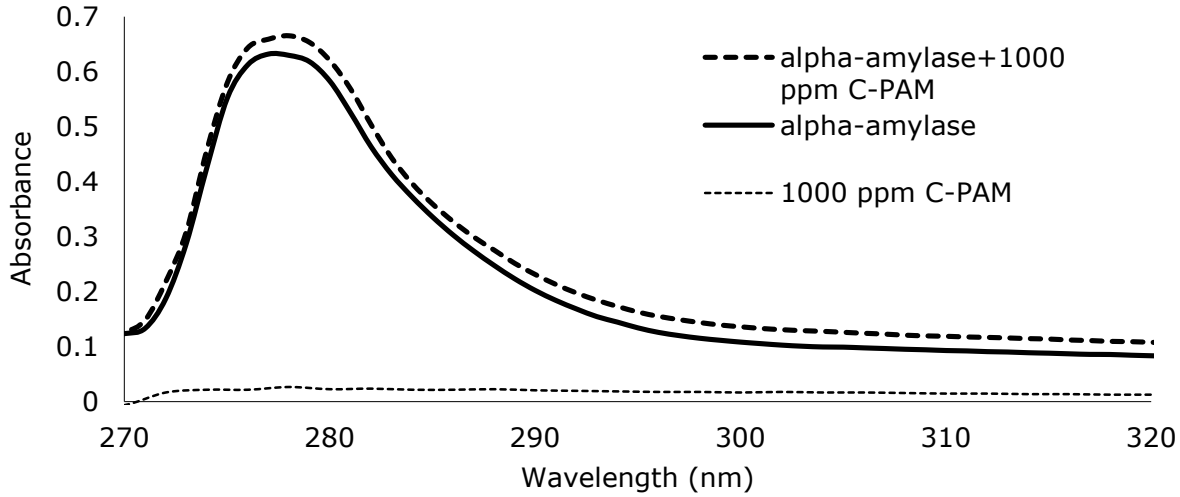

Figure 47: Amylase (0.38 mg/mL) in 0.2 M in pH 6 phosphate buffer (solid line) and in the presence of 1000 mg/l C-PAM 10025 (dashed). Absorbance of C-PAM alone is also shown (dotted). Each plot is an average of 3 measurements.

The dissociation constant, K_d, for the alpha-amylase-C-PAM complex was calculated from the absorption difference induced by C-PAM addition. To enzyme solutions of 0.38 mg/mL, C-PAM concentrations from 1-1000 mg/l were added, and spectra recorded from 270-320 nm. With the assumption that ΔA, the absorption difference at 290, is proportional to the concentration of the amylase-C-PAM complex, [EP], and ΔA_{max} is equal to the absorption difference at the saturated enzyme point, then θ, the fraction of bound enzyme as a function of C-PAM concentration (Figure 48) could be obtained according to the equation,

$$\frac{\Delta A}{\Delta A_{\max}} = \frac{[EP]}{[E_o]} = \theta \qquad (18)$$

from which the dissociation constant could be determined by a Scatchard plot (Figure 49). K_d from spectroscopy listed in Table 11 were on the order of those obtained from DLS with similar trends in data. C-PAM (10 mol% cationicity) had the weakest binding, while 80 mol% cationicity C-PAM had the strongest.

Table 11: Dissociation constants K_d for amylase to C-PAM association using spectrophotometry

C-PAM (Cationicity)	K_d (nM)
XP10023 (10%)	15.7 ± 5.0
XP10025 (40%)	7.5 ± 2
XP10033 (80%)	2.4 ± 0.2

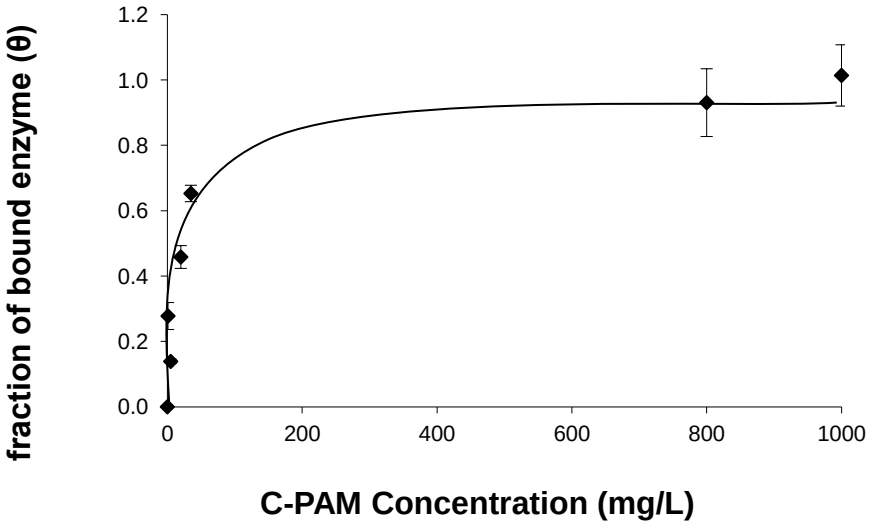

Figure 48: Adsorption isotherm for alpha-amylase to 40% cationicity C-PAM using spectrophotometry.

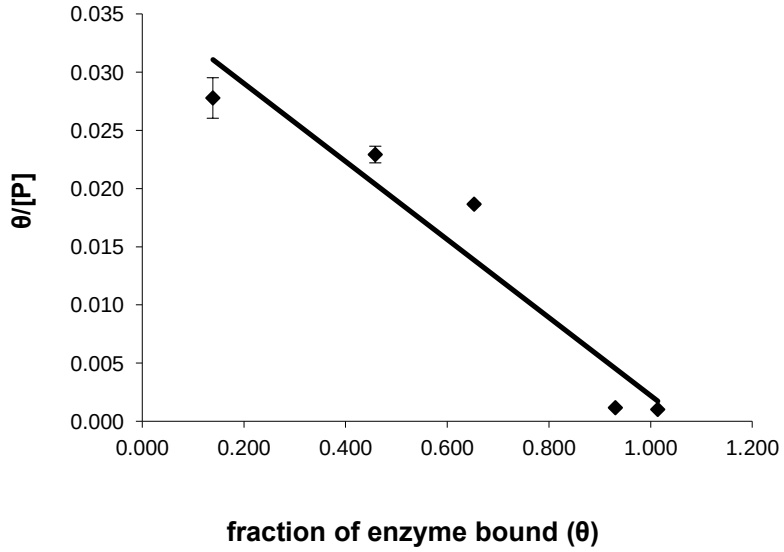

Figure 49: Plot of C-PAM to isotherm data fitted to the Scatchard equation to determine K_d using spectrophotometry (r^2=0.91).

4.3.3. Effect of C-PAM on enzyme binding to cornstarch

The purpose of this study was to determine if C-PAM inhibited or enhanced alpha-amylase binding to starch. Binding of alpha-amylase to starch was fitted well by a typical adsorption isotherm (Figure 50A), and a linearized Scatchard plot (Figure 50B). The dissociation constant of 3401 ug/mL was consistent with other literature values (Warren, et al., 2011). Dissociation constants for alpha-amylase to starch in the presence of various C-PAM polymers are shown in Table 12.

In the presence of C-PAM, the dissociation constant was significantly lower, indicating enhanced binding in the presence of C-PAM. Higher C-PAM cationicity elicited stronger binding than did lower cationicity. As a function of C-PAM concentration, lower concentration was favored over higher concentration. C-PAM at a concentration of 300 ppm gave the lowest level of binding among the C-PAM containing systems.

Table 12: Dissociation constants (K_d) for alpha-amylase to cornstarch in the presences of C-PAM at varying concentration and mol% cationicity

C-PAM mol% cationicity	C-PAM Concentration (µg/mL)	K_d (µg/mL)[a]
-	0	3401 ± 163
40	30	163 ± 13
40	100	66 ± 7
40	300	232 ± 14
10	100	200 ± 8

[a] K_d values presented as mean values ± standard deviation

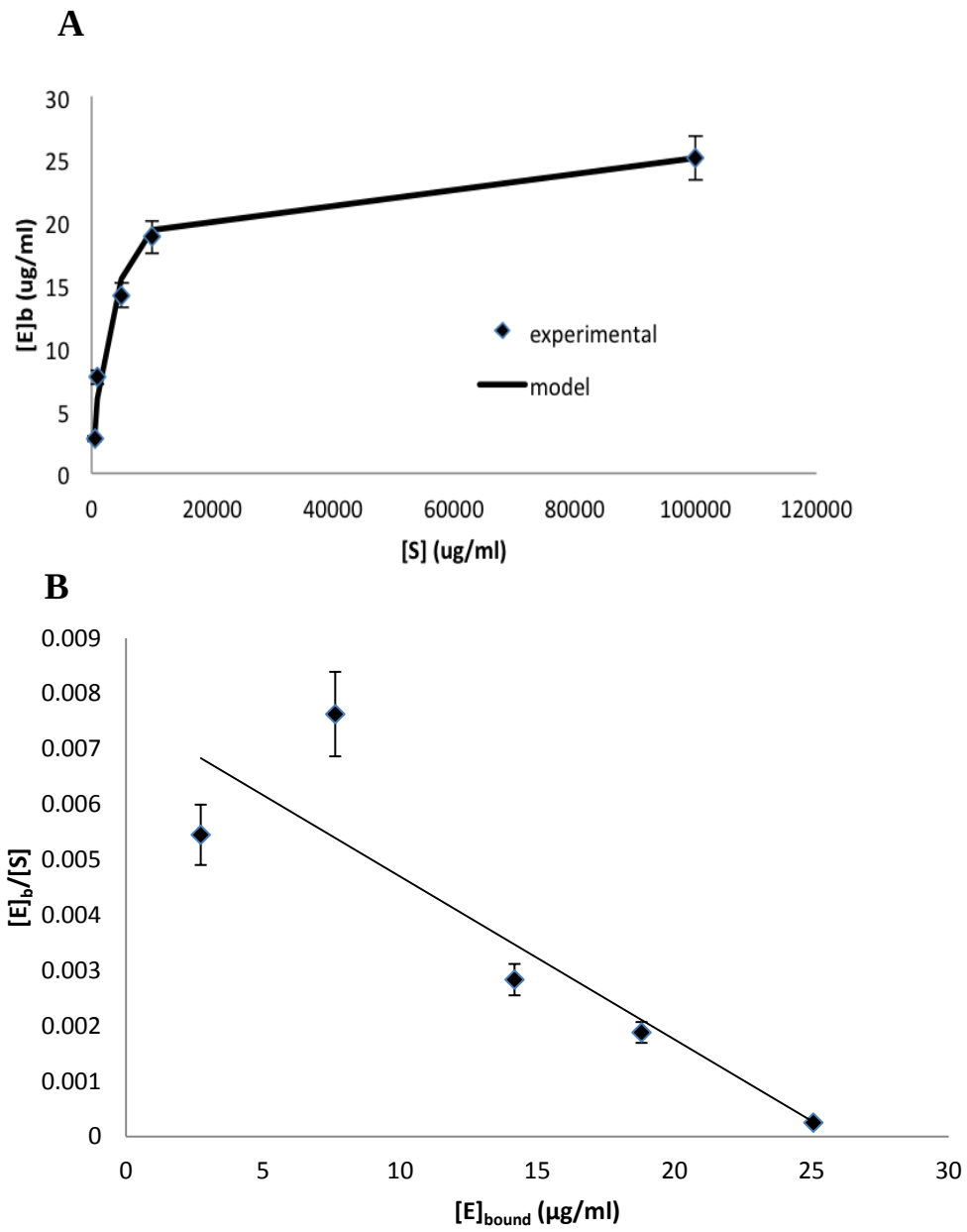

Figure 50: (A) Alpha-amylase adsorption isotherm to cornstarch granules, and (B) a plot of the adsorption data fitted to the Scatchard equation used to calculate $K_{d.}$

4.3.4. Effect of C-PAM on enzyme activity

Effect of C-PAM addition method on alpha-amylase activity

All three mixtures of C-PAM and enzyme shown in Table 13 gave equal amounts of activity demonstrating that the sequence of addition is unimportant. Since no significant difference was seen, C-PAM was added to the substrate solutions for all subsequent activity studies.

Table 13: Effect of C-PAM preparation method on the relative activity of alpha-amylase

Description	Relative amylase activity[a] (%)
1. No C-PAM (control)	100 (3.4)
2. Addition of C-PAM to substrate	130 (4.4)
3. Addition of C-PAM to enzyme	127 (4.3)
4. Addition of C-PAM to enzyme and substrate	126 (4.2)

[a] Figures in parentheses represent actual activity (U/mL) of the enzyme. Activity of regular cornstarch with no C-PAM was taken as 100%.

Effect of C-PAM concentration on alpha-amylase and glucoamylase activity

The effect of C-PAM on the activity of glucoamylase and alpha-amylase is shown in Table 14 and Figure 51. While C-PAM decreased the activity of glucoamylase to a small extent, it increased that of alpha-amylase by as much as 150%. The extent of increase was dependent on C-PAM concentration. Below 125 ppm, C-PAM had no significant effect. Further increases in concentration incrementally increased activity until a maximum activity was reached at a concentration of 833 ppm, before declining in activity upon further addition of C-PAM.

Table 14: Effect of C-PAM at three different concentrations on glucoamylase activity

C-PAM concentration (ppm)	Mass ratio of starch to C-PAM	Glucoamylase activity (U/mL)[a]	Relative % activity
0	-	152±4	100
2	5000:1	132±9	87
17	500:1	136±5	90
167	50:1	124±6	82

[a] significant at p <.001

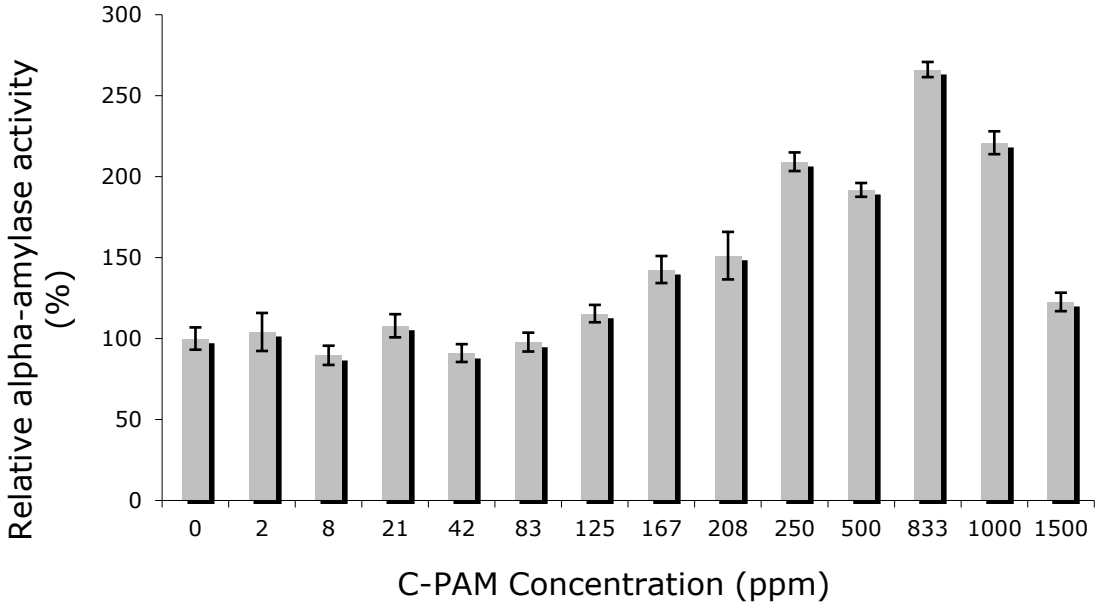

Figure 51: Effect of C-PAM on alpha-amylase activity

Table 15 shows the effect of Ca^{2+} concentration on activity with and without C-PAM. Alpha-amylase exhibited the highest activity in the presence of C-PAM without any addition of Ca^{2+} (sample 4). A 0.1 mM $CaCl_2$ concentration gave the highest activity without C-PAM. Increasing $CaCl_2$ concentration further decreased the activity of the enzyme. Addition of C-PAM and $CaCl_2$ reduced the

activity of the enzyme, likely due to charge reversal and repulsion caused by a solution excessive ionic strength.

Table 15: Effect of ionic salt concentration with and without C-PAM on the activity of alpha-amylase

Sample	C-PAM concentration (mg/l)	$CaCl_2$ concentration (mM)	U/mL activity	Standard deviation	Relative activity (%)
1	0	-	3.0	0.1	100
2	2	-	3.0	0.4	100
3	17	-	3.7	0.3	120
4	167	-	4.4	0.6	145
5	0	0.1	3.4	0.2	112
6	0	1	3.0	0.2	98
7	0	9	2.7	0.0	88
8	3	1	2.8	0.2	94
9	17	1	2.9	0.3	97
10	17	0.2	3.0	0.10	99

Effect of pH on enzyme activity with and without C-PAM

Figure 52 and Figure 53 show the relative activity of glucoamylase and alpha-amylase as a function of pH. Glucoamylase had an optimum activity at a pH of 4, but was relatively stable at in the range of 3-8 pH. Alpha-amylase had optimum activity at a pH of 6 with or without the addition of C-PAM. C-PAM increased the relative activity of alpha-amylase in the range of 3-8 pH.

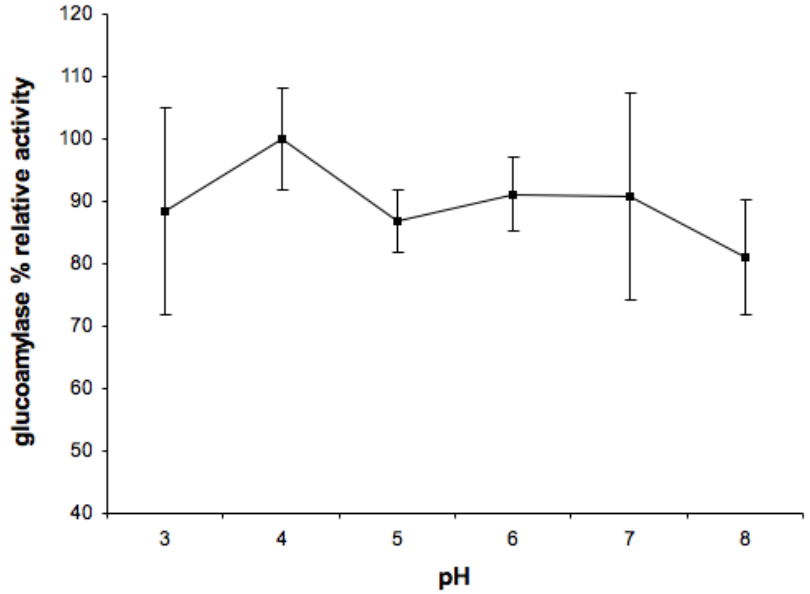

Figure 52: Effect of pH on glucoamylase activity. Activity of regular cornstarch with no C-PAM at pH 6 is taken as 100%.

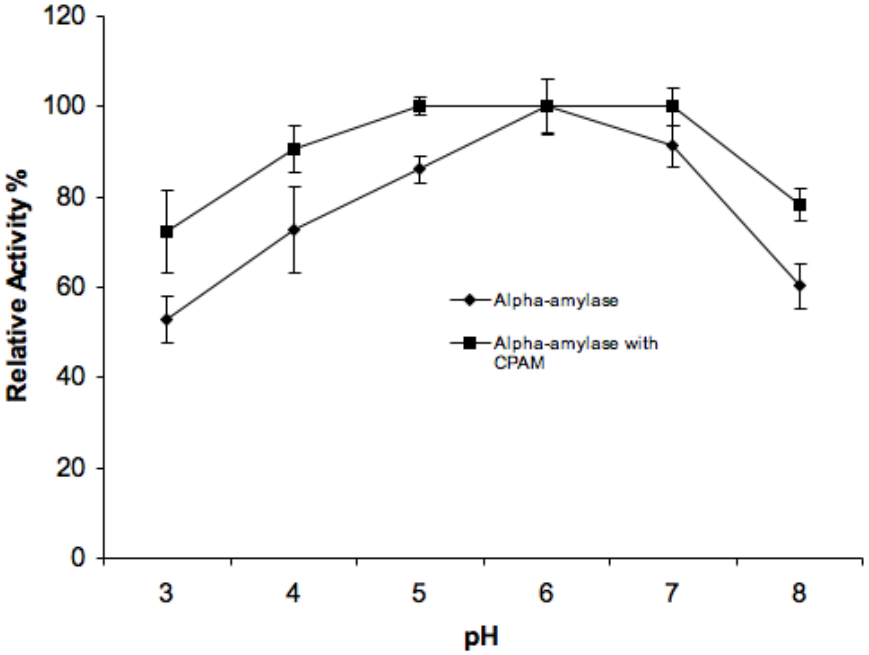

Figure 53: Effect of pH on alpha-amylase with and without C-PAM at 208 ppm. Activity of regular cornstarch with no C-PAM at pH 6 is taken as 100%.

Effect of temperature on enzyme activity stability with and without C-PAM

Figure 54 and Figure 55 show the relative activity of glucoamylase and alpha-amylase, respectively, with and without C-PAM as a function of temperature. Optimum activities for glucoamylase and alpha-amylase were at 70 ^{o}C, though glucoamylase remained relatively stable (retaining > 80% activity) for all temperatures except 90 ^{o}C. C-PAM yielded no significant increased activity for either enzyme against temperature, although it did seem to increase the stability of alpha-amylase at temperatures below 70 ^{o}C (Figure 56) to (at best) a small extent.

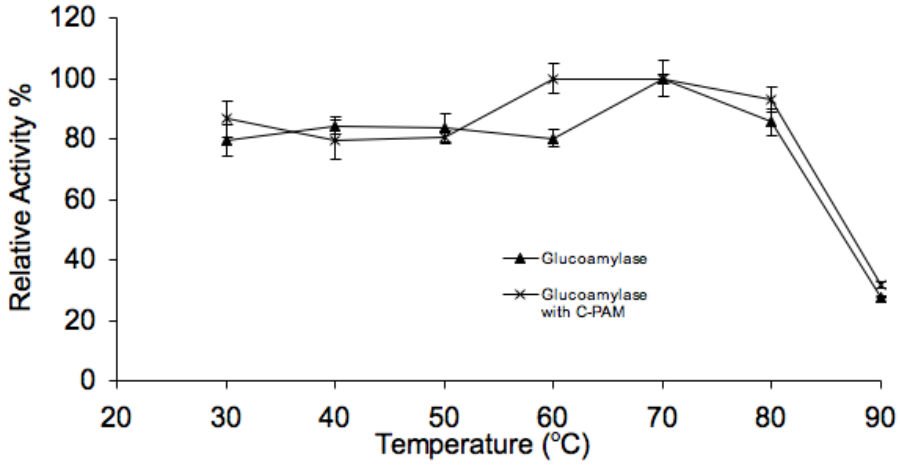

Figure 54: Effect of temperature on the activity of glucoamylase with and without 208 ppm C-PAM. Activity of regular cornstarch with no C-PAM at 70 ^{o}C is taken as 100%.

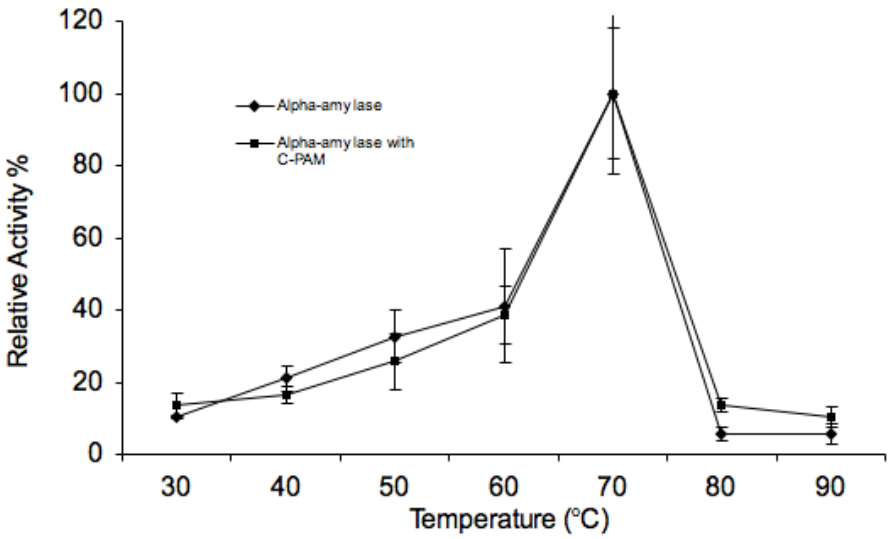

Figure 55: Effect of temperature on alpha-amylase activity with and without 208 ppm C-PAM. Activity of regular cornstarch with no C-PAM at 70 ^{o}C is taken as 100%.

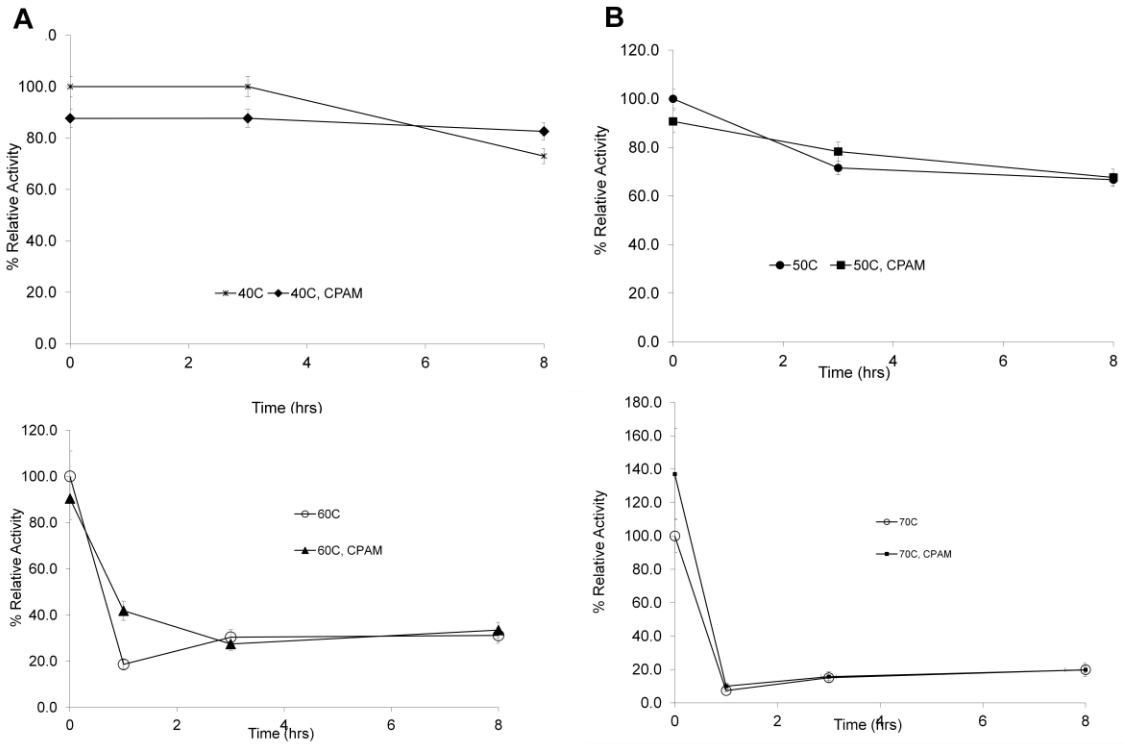

Figure 56: Effect of C-PAM (208 ppm) on alpha-amylase stability at (A) 40 ^{o}C, (B) 50 ^{o}C, (C) 60 ^{o}C, and (D) 70 ^{o}C.

4.3.5. Effect of substrate amylose/amylopectin ratio

Figure 57 shows the effect of amylose to amylopectin ratio on the activity of alhpa-amylase without the presence of C-PAM. Consistent with the literature, the activity of alpha-amylase is lowest for the high amylase cornstarch, but increases as the amylose content decreases. Due to the linear ordered conformation of the amylase polymer, it forms strong hydrogen bonds with water in solution. As a result, the amylase is relatively stable and more resistant to attack by the amylase. On the other hand, amylopectin is a much larger polymer with a more disordered structure and is readily hydrolyzed by alpha-amylase. When C-PAM was added, it significantly enhanced the activity of amylose. Amylose is already more susceptible to solubilization due to its tendency to form hydrogen bonds with water. When the C-PAM is added, the attraction of the amylose to the C-PAM further promotes solubilization of the amylose via electrostatic interactions. The increased concentration of soluble starch increases the availability of starch for enzyme to attack. In contrast, the activity of alpha-amylase towards amylopectin was inhibited in the presence of C-PAM. This is likely due to the insolubility of amylopectin.

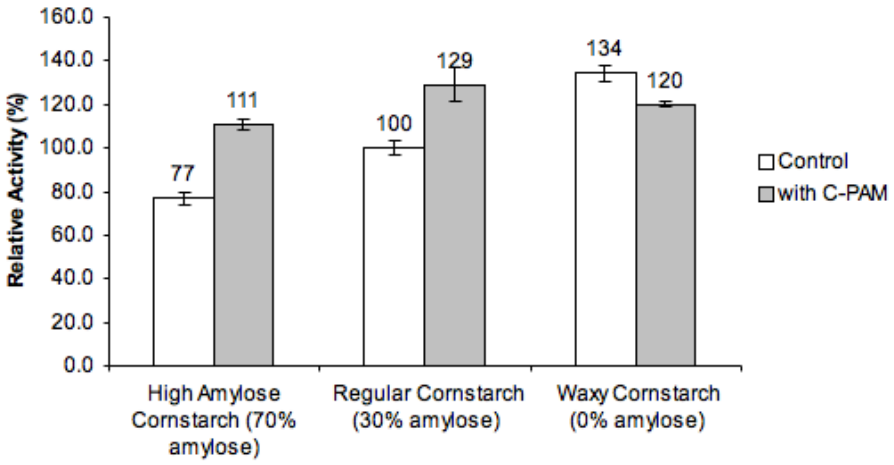

Figure 57: Activity with and without C-PAM as a function of substrate amylose/amylopectin ratio.

4.3.6. Discussion of enzyme-C-PAM interaction

DLS and UV-vis spectroscopy results both showed that there is a strong attraction between C-PAM and alpha-amylase. The dependence of the dissociation constant on mol% cationicity suggests it is largely driven by electrostatic interactions. Attraction was strongest with higher cationicity C-PAM as expected with polyelectrolytes and surfaces of opposite charge (Claesson, et al., 2005). As was shown and discussed previously, C-PAM is also strongly attracted to starch. As a result, the synergistic attraction of enzyme to C-PAM and starch to C-PAM led to a stronger level of alpha-amylase to starch binding as mediated by the C-PAM.

Since both starch and enzyme have slight negative charges, there is some level of repulsion that must be overcome before alpha-amylase can bind to starch.

When the C-PAM is adsorbed to the starch or enzyme, it partially neutralizes the surface thereby reducing the repulsion felt between starch and enzyme, thus increasing affinity of the enzyme towards starch. Lower cationicity C-PAM had a smaller effect because higher levels of polymer are able to adsorb to the starch and enzyme surfaces. If too many adsorption sites are blocked by polymer, C-PAM addition will be less effective. In much the same way, too high a concentration of C-PAM in solution will eventually began to block too many adsorption sites, thereby reducing the effectiveness of C-PAM addition. This explains the weaker binding seen in the presence of high C-PAM concentration.

C-PAM enhanced binding leads to increased alpha-amylase activity. The finding that there was no difference in activity among the different methods of mixing C-PAM in solution (Table 13) reinforces previous findings that C-PAM has a strong attraction to both enzyme and starch, and the synergistic effect of starch, enzyme, and C-PAM results in increased activity. C-PAM did not enhance glucoamylase activity (Table 14). One possible reason is the size difference between the alpha-amylase substrate (starch), and glucoamylase substrate (sugar molecules). Due to the large size of starch granules (microns), C-PAM is able to adsorb on the starch surface. On the other hand, glucoamylase is much smaller (nanometers), so C-PAM is unable to effectively adsorb to the surface, instead wrapping around the particles, resulting in inhibition of glucoamylase binding and activity.

Enzyme stabilization by polyelectrolytes has been studied by many others (Hatti-Kaul & Andersson, 1999; Khalil, et al., 2001; Yoon & Robyt, 2005). The observed stabilization of alpha-amylase against pH and temperature (Figure 53 and Figure 56) is likely a result of the formation of the C-PAM-starch-enzyme network sustaining the enzyme at the optimal conformation for activation.

4.4. Hydrolysis of Cornstarch

4.4.1. Initial studies of cornstarch hydrolysis by alpha-amylase with C-PAM

The previous sections focused on the interaction of starch and C-PAM, as well as of enzyme and C-PAM in solution. It was shown that the C-PAM increased the amount of starch solubility and alpha-amylase enzyme binding. In this section, the results and discussion will focus on the hydrolysis of cornstarch and will show that the addition of the C-PAM polymer can increase the rate and yield of enzymatic hydrolysis of starch as well as fiber substrate.

An initial lab scale study of cornstarch hydrolysis was conducted with 1 w/v% solutions of cornstarch at 50 ^{o}C. The first sample and third samples contained only 1 w/v% solution of cornstarch. The second and fourth samples contained 1 w/v% cornstarch with 40 mol% cationicity C-PAM at 100 ppm concentration. All four samples were place in a water bath at 50 ^{o}C that was shaken at an rpm of 120. To the third and fourth samples, 1 v/v% alpha-amylase was added to start the hydrolysis reaction. Samples were taken periodically and analyzed for

glucose. As a control, 100 ppm C-PAM samples were also measured. In addition, samples taken from the experiment were observed under light microscopy and analyzed using ImageJ analysis software.

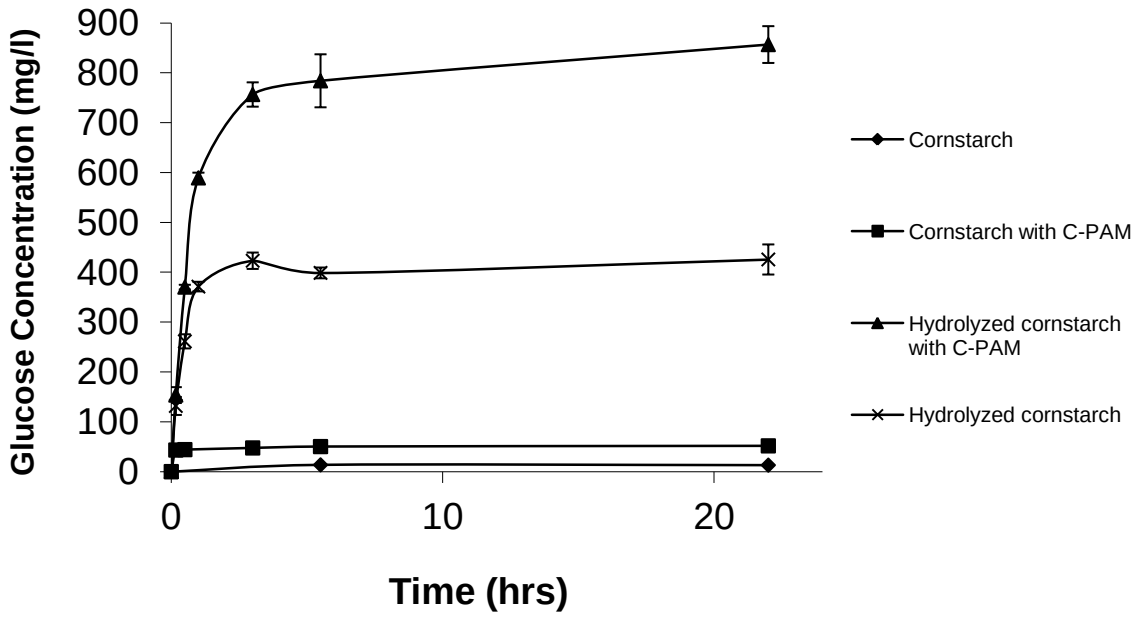

Figure 58: 1 w/v% Cornstarch at 50 ^{o}C, in the presence of 100 ppm (40 mol% cationicity) C-PAM, hydrolyzed by 1% alpha-amylase, and hydrolyzed with alpha-amylase in the presence of 100 ppm C-PAM.

C-PAM had a significant effect on the hydrolysis of cornstarch as shown in Figure 58. After 24 hours, cornstarch had produced a small amount of glucose (13±0.6 mg/l), while cornstarch in the presence of C-PAM produced 52±2 mg/l of glucose. C-PAM induced a significantly greater amount of glucose than did starch alone, consistent with the TOC solubility data of Figure 30 that showed increased solubility in the presence of C-PAM. Hydrolysis of cornstarch with alpha-amylase produced 426±30 mg/l and hydrolyzed cornstarch in the presence of C-PAM

produced 857±37 mg/l. Photographic images of the samples taken from the experiment are shown in Figure 59. There was no difference between the starch (I) and starch + C-PAM (II) (non-hydrolyzed) samples visually.

Hydrolyzed samples (III and IV) had considerably fewer granules in solution than the unhydrolyzed samples, as the majority of granules had disintegrated.

Time (hours)	(I) Cornstarch	(II) Cornstarch with100 ppm C-PAM	(III) Hydrolyzed cornstarch	(IV) Hydrolyzed cornstarch with 100 ppm C-PAM
(A) 0.5	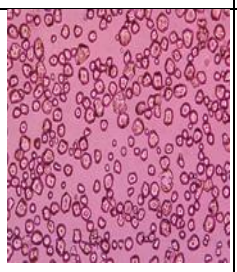	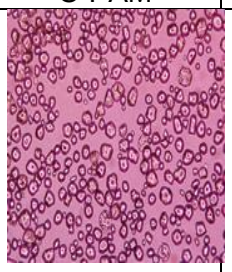	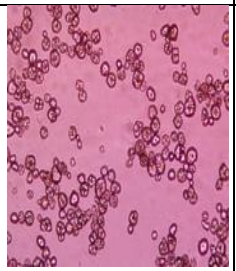	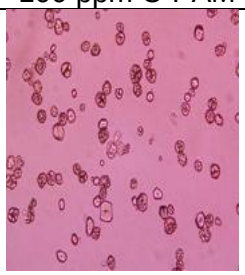
(B) 3	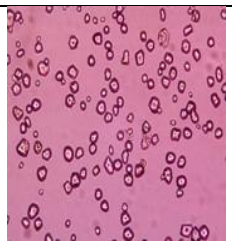		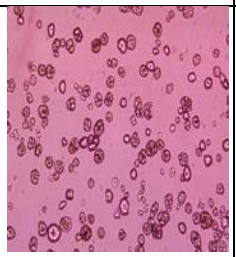	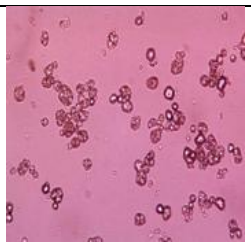
(C) 24	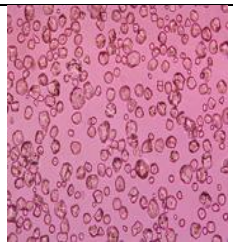	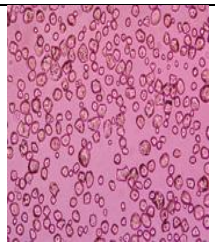	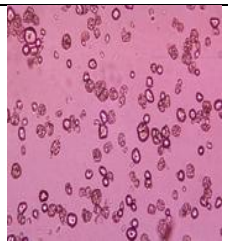	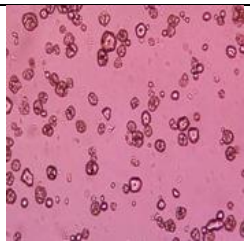

Figure 59: Images of starch granules samples taken from the initial cornstarch hydrolysis experiment at 50 ^{o}C of 1 w/v% cornstarch (I), 1 w/v% cornstarch with 100 ppm C-PAM (II), hydrolyzed cornstarch (1 w/v%) (III), and hydrolyzed cornstarch (1 w/v%) with 100 ppm C-PAM (IV) at 30 min (A), 3 hours (B), and 24 hours (C).

The hydrolyzed starch samples with C-PAM appeared to have fewer granules as compared to the hydrolyzed sample without C-PAM. The average number of granules in the images from a total of 6 images for the starch + C-PAM images was 103±14 granules per image, while that of the starch only was 123±8 granules per image. Overall, there was no significant difference in the average particle size of the granules between different samples with average particles sizes for the group 1, 2, 3, and 4 of 14.6±9, 14.4±9, 15.3±8, and 13.8±9 μm, respectively.

4.4.2. Cornstarch hydrolysis by glucoamylase with C-PAM

There was no significant effect of C-PAM on saccharification by glucoamylase. Saccharification of 8 w/v% cornstarch at 50 ^{o}C for 3 hours with C-PAM (100 mg/l) produced a glucose yield of 62,289± 640 mg/l, while without C-PAM 62,607±1470 mg/l was produced. Because C-PAM addition offered no further enhancement to hydrolysis with glucoamylase, the remaining hydrolysis experiments focused on hydrolysis with alpha-amylase.

4.4.3. Effect of C-PAM properties: concentration, cationicity, MW, and addition point

Figure 60 and Figure 61 show hydrolysis of cornstarch by alpha-amylase with C-PAM as a function of C-PAM cationicity and concentration, as measured by Brix level. As a function of cationicity, 40 mol% increased sugar production by the greatest amount (7%), followed by 80 mol% (5%). Addition of 10 mol% reduced production of glucose by 20%. As a function of concentration, sugar yield was

optimal with lower concentration, increasing yield with 30 and 100 ppm C-PAM by 12% and 7%, respectively. C-PAM at high concentration (300 ppm) reduced yield by approximately 12%.

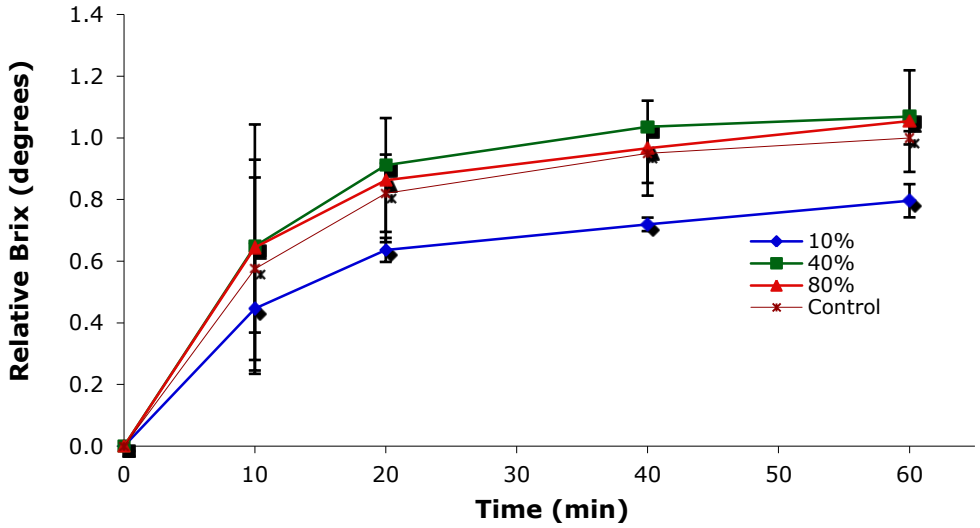

Figure 60: Effect of C-PAM cationicity on sugar generation at 70 ^{o}C. C-PAM concentration is 100 ppm.

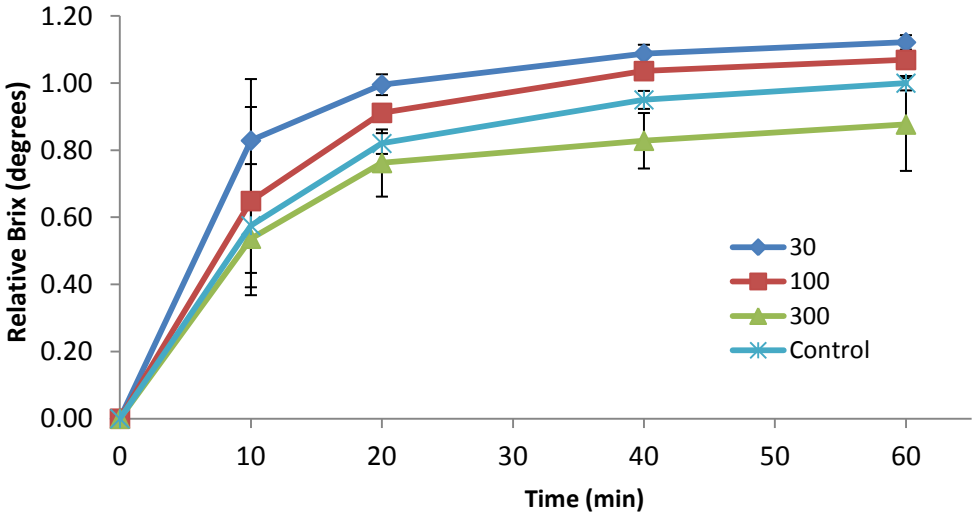

Figure 61: Effect of C-PAM concentration (XP10025) on sugar generation at 70 ^{o}C. C-PAM concentration is 100 ppm.

Viscosity was measured using a Grace Instruments M3500 viscometer. Due to the limitations of the viscometer, cornstarch concentration for these experiments was decreased to 8 w/v%. Three different types of C-PAM with cationicity of 10%, 40%, 80% at concentrations of 30, 100, and 300 mg/L were used in this experiment. The viscosity of the cornstarch suspensions (control), or cornstarch-C-PAM mixtures was measured as they were heated from 20 ^{o}C to 90 ^{o}C (2.5 ^{o}C/min) at a shear rate of 400 s^{-1}. Peak viscosities and sugar yield as measured by Brix analysis are reported in Table 18. Trends that were observed at 30 w/v% cornstarch concentration were upheld at 8 w/v% cornstarch concentration. The effect of C-PAM cationicity on peak viscosity and Brix is illustrated in Figure 62. The mirror-image relationship demonstrates that hydrolysis is suppressed at high viscosity. High viscosity is known to reduce reaction rates by affecting Brownian motion and the conformational changes undergone by the enzyme. In this case the polymer can agglomerate the substrate thereby reducing the surface area. This is likely the case at 10% cationicity. The particles take on a net positive charge at higher cationicity, and repulsion among particles reduces the degree of agglomeration. This effect is well established in the literature of sludge dewatering. A similar effect is seen in Figure 63, which illustrates the effect of changing concentration of a 40% cationicity C-PAM on Brix and viscosity. The agglomeration that occurs at low c-PAM concentration is reversed as the c-PAM concentration is raised. For this application a 40% cationicity C-PAM is optimal. Again, the hydrolysis is most efficient at low viscosity. Increasing C-PAM concentration is analogous to using a higher charged c-PAM in the previous

example in that charge repulsion reduces the tendency of the particles to agglomerate.

Table 16: Peak viscosity vs. sugar yield during hydrolysis for 8 w/v% cornstarch as a function of C-PAM cationicity and concentration

Sample	Peak viscosity (cP)	Sugar yield (^{o} Brix)
Cornstarch	104±4	7.75±.1
Cornstarch and 10% cationicity C-PAM (30 ppm)	148±3	7.65±.05
Cornstarch and 40% cationicity C-PAM (30 ppm)	85±7	8.40±.1
Cornstarch and 40% cationicity C-PAM (300 ppm)	196±15	8.25±.1
Cornstarch and 80% cationicity C-PAM (30 ppm)	76±5	8.25±.1

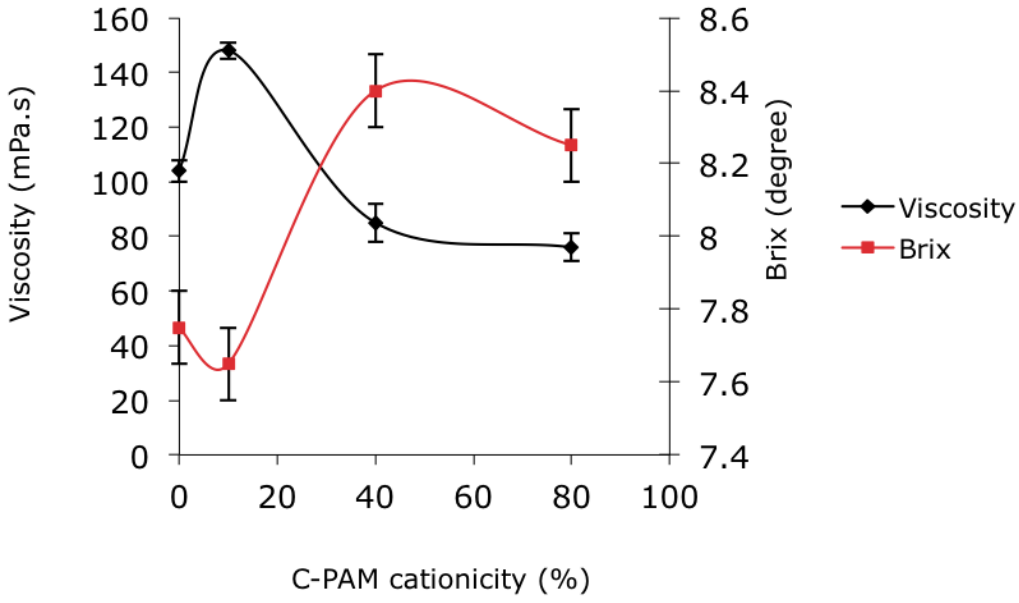

Figure 62: Peak viscosity (mPa·s) and hydrolysis yield (degree Brix) as a function of C-PAM cationicity.

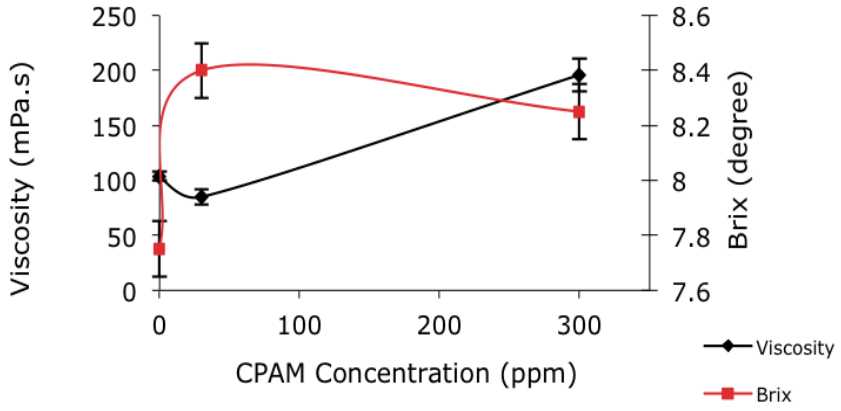

Figure 63: Peak viscosity (mPa·s) and hydrolysis yield (degree Brix) as a function of C-PAM concentration

The effect of C-PAM molecular weight on 8 w/v% cornstarch is shown in Table 17. Sugar yield was increased at all molecular weights tested. The highest molecular weight polymer yielded a slightly lower amount of sugar than the lower molecular weight polymers.

Table 17: Effect of molecular weight on sugar yield during hydrolysis of 8 w/v% cornstarch with C-PAM XP10025 at 30 ppm

C-PAM average molecular weight range, M_n x10^6 Daltons	Sugar yield (degree Brix)
No C-PAM (control)	7.75±.1
5	8.40±.1
9	8.50±.1
11	8.15±.1

The point at which C-PAM was added to the system affected total yield of glucose (Table 18). When C-PAM was added prior to addition of alpha-amylase (and reaction start), glucose yield was significantly greater than the control (p-

value = 0.0335). When C-PAM was added after enzyme addition, glucose production was significantly less than that of the control (p-value = 0.0397).

Table 18: Effect of C-PAM addition point: glucose yield after one hour hydrolysis at 70 ^{o}C

Sample description	Glucose yield (mg/l)
Control	13,115 ± 207
C-PAM added before enzyme	13,539 ± 102
C-PAM added after enzyme	12,733 ± 75

4.4.4. Effect of enzyme loading

The degree to which C-PAM can lower enzyme dosage is shown in Figure 64, where the alpha-amylase dose was progressively reduced in the presence of 100 ppm C-PAM. The cornstarch was present at 30% and the enzyme was applied at 0.067% by volume. The hydrolysis was run at 70 ^{o}C. Interpolation shows that the C-PAM reduces the enzyme loading required to produce the same Brix level obtained in the control by 62%. The C-PAM is cheaper than the enzyme so major savings in enzyme costs are possible.

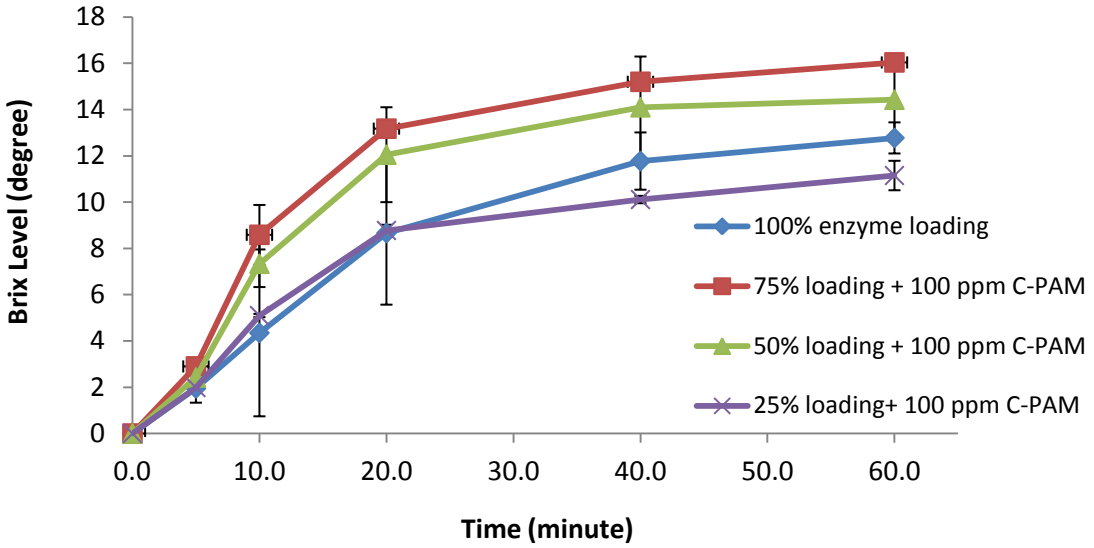

Figure 64: Effect of enzyme load with C-PAM at 100 ppm for hydrolysis of 30% cornstarch.

4.4.5. Effect of process conditions: temperature and agitation

Hydrolysis of 1 w/v% cornstarch with concentrations of C-PAM at 50 ^{o}C and 70 ^{o}C is shown in Figure 65. At this starch concentration, C-PAM greatly enhanced hydrolysis at pre (50 ^{o}C) and post (70 ^{o}C) gelatinization temperatures. At both temperatures, the yield of glucose increased with C-PAM concentration. C-PAM yielded more glucose at 50 ^{o}C than 70 ^{o}C at a constant C-PAM concentration.

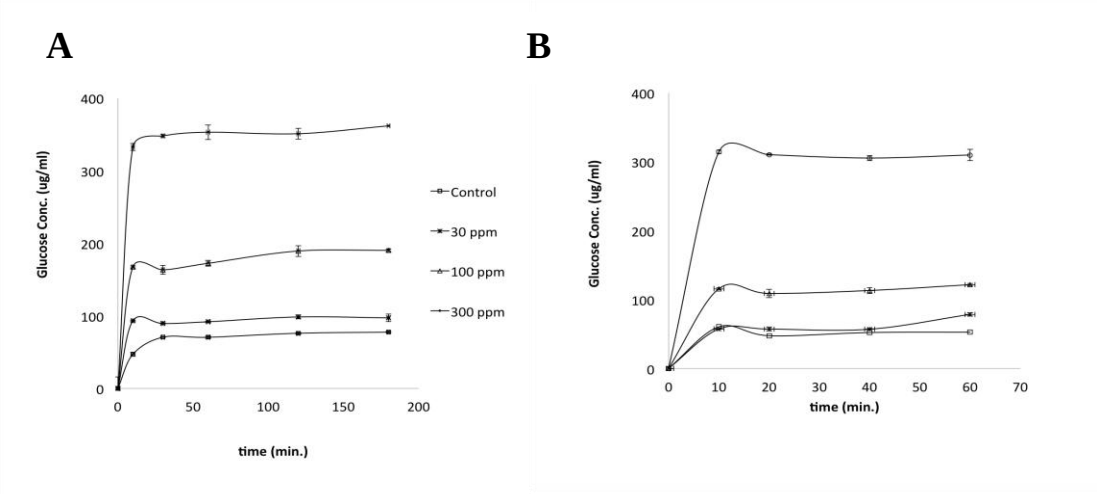

Figure 65: Temperature effects on C-PAM aided hydrolysis for hydrolysis of 1% w/v cornstarch at (A) 50 ^{o}C, and (B) 70 ^{o}C at 0.004 v/v% enzyme loading.

Relative sugar yields with and without C-PAM at three levels of agitation are shown in Figure 66. Consistent with literature values (Ariff et al., 1997), sugar yield increased as degree of agitation increased for hydrolysis of cornstarch. In the presence of C-PAM, hydrolysis at the highest level of agitation was slightly inhibited by the addition of C-PAM.

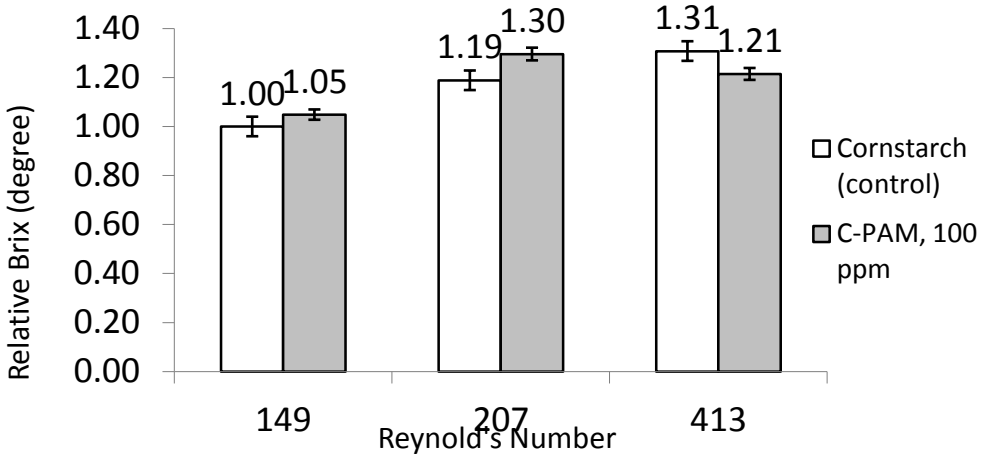

Figure 66: Effect of agitation on C-PAM aided hydrolysis of 30 w/v% starch with an enzyme load of 0.6 v/v%.

4.4.6. Comparison of fiber to cornstarch hydrolysis

A study was performed to compare the hydrolysis of cornstarch to fiber in the presence of cationic polyelectrolytes with varying properties. The fiber substrate was a softwood bleached Kraft fiber, and the starch substrate was regular cornstarch (27% amylose, 73% amylopectin) purchased from Sigma-Aldrich. Ashland Water Technologies supplied the polyelectrolytes with varying properties for this study, which are summarized in Table 19. C-PAM samples came in either emulsion or dry powdered solids form. The chemical structure of the monomer units in the polymers used in the experiment are shown in Figure 67. Using charge titration, polymer charges (C/g) were determined for each of the polymer series, to further characterize the C-PAM samples. As mol% cationicity data was not explicitly given values were estimated based on a calibration of known polymer cationicity values.

Group 1 series polymers was a branched co-polymer of acrylamide (AM), and [2-(acryloyloxy)ethyl]trimethylammonium chloride (Q-9) of increasing cationicity. Group 2 and Group 3 series were linear (AM/Q-9) polymers of increasing cationicity, with the exception of sample K295FL which was the only hompolymer of the sample set, consisting of only Q-9. Groups 4 and 5 were C-PAM samples which came in dry powdered form. Group 4 was a series consisted of linear polymers with AM and Q-9 co-monomers, of increasing cationicity and viscosity. Group 5 was also a linear polymer, which made up of AM and the (3-acrylamidopropyl) trimethylammonium chloride monomer (APTAC) of increasing

cationicity. All of the polymers had molecular weights in the range from 2-5 10^6 Daltons. Overall, Group 4 had the highest cationicity. For fiber experiments, 1 w/v% fiber was added to C-PAM so that the final concentration of C-PAM was 500 ppm. For starch samples, 1 w/v% starch was added to C-PAM of 100 ppm final concentration. C-PAM concentrations were determined in a previous experiment to be optimum for each substrate. To start the reactions, 1 v/v% cellulase or 1 v/v% amylase was added to the fiber and starch samples. Each sample was placed in a water bath at 50 ^{o}C, and agitated by shaking at 150 rpm. The samples were allowed to react for six hours before performing glucose analysis of each of the samples.

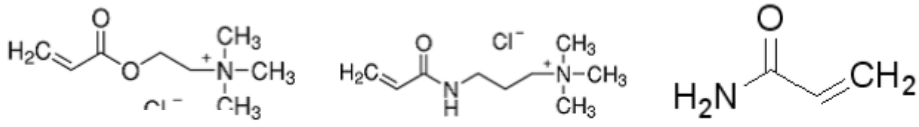

Figure 67: Monomer units of C-PAM used in fiber vs. cornstarch screening: (left) [2-(acryloyloxy)ethyl]trimethylammonium chloride (Q-9),(center) (3-acryl amidopropyl)trimethylammonium chloride (APTAC), and (right) acrylamide (AM).

Table 19: Properties of cationic polyelectrolyte used in fiber vs. cornstarch hydrolysis study

								Viscosity	
Group	Sample	Polymer type	co-monomer	Stock Form (Dry or Emulsion)	Avg Charge (C/g)	std. dev.	Estimated Cationicity (mol%)	0.5% wt (mPa-s)	0.1% wt (mPa-s)
1	K226FLX	Branched	AM/Q-9	Emulsion	58	0.7	1		
	K274FLX	Branched	AM/Q-9	Emulsion	60	1.0	1		
	K275FLX	Branched	AM/Q-9	Emulsion	130	7.0	12		
	K279FLX	Branched	AM/Q-9	Emulsion	119	7.2	10		
	K290FLX	Branched	AM/Q-9	Emulsion	169	15.7	18		
2	K111L	Linear	AM/Q-9	Emulsion	58	2.4	1		
	K122L	Linear	AM/Q-9	Emulsion	89	1.8	6	4500	1000
	K133L	Linear	AM/Q-9	Emulsion	105	5.3	7	4500	900
	K136L	Linear	AM/Q-9	Emulsion	127	13.0	11		
	K148L	Linear	AM/Q-9	Emulsion	127	5.0	11		
3	K260FL	Linear	AM/Q-9	Emulsion	123	2.9	11		
	K290FL	Linear	AM/Q-9	Emulsion	123	3.0	11		
	K295FL	homo-polymer	Q-9	Emulsion	188	2.8	21		
4	835BS	Linear	AM/Q-9	Dry solid	160	6.2	17	3500	100
	855BS	Linear	AM/Q-9	Dry solid	315	4.0	40	4000	150
	857BS	Linear	AM/Q-9	Dry solid	312	5.3	40	6000	200
	858BS	Linear	AM/Q-9	Dry solid	420	2.9	56	6500	200
	859BS	Linear	AM/Q-9	Dry solid	391	8.0	52	6500	200
5	610BC	Linear	AM/APTAC	Dry solid	43	0.6	1	450	35
	611BC	Linear	AM/APTAC	Dry solid	109	0.7	9	450	35
	644BC	Linear	AM/APTAC	Dry solid	262	4.2	32	700	70
	650 BC	Linear	AM/APTAC	Dry solid	189	3.7	21	700	65

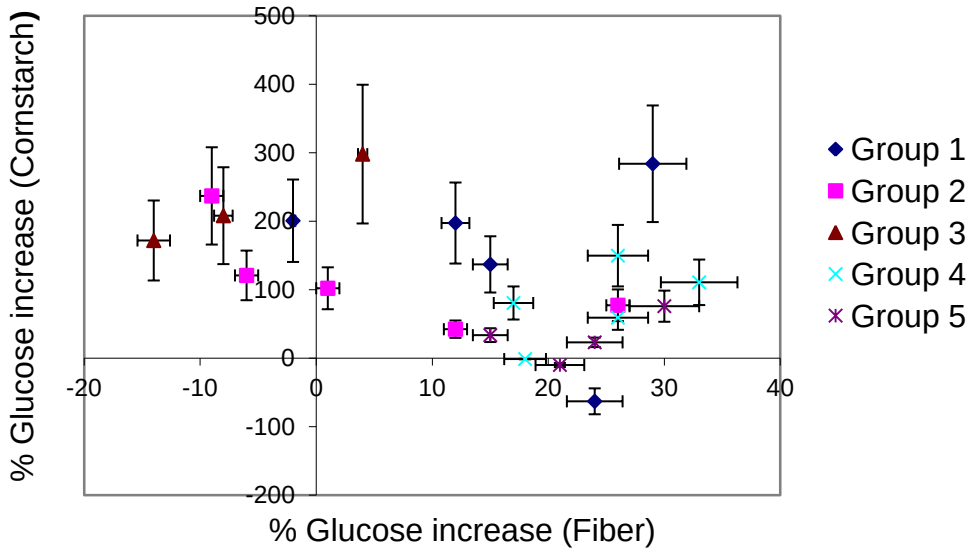

Figure 68: Glucose yield (normalized) from screening of various C-PAM polymers on both cornstarch and fiber substrates.

The results for the hydrolysis screening are reported in Figure 68. Glucose yields after 6 hours from cornstarch and fiber with each C-PAM as a function of the increase in glucose as compared to the control are shown. As can be seen, C-PAM polymers with a wide range of properties were able to enhance the hydrolysis of both fiber and cornstarch to varying degrees, though no one trend could be determined as being the most significant factor for increasing glucose yield. Each of the polymers was able to increase the rate of glucose generation of at least one of the substrates, and there was no C-PAM that inhibited both fiber and starch hydrolysis. The C-PAM series which worked best for both the starch and fiber substrate was the group 1 series of branched AM/Q-9 C-PAMs. For starch alone, the best overall series of polymers were that of Group 3, a linear AM/Q-9 series. For fiber, group 4 and 5, linear co-polymers of AM/Q-9 and

AM/APTAC, worked best overall. A breakdown of the glucose yield with C-PAM of the starch substrate by polymer series is shown in Figure 69. In general, as cationicity increased across a polymer series, the glucose yield increased as well. The emulsion based polymers were more favorable than the dry powder based solutions, most likely a result of the powder based solutions having a higher viscosity than emulsion based C-PAM solutions.

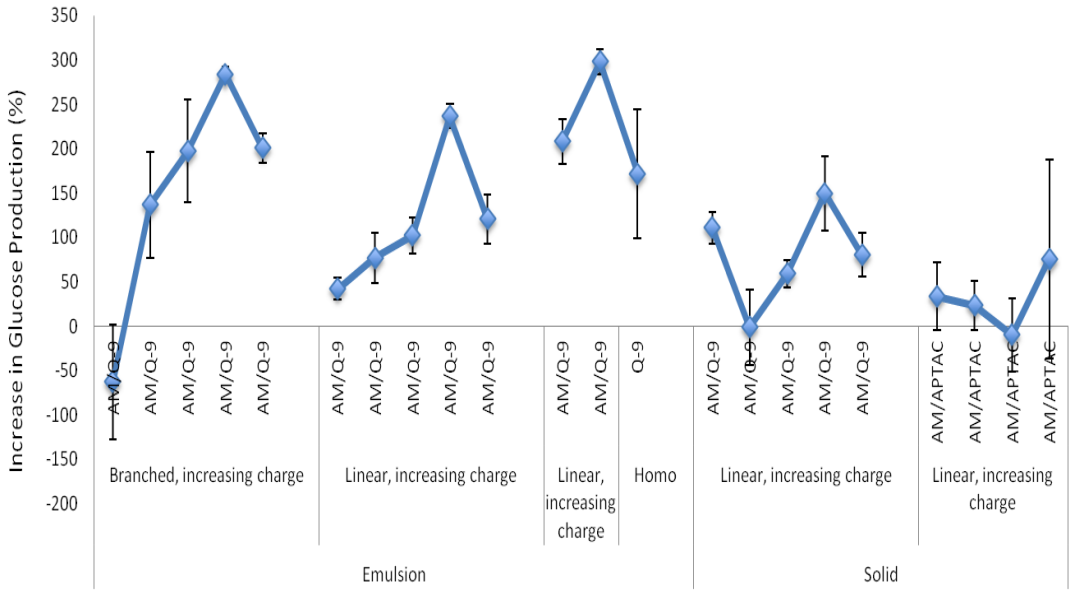

Figure 69: Increase in glucose production (%) as a function of C-PAM series

4.4.7. Discussion of hydrolysis results

There was no significant effect on hydrolysis by glucoamylase with C-PAM. This is likely due to the difference in size of the alpha-amylase substrate (starch) and glucoamylase substrate (dextrin). However, there was a reduction in activity caused by C-PAM, as was discussed previously. The importance of substrate

size is further seen by the dependence of glucose yield on point of C-PAM addition (Table 18). When C-PAM is added before enzyme, C-PAM is able to adsorb to starch and C-PAM surfaces, reduce surface charge repulsion, and enhance binding. Glucoamylase yield is reduced when added after the enzyme because by the time C-PAM is added, starch substrate has already been broken down by enzyme, so that C-PAM would be much larger in size than the starch fragments. As a consequence, C-PAM would not be able to adsorb to the surface to reduce repulsion. Instead the C-PAM would destabilize starch fragments and “floc” the components, minimizing further hydrolysis.

Hydrolysis with C-PAM as a function of cationicity and concentration were consistent with binding data. Binding increased to a greater extent than starch hydrolysis. This is likely evidence that some of the increased binding in the presence of C-PAM was nonproductive binding. The inhibition of hydrolysis by the 10 mol% cationicity was likely caused by high levels of adsorption by the low cationicity C-PAM, which would inhibit hydrolysis by reducing the availability of surface sites for alpha-amylase binding. Though binding with 10 mol% cationicity was weaker than with the other C-PAM, it was still greater than without C-PAM. For hydrolysis, 10 mol% cationicity reduced yield. The effect of 10 mol% cationicity was more pronounced during hydrolysis because of the negative effect of viscosity. The inhibition of hydrolysis by high C-PAM concentration was likely caused by excessive adsorption as well. The molecular weight of C-PAM was less important than its cationicity.

For hydrolysis runs made at low starch concentration, C-PAM was able to increase glucose yield at both pre- and post gelatinization temperatures. Viscosity is not a factor at low starch concentration, but should be increasingly important at higher starch levels. Shearing of enzyme-C-PAM complex likely causes the apparent inhibition of glucose yield at high agitation**.** As a result, optimization of mixing conditions is necessary to achieve highest sugar yields possible.

C-PAM is likely accelerating hydrolysis of cornstarch due to its conventional role as a flocculant. Previous studies by Reye (Reye, Maxwell, et al., 2011; Reye, et al., 2009), found that C-PAM also increased binding and hydrolysis of fiber by cellulase enzyme to the same order of magnitude. In this study it was shown that C-PAM enhances the hydrolysis of both fiber and starch at comparable levels. Since starch-amylase and fiber-cellulase systems are very different, their similar response to the presence of C-PAM suggests a physical rather than a biochemical mechanism. As with fiber hydrolysis, it is believed that the C-PAM is operating via a “patching”, or charge neutralization mechanism. Based on experimental results, it is believed that C-PAM first adsorbs to the substrate surface. The adsorption of the oppositely charge polymer reduces the charge of the substrate and starch surfaces, reducing the amount of repulsion between starch and enzyme. This, in turn, increases the affinity of the enzyme to

substrate, and binding is increased. Because more enzyme is able to bind to substrate, more starch is broken down and converted to glucose.

CHAPTER 5: Conclusions

5.1. Introduction

This dissertation has investigated the mechanism through which cationic polyacrylamide (C-PAM) increases the rate of enzymatic hydrolysis of cornstarch. This chapter summarizes the results and conclusions in light of the original objectives, then discusses the contributions to knowledge of this body of work and implications for practical use, and concludes with recommendations for future work.

5.2. Research Objectives: Summary of Findings and Conclusions

The first objective was to study starch-C-PAM interactions and understand the role of these interactions in acceleration of C-PAM mediated starch hydrolysis. The second was to study the enzyme-C-PAM interactions and understand their role in C-PAM mediated starch hydrolysis. Finally, the last objective was to propose a mechanism for enzymatic hydrolysis in the presence of C-PAM that accounts for these starch-enzyme-C-PAM interactions.

The main results found that address the objectives of this dissertation are:

1. C-PAM has a high affinity for and adsorbs strongly to the starch surface.
2. The adsorbed C-PAM does not significantly affect swelling but does increase the amount of starch fragments that solubilizes below gelatinization temperatures.

3. The association of C-PAM to alpha-amylase is driven by electrostatic interactions. Adsorption strength increases as cationicity increases.
4. C-PAM greatly increases alpha-amylase starch binding ability. Optimum binding occurred with low concentration and higher mol% cationicity.
5. The activity of alpha-amylase increases with increasing C-PAM concentration until a maximum is reached at saturation.
6. C-PAM inhibited the activity and yield of glucoamylase, most likely due to the difference in size of the alpha-amylase substrate (on the order of 10^6) and glucoamylase substrate (on the order of 10^9).
7. Hydrolysis yield was affected by C-PAM in the same manner as alpha-amylase binding was; as with binding, sugar yield was lowest with C-PAM of low cationicity C-PAM and high concentration.
8. Hydrolysis is suppressed at high viscosity. The lower cationicity C-PAM-starch systems had higher viscosity, and as a result had lower sugar yields. Because low cationicity C-PAM has a lower level of intra-molecular repulsion, it is able to agglomerate more particles than the higher cationicity C-PAM, which causes the system to be more viscous. Increasing C-PAM concentration has the analogous affect as lowering the cationicity of the C-PAM.
9. C-PAM increases the yield from both cornstarch and wood pulp fiber substrate, suggesting a nonspecific biochemical mechanism of action

Taken together, these results suggest that the enhancement of hydrolysis is due to increased alpha-amylase binding to starch, induced by C-PAM. C-PAM increases alpha-amylase binding by reducing the charge repulsion of both alpha-amylase and starch when adsorbed by C-PAM. The degree of binding and subsequent hydrolysis is largely dependent on the concentration and properties of the C-PAM.

5.3. Contributions to knowledge and implications for practical use

These findings add to our understanding of a novel method for increasing efficiency of enzymatic starch hydrolysis, and serves as a base for future studies in enzymatic hydrolysis enhanced by cationic polymers. A list of publications and presentations to date from this work is shown below.

- Reye, J.T., **Maxwell, K**., Rao, S. Lu, J., Banerjee, S. (2009). *Cationic polyacrylamides enhance rates of starch and cellulose saccharification*. Biotechnology Letters. 31: 1613-1616
- Reye, J.T., **Maxwell, K**., Banerjee, S. (2011). *Cationic polyacrylamides promote binding of cellulose and amylase.* Journal of Biotechnology. 154: 269-273
- Reye, J.T.,Lu, Jian **Maxwell, K**., Banerjee, S. (2011). *Enhancement of cellulase catalysis of wood pulp fiber by cationic polyelectrolytes.* Biomass and Bioenergy. 35(12): 4887-4891.
- Publication: **Maxwell, K**, Krantz, A., Banerjee, S. (2012) *Cationic Polyacrylamides increase the rate of liquefaction and saccharification of cornstarch. AIChEJ, in final revision.*

- Maxwell, K. (2011). *Polymer Accelerated Hydrolysis of Starch for the Production of Biofuels*, American Institute of Chemical Engineers Spring Meeting, Chicago, Il. (presentation)
- Maxwell, K. (2009). *Accelerated Hydrolysis of Starch for Biofuel Production*, National Society of Black Engineers Annual Convention, Las Vegas, NV. (presentation)

An important practical implication of these findings is that substantial reductions in enzyme usage would be possible with the addition of a small dosage of C-PAM during the industrial hydrolysis of cornstarch, with no major alterations to the existing set-up. However as shown with this study, C-PAM properties such as concentration, cationicity, and molecular weight, and process conditions such as viscosity and agitation must be taken into account in order to achieve optimal yield.

5.4. Recommendations for future research and direction

Finally, though measures were taken to model industrial cornstarch hydrolysis condition, there were still some limitations to this study. The most important limitation was that all experiments were conducted at the lab scale with the assumption that results would apply to scaled up conditions. Also purified cornstarch was used as a model substrate, as opposed to the mashed corn mixture that would be used in industry. This was done in order to have a consistent starting substrate with which to evaluate and compare results. Further study could compare the hydrolysis a raw corn mass suspension to that of the

purified cornstarch suspension. In addition, further research regarding the role of substrate size on the mechanism would prove useful in determining other potential biomass substrates for this method of hydrolysis enhancement.

There are two main areas that are recommended for future research direction. First, an investigation into the effectiveness of other positively charge polymers would be very beneficial. Experiments are already underway into the use of polydiallyl dimethyl ammonium chloride (PDADMAC) as an alternative to C-PAM, and have been successful in increasing enzymatic hydrolysis of both starch and fiber. Therefore other positively charged polymers such as polyethyleneimine (PEI), or poly aluminum chloride (PAC) might also prove beneficial. PDADMAC, PEI, and PAC would be alternatives that are more health and environmentally sustainable than the acrylamide based C-PAM. As an extension to the above study, it is recommended that further exploration be done on the use and effectiveness of a non-synthetic polymer. If a non-renewable charged polymer source was proven successful, it would open the door to opportunities for expansion of the applications this method could be used for.

The second major area of future work should be directed toward the exploration of the use of other biomass material as substrate. Since C-PAM was successful in increasing hydrolysis of both fiber and cornstarch and it was shown to enhance hydrolysis via a nonspecific mechanism, the enhancement of other biomass conversion systems seems highly likely. Corn stover, switchgrass, bagasse, and

wheat straw are examples of biomass material that might deem beneficial from this method of hydrolysis and would add to the practical applications of this work.

REFERENCES

Aksberg, R., & Wagberg, L. (1989). Hydrolysis of cationic polyacrylamides. *Journal of Applied Polymer Science, 38*(2), 297-304.

Ariff, A. B., Asbi, B. A., Azudin, M. N., & Kennedy, J. F. (1997). Effect of mixing on enzymatic liquefaction of sago starch. *Carbohydrate Polymers, 33*(2), 101-108.

BeMiller, J. (2011). Pasting, paste, and gel properties of starch-hydrocolloid combinations. *Carbohydrate Polymers, 86*, 386-423.

Berg, J. M., Claesson, P. M., & Neuman, R. D. (1993). Interactions between Mica Surfaces in Sodium Polyacrylate Solutions Containing Calcium Ions. *Journal of Colloid and Interface Science, 161*(1), 182-189. doi: 10.1006/jcis.1993.1457

Bothast, R. J., & Schlicher, M. A. (2005). Biotechnological processes for conversion of corn into ethanol. *Appl Microbiol Biotechnol, 67*(1), 19-25. doi: 10.1007/s00253-004-1819-8

Bratby, J. (1980). *Coagulation and Flocculation*. Croydon: Uplands Press.

Brumm, P. J., & Teague, W. M. (1989). Effect of additives on the thermostability of *Bacillus stearothermophilus* alpha-amylase. *Biotechnology Letters, 11*, 541-544.

Claesson, P. M., Poptoshev, E., Blomberg, E., & Dedinaite, A. (2005). Polyelectrolyte-mediated surface interactions. *Adv Colloid Interface Sci, 114-115*, 173-187. doi: S0001-8686(05)00011-4 [pii]
10.1016/j.cis.2004.09.008

De Witt, J. A., & Van de Ven, T. (1992). Kinetics and reversibility of the adsorption of poly(vinyl alcohol) onto polystyrene latex particles. *Langmuir, 8*(3), 788-793.

Declerck, N., Machius, M., Joyet, P., & Wiegand, G. (2003). Hyperthermostabilisation of *Bacillus licheniformis* alpha-amylase and modulation of its stability over a 50 ^{o}C temperature range. *Protein Engineering, 16*, 287-293.

Dobrynin, A. V., & Rubinstein, M. (2005). Theory of polyelectrolytes in solutions and at surfaces. *Progress in Polymer Science, 30*, 1049-1118.

Elodi, P., Mora, S., & Krysteva, M. (1972). Investigation of Active Center of Porcine-Pancreatic Amylase. *European Journal of Biochemistry, 24*(3), 577-582.

Enarsson, L. E., & Wagberg, L. (2008). Adsorption kinetics of cationic polyelectrolytes studied with stagnation point adsorption reflectometry and quartz crystal microgravimetry. *Langmuir, 24*, 7329-7337.

Fitter, J. (2005). Structural and dynamical features contributing to thermostability in alpha-amylases. *Cell Mol Life Sci, 62*(17), 1925-1937. doi: 10.1007/s00018-005-5079-2

Gangadhara, D., Nampoothiri, M. K., Sivaramakrishnan, S., & Pandey, A. (2009). Immobilized bacterial alpha-amylase for effective hydrolysis of raw and soluble starch. *Food Research International, 42*, 436-442.

Gregory, J., & Barany, S. (2011). Adsorption and flocculation by polymers and polymer mixtures. *Advances in Colloid and Interface Science, 169*(1), 1-12. doi: 10.1016/j.cis.2011.06.004

Guillen, D., Santiago, M., Linares, L., Perez, R., Morlon, J., Ruiz, B., . . . Rodriquez-Sanoja, R. (2007). Alpha-Amylase Starch Binding Domains: Cooperative Effects of Binding to Starch Granules of Multiple Tandemly Arranged Domains. *Applied and Environmental Microbiology, 73*(12), 3822-3837.

Haefele, D., Owens, F., O'Bryan, K., & Sevenich, D. (2004). *Selection and Optimization of Corn Hybrids for Fuel Ethanol Production.* Paper presented at the 59th Annual Corn and Sorghum Research Conference, Alexandria, VA.

Hatti-Kaul, R., & Andersson, M. (1999). Protein stabilising effect of polyethyleneimine. *Journal of Biotechnology, 72*, 21-31.

Hogg, R. (1999). The role of polymer adsorption kinetics in flocculation. [Article]. *Colloids and Surfaces a-Physicochemical and Engineering Aspects, 146*(1-3), 253-263. doi: 10.1016/s0927-7757(98)00723-7

Hubbe, M. A., Nanko, H., & McNeal, M. R. (2009). Retention aid polymer interactions with cellulosic surfaces and suspensions: A review. *Bioresources, 4*(2), 850-906.

Iefuji, H., Chino, M., Kato, M., & Limura, Y. (1996). Raw starch-digesting and thermostable alpha-amylase from the yeast *Cryptococcus sp. S-2*:

Purification, characterization, cloning and sequencing. *Biochemistry Journal, 318*, 989-996.

Iyer, P. V., & Ananthanarayan, L. (2008). Enzyme stability and stabilization-Aqueous and non-aqueous environment. *Process Biochemistry, 43*, 1019-1032.

James, J. A., & Lee, B. H. (1997). Glucoamylases: Microbial Sources, Industrial Applications and Molecular Biology- A Review. *Journal of Food Biochemistry, 21*, 1-52.

Jane, J.-l. (1993). Mechanism of Starch Gelatinization in Neutral Salt Solutions. *starch/starke, 45*(5), 161-166.

John, G. (1973). Rates of flocculation of latex particles by cationic polymers. *Journal of Colloid and Interface Science, 42*(2), 448-456. doi: 10.1016/0021-9797(73)90311-1

John, G. (1988). Polymer adsorption and flocculation in sheared suspensions. *Colloids and Surfaces, 31*(0), 231-253. doi: 10.1016/0166-6622(88)80196-3

Kaur, L., Singh, J., Singh, H., & McCarthy, O. (2008). Starch-cassia gum interactions: A microstructure-Rheology study. *Food Chemistry, 111*, 1-10.

Khalil, M., Meier, P., Brainard, J., Vanderberg, L., Sauer, N., & Foreman, T. (2001). Effects of Charged Water Soluble Polymers on the Stability and Activity of Yeast Alcohol Dehydrogenase and Subtilizing Carlsberg. *Biotechnology and Bioengineering, 76*(3), 241-246.

Kinniburgh, D. G. (1986). General purpose adsorption isotherms. *Environmental Science Technology, 20*(9), 895-904.

Kwiatkowski, J. R., McAloon, A. J., Taylor, F., & Johnston, D. B. (2006). Modeling the process and costs of fuel ethanol production by the corn dry grind process. *Industrial Crops and Products, 23*, 288-296.

La Mer, V. K. (1966). Filtration of colloidal dispersions flocculated by anionic and cationic polyelectrolytes. *Discussions of the Faraday Society, 42*, 248-254.

Leloup, V. M., Colonna, P., & Ring, S. G. (1991). Alpha-Amylase Adsorption on Starch Crystallites. *Biotechnology and bioengineering, 38*(2), 127-134.

Lim, H. L., Macdonald, D. G., & Hill, G. A. (2003). Hydrolysis of starch particles using immobilized barley alpha-amylase. *Biochemical Engineering Journal, 13*(53-62).

Mandala, I. G., & Bayas, E. (2004). Xanthan effect on swelling, solubility and viscosity of wheat starch dispersions. *Food Hydrocolloids, 18*, 191–201.

Michaels, A. S. (1954). Aggregation of Suspension by Polyelectrolytes. *Ind. Eng. Chem., 46*, 1485.

Montalbo-Lomboy, M. (2008). *Ultrasonic pretreatment for enhanced saccharification and fermentation of ethanol production from corn.* Phd, Iowa State University.

Mora, S., Lu, J., & Banerjee, S. (2011). Mechanism of rate enhancement of wood fiber saccharification by cationic polyelectrolytes. *Biotechnology Letters, 33*(9), 1805-1808.

Mortimer, D. (1991). Synthetic Polyelectrolytes-A Review. *Polymer International, 25*, 29-41.

Mussatto, S., Dragone, G., Guimaraes, P., Silva, J., Carneiro, L., Roberto, I., & Teixeira, J. (2010). Technological trends, global market, and challenges of bio-ethanol production. *Biotechnology Advances, 28*, 817-830.

Napper, D. H. (1983). *Polymeric stabilization of colloidal dispersions*. London Academic Press.

Nigam, P. S., & Singh, A. (2011). Production of liquid biofuels from renewable resources. *Progress in Energy and Combustion Science, 37*, 52-68.

Nishibue, H., Ogawa, H., Kozono, H., Morita, K., Matsuyama, H., & Teramoto, M. (1996). Effect of addition of water soluble cationic polymers on thermal stability and activity of glucose dehydrogenase. *Colloids and Surfaces B; Biointerfaces 7*, 165-171.

Noh, H., & Vogler, E. (2006). Volumetric interpretation of protein adsorption: Partition coefficients, interphase volumes, and free energies of adsorption to hydrophobic surfaces. *Biomaterials, 27*(34), 5780-5793.

O'Gorman, J. V., & Kitchener, J. A. (1974). The flocculation and de-watering of kimberlite clay slimes. *International Journal of Mineral Processing, 1*(1), 33-49. doi: 10.1016/0301-7516(74)90025-8

Ozeroglu, C., Guney, O., Sarac, A. S., & Mustafaev, M. I. (1996). The polymerization of acrylamide initiated with Ce(IV) and KMnO4 redox systems in the presence of glycine. *Journal of Applied Polymer Science, 60*(5), 759-765.

Pfau, A., Schrepp, W., & Horn, D. (1999). Detection of a single molecule adsorption structure of poly(ethylenimine) macromolecules by AFM. *Langmuir, 15*(9), 3219-3225.

Rendleman, M., & Shapouri, H. (2007). *New Technologies in Ethanol Production*. (842).

Reye, J., Lu, J., Maxwell, K., & Banerjee, S. (2011). Enhancement of cellulase catalysis of wood pulp fiber by cationic polyelectrolytes. *Biomass and Bioenergy, 35*(12), 4887-4891.

Reye, J., Maxwell, K., & Banerjee, S. (2011). Cationic polyacrylamides promote binding of cellulase and amylase. *Journal of Biotechnology, 154*, 269-273.

Reye, J., Maxwell, K., Banerjee, S., Rao, S., & Lu, J. (2009). Cationic polyacrylamides enhance rates of starch and cellulose saccharification. *Biotechnology Letters, 31*(10), 1613-1616.

RFA. (2011). Ethanol Industry Outlook: Renewable Fuels Association.

Robertson, G. H., Wong, D. W., Lee, C. C., Wagschal, K., Smith, M. R., & Orts, W. J. (2006). Native or raw starch digestion: a key step in energy efficient biorefining of grain. *J Agric Food Chem, 54*(2), 353-365. doi: 10.1021/jf051883m

Sanchez, O. J., & Cardona, C. A. (2008). Trends in biotechnological production of fuel ethanol from different feedstocks. *Bioresour Technol, 99*(13), 5270-5295. doi: S0960-8524(07)00937-6 [pii]
10.1016/j.biortech.2007.11.013

Sarbatly, R., & England, R. (2004). Critical review of membrane bioreactor system used for continuous production of hydrolyzed starch. *Chemical and Biochemical Engineering, 18*(2), 155-165.

Shatat, R., Ariffin, A., Rahman, N. N. A., & Kadir, M. O. A. (2008). The effect of molecular weight and charge density on floc size distribution of palm oil mill effluent flocculated with cationic polyelectrolytes. *Journal of Basic and Applied Sciences, 4*(2), 95-103.

Shaw, A., Bott, R., & Day, A. G. (1999). Protein Engineering of alpha-amylase for low pH performance. *Protein technologies and commercial enzymes, 10*(349-352).

Sivaramakrishnan, S., Gangadharan, D., Nampoothiri, K. M., Soccol, C. R., & Pandey, A. (2006). Alpha-Amylases from Microbial Sources- An Overview

on Recent Developments. *Food Technology and Biotechnology, 44*(2), 173-184.

Smith-Palmer, T., & Pelton, R. (2002). Flocculation of particles *Encyclopedia of Surface and Colloid Science* (Vol. 2, pp. 2207-2224).

Solberg, D., & Wagberg, L. (2003). Adsorption and flocculation behavior of cationic polyacrylamide and colloidal silica. [Article]. *Colloids and Surfaces a-Physicochemical and Engineering Aspects, 219*(1-3), 161-172. doi: 10.1016/s0927-7757(03)00029-3

Street, H., & Close, J. (1956). Determination of Amylase Activity in Biological Fluids. *Clinica Chimica Acta, 1*(3), 256-268.

Sukhishvili, S. A., & Granick, S. (1998). Polyelectrolyte adsorption onto an initially-bare solid surface of opposite electrical charge. [Article]. *Journal of Chemical Physics, 109*(16), 6861-6868. doi: 10.1063/1.477253

Taylor, F., McAloon, A. J., Craig, J. C., Yang, P., Wahjudi, J., & Eckhoff, S. R. (2001). Fermentation and Costs of Fuel Ethanol from Corn with Quick-Germ Process. *Applied Biochemistry and Biotechnology 94*, 41-49.

Tester, R. F., & Sommerville, M. D. (2003). The effects of non-starch polysaccharides on the extent of gelatinization, swelling, and alpha-amylase hydrolysis of maize and wheat starches. *Food Hydrocolloid, 17*, 41-54.

Van Beynum, G. M. A., & Roels, J. A. (Eds.). (1985). *Starch Conversion Technology* (Vol. 14). New York: Marcel Dekker, INC.

Van De Ven, T. (1994). Kinetic aspects of polymer and polyelectrolyte adsorption on surfaces. *Advances in Colloid and Interface Science, 48*(15), 121-140.

Warren, F., Royall, P., Gaisford, S., Butterworth, P., & Ellis, P. (2011). Binding interactions of alpha-amylase with starch granules: The influence of supramolecular structure and surface area. *Carbohydrate Polymers, 86*, 1038-1047.

Wong, S. S., Teng, T. T., Ahmad, A. L., Zuhairi, A., & Najafpour, G. (2006). Treatment of pulp and paper mill wastewater by polyacrylamide (PAM) in polymer induced floccuation. *Journal of Hazardous Materials, 135*, 378-388.

Xie, F., Liu, H., Chen, P., Xue, T., Chen, L., Yu, L., & Corrigan, P. (2006). Starch Gelatinization under Shearless and Shear Conditions. *International Journal of Food Engineering, 2*(5), 1-29.

Yoo, Y., Hong, J., & Hatch, R. (1987). Comparison of Alpha-Amylase Activities from Different Assay Methods. *Biotechnology and Bioengineering, 30*(1), 147-151.

Yoon, S., & Robyt, J. (2005). Activation and stabilization of 10 starch degrading enzymes by Triton-X-100, polyethylene glycols, and polyvinyl alcohols. *Enzyme and Microbial Technology, 37*(556-562).

Zhu, W. X., Gayin, J., Chatel, F., Dewettinck, K., & Wan der Meeren, P. (2009). Influence of electrolytes on the heat-induced swelling of aqueous dispersions of native wheat starch granules. *Food Hydrocolloid, 23*, 2204-2211.